

AperTO - Archivio Istituzionale Open Access dell'Università di Torino

**Fructose liquid and solid formulations differently affect gut integrity, microbiota composition and related liver toxicity: a comparative in vivo study**

**This is the author's manuscript**

*Original Citation:*

*Availability:*

This version is available <http://hdl.handle.net/2318/1661849> since 2019-04-15T11:21:58Z

*Published version:*

DOI:10.1016/j.jnutbio.2018.02.003

*Terms of use:*

Open Access

Anyone can freely access the full text of works made available as "Open Access". Works made available under a Creative Commons license can be used according to the terms and conditions of said license. Use of all other works requires consent of the right holder (author or publisher) if not exempted from copyright protection by the applicable law.

(Article begins on next page)

# **Fructose liquid and solid formulations differently affect gut integrity, microbiota composition and related liver toxicity: a comparative *in vivo* study.**

Mastrocola R, Ferrocino I, Liberto E, Chiazza F, Cento AS, Querio G., Nigro D, Bitonto V, Cutrin JC, Rantsiou K, Durante M, Masini E, Aragno M<sup>1</sup>, Cordero C, Cocolin L, Collino M.

## **HIGHLIGHTS**

1. Solid and liquid fructose are differently absorbed by intestinal barrier
2. Solid and liquid fructose differently affects gut microbiota population
3. Altered microbiota and AGEs accumulation disrupt intestinal barrier
4. Solid fructose absorption is linked to increased hepatic inflammasome activation.

1 **Fructose liquid and solid formulations differently affect gut integrity,**  
2 **microbiota composition and related liver toxicity: a comparative *in***  
3 ***vivo* study.**

4 Mastrocola R<sup>1,2</sup>, Ferrocino I<sup>3</sup>, Liberto E<sup>4</sup>, Chiazza F<sup>4</sup>, Cento AS<sup>1</sup>, Collotta D<sup>4</sup>, Querio G.<sup>4</sup>, Nigro D<sup>1</sup>,  
5 Bitonto V<sup>5</sup>, Cutrin JC<sup>5</sup>, Rantsiou K<sup>3</sup>, Durante M<sup>6</sup>, Masini E<sup>6</sup>, Aragno M<sup>1</sup>, Cordero C<sup>4</sup>, Cocolin L<sup>3\*</sup>,  
6 Collino M<sup>3\*</sup>

7  
8 *\*shared senior authors of this study.*

9  
10 <sup>1</sup>Dept. of Clinical and Biological Sciences, University of Turin, Italy;

11 <sup>2</sup>Dept. Internal Medicine, University of Maastricht, The Netherlands;

12 <sup>3</sup>Dept. of Agricultural, Forest and Food Sciences, University of Turin, Italy;

13 <sup>4</sup>Dept. of Drug Science and Technology, University of Turin, Italy;

14 <sup>5</sup>Dept. of Molecular Biotechnology and Sciences for the Health, University of Turin, Italy;

15 <sup>6</sup>Dept. of Neuroscience, Psychology, Drug Research and Child Health, University of Florence, Italy.

16

17

18

19

Corresponding author:

20

Massimo Collino

21

Department of Drug Science and Technology,

22

University of Turin via P. Giuria 9, 10125 Torino, Italy.

23

Tel: +39 011 6706861 Fax: +39 011 2367955

24

E-mail address: massimo.collino@unito.it

25

26

Luca Cocolin

27

DISAFA, University of Turin

28

Largo Braccini 2, 10095 Grugliasco, Italy.

29

Tel: +39 011 6708553 Fax: +39 011 2368549

30

E-mail address: lucasimone.cocolin@unito.it

31

32

33 **Running title:** Liquid vs. solid fructose in gut/liver toxicity

34 **Abstract**

35 Despite clinical findings suggest that the form (liquid versus solid) of the sugars may significantly  
36 affect the development of metabolic diseases, no experimental data are available on the impact of  
37 their formulations on gut microbiota, integrity and hepatic outcomes.

38 In the present study, C57Bl/6j mice were fed a standard diet plus water (SD), a standard diet plus  
39 60% fructose syrup (L-Fr), or a 60% fructose solid diet plus water (S-Fr), for 12 weeks. Gut  
40 microbiota was characterized through 16S rRNA phylogenetic profiling and shotgun sequencing of  
41 microbial genes in ileum faecal content and related volatilome profiling.

42 Fructose feeding led to alterations of the gut microbiota depending on the fructose formulation, with  
43 increased colonization by Clostridium, Oscillospira, and Clostridiales phyla in the S-Fr group and  
44 Bacteroides, Lactobacillus, Lachnospiraceae, and Dorea in the L-Fr. S-Fr evoked the strongest  
45 accumulation of Advanced Glycation End Products (AGEs) and barrier injury in the ileum intestinal  
46 mucosa, leading to increased lipopolysaccharide (LPS) levels in the portal plasma. These effects  
47 were associated to a stronger activation of the LPS-dependent pro-inflammatory TLR4/NLRP3  
48 inflammasome pathway in the liver of S-Fr mice than of L-Fr mice. In contrast, L-Fr intake induced  
49 higher levels of hepatosteatosis and markers of fibrosis than S-Fr. Fructose-induced *ex novo*  
50 lipogenesis with production of SCFA and MCFA was confirmed by metagenomic analysis.

51 These results suggest that consumption of fructose under different forms, liquid or solid, may  
52 differently affect gut microbiota, thus leading to impairment in intestinal mucosa integrity and liver  
53 homeostasis.

54

55 **Keywords:** Fructose; Microbiota; Advanced Glycation End-products; Faecal volatilome;  
56 Inflammasome

57

## 58 1. Introduction

59 Over the last decades, the dietary intake of fructose has rapidly increased in industrialized countries  
60 due to changes in dietary behaviors, such as the rise in sugar-sweetened beverages and sugar-rich  
61 processed foods consumption [1, 2]. The increase in fructose consumption has been associated to  
62 higher prevalence of metabolic diseases, such as dyslipidemia, insulin resistance, high blood  
63 pressure, hepatic steatosis, and nonalcoholic fatty liver diseases (NAFLD) [3, 4], which are related  
64 to the high lipogenic power of fructose [5, 6]. The peculiar lipid deposition induced by excessive  
65 fructose consumption in ectopic tissues, such as liver and skeletal muscle, without significantly  
66 affecting body weight and adipose tissue mass, has been previously described [7-9].

67 Fructose is absorbed in the small intestine by the specific facilitative transporters expressed in both  
68 the apical and basolateral membrane of enterocytes [10]. After absorption, fructose is primarily  
69 metabolized in the liver which takes up at least 50% of the initial fructose flux [11].

70 The fructose intake exceeding the absorption capacity of small intestine passes to the large intestine  
71 where it becomes fermentable substrate for the microbiota. It has been reported that high fructose  
72 intake alters microbiota composition, resulting in reduced bacterial diversity and altered expression  
73 of genes involved in specific metabolic pathways [12].

74 We recently demonstrated that a high fructose intake induces Advanced Glycation End Products  
75 (AGEs) accumulation in liver, **contributing to increase the endogenous synthesis of fatty acids**  
76 **(known as *ex novo* lipogenesis)** and to intracellular lipids deposition, and evoking a pro-  
77 inflammatory response [13, 14]. Fructose-derived AGEs might also impair gut homeostasis,  
78 stimulating the growth of detrimental colonic bacteria (*Clostridia* and/or *Bacteroides*). So far, this  
79 hypothesis has never been investigated despite recent studies indicate that exposure to diet-derived  
80 AGEs for 2 weeks is sufficient to alter the colonic bacteria profile in humans [15]. As a  
81 consequence, increased gastrointestinal permeability may allow the translocation of toxic  
82 compounds from the gut into the circulation, activating systemic immune responses and  
83 inflammatory signals.

84 Another recent intriguing finding is that liquid high-sugar diets differentially modulate feeding  
85 behavior, as well as intestinal sugar transporters and hormones expression, when compared to solid  
86 high-sugar diets [16]. This experimental evidence may suggest that not only the type (e.g. fructose  
87 versus glucose), but also the form (liquid versus solid) of the sugars may significantly affect the  
88 development of obesity, insulin resistance and/or fatty liver disease. Despite the paucity of  
89 experimental data, this topic deserves better elucidation as sweeteners, including fructose, can be  
90 ingested as both liquid and solid formulations. Unfortunately, to date, the peculiar effects of intake  
91 of different forms of fructose, liquid or solid, on intestine integrity and microbiota, and hepatic  
92 outcomes have never been investigated.

93 Hence, the present study aimed at investigating the effects of fructose-derived AGEs on gut  
94 microbiota composition and function as well as on the impact on the intestinal barrier and the  
95 following consequences on the main target organ of fructose metabolism: the liver. Most notably,  
96 the study was designed to elucidate potential toxicological differences due to the sugar  
97 formulations.

98

99

## 100 **2. Materials and Methods**

### 101 **2.1 Animal model and procedures**

102 Male C57Bl/6j mice (Charles River Laboratories, Calco, Italy) of 4 weeks of age were cared in  
103 compliance with the European Council directives (No. 86/609/EEC) and with the Principles of  
104 Laboratory Animal Care (NIH No. 85–23, revised 1985). The scientific project was approved by the  
105 Ethical Committee of the Turin University (permit number: D.M. 94/2012-B). Mice were divided  
106 into three groups: a group fed with a standard diet and drinking tap water (SD group,  $n = 10$ ), a  
107 group fed with a standard diet and drinking a 60% fructose (w/vol) syrup solution (L-Fr group,  $n =$   
108 10), and a group fed with a solid diet providing the 60% of calories from fructose and drinking tap  
109 water (S-Fr group,  $n = 10$ ), for twelve weeks. Standard diet (Sniff Spezialdiäten GmbH, Soest,  
110 Germany) composition was: 62.1% of calories in carbohydrates (36.2% from corn starch, 14.9%  
111 from dextrin and 11% from sucrose), 5.1% of calories in fat, 5% of calories in fibres and 17.6% of  
112 calories from proteins. L-Fr syrup was prepared dissolving 60% of fructose in water with 3.5%  
113 citric acid as preservative. S-Fr diet (Sniff Spezialdiäten GmbH, Soest, Germany) composition was:  
114 70% of calories in carbohydrates (8.9% from corn starch, 1% from sugar and 60% from fructose),  
115 10% of calories in fat, and 20% of calories from proteins. **The SD and S-Fr diets provided the same**  
116 **amount of calories (3.85 kcal/g). The percentage of fructose has been chosen according to our**  
117 **previous studies, in which we demonstrated that 60% fructose diet for 12 weeks was able to evoke**  
118 **significant derangements in key end-organs of metabolic diseases [14, 17, 18]. Mice of both S-Fr**  
119 **and L-Fr groups were fed with the same amount of daily fructose intake.** All groups received drink  
120 and food *ad libitum*.

121 Body weight and food intake were recorded weekly. Fasting glycemia was measured at the start of  
122 the protocol and every 4 weeks by saphenous vein puncture using a glucometer (GlucoGmeter,  
123 Menarini Diagnostics). Urine samples were collected for 18 hours from mice in individual  
124 metabolic cages. After 12 weeks, mice were anesthetized and sacrificed by cardiac exsanguination.  
125 Blood was collected and liver and small intestine (ileum) were rapidly removed. A portion of each

126 tissue, liver and ileum, was cryoprotected in OCT (Optimal Cutting Temperature) compound and  
127 frozen in N<sub>2</sub> for cryostatic preparations. Fragments from the left lateral lobe of liver and from ileum  
128 tract of intestine were fixed overnight in 4% buffered formaldehyde solution for paraffin inclusion  
129 and morphology evaluation. Other portions of tissues and the luminal faecal content of the ileum  
130 were frozen in N<sub>2</sub> and stored at -80°C for analysis.

131

## 132 **2.2 Plasma analyses**

133 Plasma and tissue triglyceride levels (TG) were determined by standard enzymatic procedures using  
134 reagent kits (Hospitex Diagnostics, Florence, Italy). Plasma insulin level was measured using an  
135 enzyme-linked immunosorbent assay (ELISA) kit (Merckodia AB, Uppsala, Sweden). Plasma LPS  
136 levels were determined by Pierce LAL Chromogenic Endotoxin Quantitation Kit (Thermo  
137 Scientific, Waltham, MA, USA). After incubation of samples with Limulus Amebocyte Lysate  
138 (LAL), chromogenic substrate and stop reagent, we measured absorbance at 410 nm.

139

## 140 **2.3 Urine analysis**

141 Glucose and fructose urinary concentrations were determined by gas chromatography coupled with  
142 mass spectrometric detection (GC-MS) after suitable derivatization. Urine samples were submitted  
143 to derivatization consisting of oximation/silylation according to a reference protocol [19]: 200 µL of  
144 urine and internal standard (*p*-Chlorophenylalanine 10 g/L) were diluted with methanol and  
145 carefully mixed (Whirlimixer vortex, Fisher Scientific, Loughborough, Leicestershire, UK). Then,  
146 30 µL of MOX were added to 20 µL of that solution and incubated for 2 hours at 60°C. Next, 30 µL  
147 of MSTFA were added and incubated at 100 °C for 60 minutes. The resulting sample was diluted in  
148 dichloromethane and immediately analyzed in duplicate or stored at -80°C until analysis.  
149 Quantitation was done by external standard calibration according to a previous study [20].  
150 GC-MS analyses were run with an Agilent 6890 GC unit coupled to an Agilent 5975C MS detector  
151 (Agilent, Little Falls, DE, USA) operating in EI mode at 70 eV. The GC transfer line was set at



152 300°C. An Auto Tune option was used and the scan range was set to m/z 50-350 with a scanning  
153 rate of 2,500 amu/s. The column consisted of a 30 m × 0.25 mm  $d_c$  × 0.25  $\mu$ m  $d_f$  SE52 (95%  
154 polydimethylsiloxane, 5% phenyl) from Mega (Legnano, Milan, Italy). The carrier gas was helium  
155 delivered at constant flow of 1.2 mL/min. Injection was by split/splitless injector, split mode, split  
156 ratio 1/20, injector temperature 280°C, and injection volume 2 $\mu$ L. The oven temperature  
157 programme was 80°C (1 min) to 300°C (10 min) at 4.0°C/min.

158

## 159 **2.4 Histological analysis**

### 160 *2.4.1 Hematoxylin/eosin staining and histology score on liver sections*

161 **Liver and ileum mucosa morphology was evaluated by standard hematoxylin/eosin (H&E) staining**  
162 **on de-waxed 5  $\mu$ m sections. The NAFLD activity score (NAS) evaluating the grade of steatosis, the**  
163 **umber of inflammatory foci, the presence of ballooning, and the fibrosis staging has been performed**  
164 **as described by Kleiner et al. [21] paralleled by the histology activity index of damage (HAID), a**  
165 **semi-quantitative necro-inflammatory grading based in the Knodell score system [22] which**  
166 **evaluates the degree of periportal interface hepatitis, focal lytic necrosis, apoptosis, and focal**  
167 **inflammation. Histologic scores have been performed on ten fields at 200x magnification per liver**  
168 **section by a blinded pathologist.**

### 169 *2.4.2 Oil Red O staining*

170 Liver lipid accumulation was evaluated by Oil Red O staining on 7  $\mu$ m ileum cryostatic sections.  
171 Stained tissues were viewed under an Olympus Bx4I microscope (X10 magnification) with an  
172 AxioCamMR5 photographic attachment (Zeiss, Gottingen, Germany).

### 173 *2.4.3 Indirect immunofluoresce*

174 Indirect immunofluorescence on 7  $\mu$ m cryostatic sections was performed for intestinal expression  
175 and localization of GLUT-5, both intestinal and hepatic expression and localization of GLUT-2, as  
176 well as intestinal CML, CEL, and RAGE expression. Sections were blocked for 1 h with 3% BSA  
177 in PBS added with unconjugated goat anti-mouse IgG (Sigma Chemical Co., St. Louis, MO, USA)

178 to prevent interferences between endogenous mouse IgG and secondary antibody against mouse  
179 IgG. Sections were then incubated overnight with primary antibodies: rabbit anti-GLUT-2 (Santa  
180 Cruz Biotechnology, Dallas, Texas, USA), mouse anti-CML (R&D Systems, Inc. Mineapolis, MN,  
181 USA), mouse anti-CEL (TransGenic Inc., Kobe, Japan), and mouse anti-RAGE (Abcam), and  
182 subsequently for 1 h with Cy3-labeled secondary antibody (Sigma Chemical Co.). Negative controls  
183 were prepared incubating sections only with secondary antibodies. Nuclei were stained with  
184 Hoechst dye and sections were then examined using a Leica Olympus epifluorescence microscope  
185 (Olympus Bx4I) with a photographic attachment. CML, CEL and RAGE immunoreactivity has  
186 been quantified by using Image J software (NIH).

187

## 188 **2.5 Intestinal alkaline phosphatase (IAP) activity**

189 Alkaline phosphatase activity has been detected in ileum protein extracts with SensoLite pNPP  
190 Alkaline Phosphatase colorimetric assay kit (AnaSpec Inc, Fremont, CA, USA) following  
191 manufacturer's instructions for kinetic reading.

192

## 193 **2.6 Gene and protein expression analysis**

### 194 *2.6.1 Preparation of tissue extracts*

195 Cytosolic and nuclear extracts from livers were prepared as previously described [23]. Total protein  
196 from intestinal tissue was obtained by the AllPrep® DNA/RNA/protein Kit (Qiagen) and protein  
197 content was determined using the Bradford assay (BioRad, Hercules, CA, USA).

### 198 *2.6.2 Western blotting*

199 Equal amounts of proteins were separated by SDS-PAGE and electrotransferred to nitrocellulose  
200 membrane (GE-Healthcare Europe, Milano, Italy). Membranes were probed with mouse anti-CML  
201 (R&D Systems), rabbit anti-SCAP (Abcam), rabbit anti-SREBP1 (Abcam), rabbit anti-ACC (Cell  
202 Signaling Technology, Danver, MA, USA), mouse anti-FASN (Santa Cruz Biotechnology, Dallas,  
203 Texas, USA), rabbit anti-NLRP3 (Abcam), rabbit anti-caspase-1 (Abcam), mouse anti-IL-1 $\beta$  (Santa

204 Cruz Biotechnology), rabbit anti-TGF- $\beta$  (Abcam), rabbit anti-SMAD (Cell Signaling), rabbit anti-  
205 pSMAD (Cell Signaling), rabbit anti-fibronectin (Abcam), rabbit anti-vimentin (Cell Signaling), rat  
206 anti-ZO-1 (Santa Cruz), mouse anti-occludin (Santa Cruz), mouse anti-TLR-4 (Santa Cruz), mouse  
207 anti-MyD88 (Santa Cruz), and rabbit anti-IRAK1 (Santa Cruz) followed by incubation with  
208 appropriated HRP-conjugated secondary antibodies (Sigma).

209 Proteins were detected with Clarity Western ECL substrate (BioRad) and quantified by  
210 densitometry using analytic software (Quantity-One, Bio-Rad). Results were normalized with  
211 respect to densitometric value of mouse anti-GAPDH (Santa Cruz Biotechnology) for cytosolic and  
212 total proteins, and mouse anti-histone H3 (Abcam) for nuclear proteins.

### 213 *2.6.3 Real-time PCR (RT-PCR)*

214 Total RNA was isolated from ileum and liver tissue samples. Briefly, tissue samples were collected  
215 in Allprotect Tissue Reagent and stored at -80 °C. Total RNA was then obtained by the AllPrep®  
216 DNA/RNA/protein Kit and reverse transcribed into 20  $\mu$ L cDNA (complementary DNA) reaction  
217 volume, using the QuantiTect® Reverse Transcription Kit. Quantitative RT-PCR was performed for  
218 specific genes (GLUT-2, GLUT-5, occludin, and ZO-1) using the SsoFast™ EvaGreen. The  
219 transcript of the reference gene ribosomal 18s RNA (RNR18) was used to normalize mRNA data,  
220 and real-time PCR was performed by a MiniOpticon™ Real Time PCR system (Bio-Rad). The PCR  
221 protocol conditions were as follows: HotStarTaq DNA polymerase activation step at +95 °C for 30  
222 sec, followed by 40 cycles at +95 °C for 5 seconds and +55 °C for 10 sec. All runs were performed  
223 with at least three independent cDNA preparations per sample and all samples were run in  
224 duplicate. At least two non-template controls were included in all PCR runs. The quantification data  
225 analyses were performed using the Bio-Rad CFX Manager Software version 3.0 (Bio-Rad)  
226 according to the manufacturer's instructions.

227

## 228 **2.7 Microbiota analysis**

### 229 *2.7.1 Samples preparation and DNA extraction.*

230 To reduce the inter-sample variability a pool of the faecalileum content samples from each dietary  
231 intervention was obtained (three samples pools). The faecal samples pool (100 mg) were  
232 homogenized and washed twice in 500  $\mu$ L of PBS (Phosphate-Buffered Saline, pH 7.4) and DNA  
233 extraction was carried out by using MasterPure Complete DNA & RNA Purification kit (Illumina,  
234 San Diego, California). RNA was removed by a treatment with RNase (Ambion, Foster City,  
235 California) for 45 min at 37 °C. The Qubit and the Qubit DNA Assay kit (Life Technologies,  
236 Carlsbad, California) were used for quantification.

### 237 *2.7.2 16S rRNA phylogenetic profiling and shotgun sequencing of microbial genes*

238 The microbial diversity was studied by high throughput amplicon target sequencing of the amplified  
239 V3–V4 region of the 16S rRNA as reported elsewhere (Klindworth et al., 2013). The PCR products  
240 were purified by means of an Agencourt AMPure kit (Beckman Coulter, Milan, Italy), and the  
241 resulting products were tagged by using the Nextera XT Index Kit (Illumina). Sequencing was  
242 performed with a MiSeq Illumina instrument with v3 chemistry and generated 250 bp paired-end  
243 reads. The software used for the base-calling and Illumina barcode demultiplexing processes, were  
244 the MiSeq Control Soft. V2.3.0.3, the RTA v1.18.42.0 and the CASAVA v1.8.2.

245 DNA directly extracted from faecal samples was then subject to shotgun sequencing. Shotgun  
246 libraries were fragmented and tagged with sequencing adapters by using the TruSeqDNA library  
247 preparation kit (Illumina). Shotgun sequencing was performed with a NextSeq 500 platform  
248 (Illumina) according to the manufacturer's instructions, by G4L company (Salerno, Italy) and  
249 generated 100 bp paired-end reads.

### 250 *2.7.3 Bioinformatics and data analysis*

251 16S rRNA amplicon reads were analyzed by using QIIME 1.9.0 software (Caporaso et al., 2010).  
252 OTUs defined by a 97% of similarity were picked using the uclust pipeline and the representative  
253 sequences were submitted to the RDP-II classifier to obtain the taxonomy assignment and the  
254 relative abundance of each OTU using the Greengenes 16S rRNA gene database. The whole  
255 metagenome data analysis was carried out as follows: raw reads quality (Phred scores) was

256 evaluated by using the FastQC toolkit (<http://www.bioinformatics.babraham.ac.uk/projects/fastqc/>).  
257 The raw sequences were trimmed to Qscore of 20 with the SolexaQA++ software (Cox et al., 2010).  
258 Duplicate sequences and sequences less than 50 bp were discarded by using Prinseq (Schmieder and  
259 Edwards, 2011). The obtained trimmed reads were then mapped to the draft genome of *Mus*  
260 *musculus* ([ftp://ftp.ncbi.nlm.nih.gov/genomes/Mus\\_musculus/Assembled\\_chromosomes](ftp://ftp.ncbi.nlm.nih.gov/genomes/Mus_musculus/Assembled_chromosomes)) by using  
261 Bowtie2 (Langmead and Salzberg, 2012) in end-to-end, sensitive mode. Clean reads were aligned  
262 against the Kyoto Encyclopedia of Genes and Genomes (KEGG) database version April 2011 by  
263 using Bowtie2 software in end-to-end, sensitive mode. The number of reads uniquely mapped to  
264 each gene in the KEGG database was extracted by using SAMtools and normalized to total read  
265 mapped to the whole catalogue.

266 The metabolic reconstruction of the mice faecal microbiota was performed as follow: clean non host  
267 reads were then assembled with SPAdes v3.10.0 [24] and comparison of assemblers was performed  
268 by using QUAST v4.1 [25]. Each contig was run through an automated gene annotation pipeline  
269 utilizing MetaGeneMark. The predicted genes were then aligned against the NCBI-NR database by  
270 using blastx in order to obtain the gene annotation. The number of reads mapped to each gene were  
271 then used for the metabolic pathways reconstruction based on the Kyoto Encyclopedia of Genes and  
272 Genomes (KEGG) version April 2011 and visualized by using MEGAN software v5.

273 The functional gene count table was internally normalized in MEGAN by checking the “use  
274 normalized count” option. Rarefaction analysis was performed based on the leaves of the tree in  
275 MEGAN.

#### 276 *2.7.4 Sequences accession numbers.*

277 The 16S rRNA and the metagenome sequences are available at the Sequence Read Archive (SRA)  
278 of the National Center for Biotechnology Information (NCBI) under accession numbers SRP100599  
279 and SRP100623, respectively.

280

## 281 **2.8 Faecal volatilome profiling**

282 *2.8.1 Volatiles sampling by Head Space Solid-Phase Micro Extraction (HS-SPME): devices and*  
283 *conditions*

284 HS-SPME analysis were carried out on a GC×GC system coupled with a time of flight mass  
285 spectrometer (TOF-MS) operating in tandem ionization mode. SPME fibers,  
286 Divinylbenzene/Carboxen/ Polydimethylsiloxane (DVB/CAR/PDMS)  $d_f$  50/30  $\mu$ m - 2 cm were  
287 from Supelco (Bellefonte, PA, USA). Fibers were conditioned before use as recommended by the  
288 manufacturer. The standard-in-fiber procedure was adopted to pre-load the ISTD ( $\alpha$ -thujone) onto  
289 the fiber before sampling. 5.0  $\mu$ L of ISTD solution (100 ppm) were placed into a 2 mL glass vial  
290 and submitted to HS-SPME at 70°C for 10 min. Faecal samples were exactly weighted (10 mg) in  
291 glass vials (2.0 mL) and submitted to manual HS-SPME sampling. After ISTD loading step, the  
292 SPME device was exposed to the sample headspace for 30 min at 70°C. Extracted analytes were  
293 recovered by thermal desorption of the fiber into the S/SL injection port of the GC×GC system at  
294 250°C for 5 min. Each sample was analyzed in triplicate.

295 *2.8.2 GC×GC-TOF-MS instrument set-up and analytical conditions*

296 GC×GC analyses were performed on an Agilent 6890 GC unit coupled with a Markes BenchTOF-  
297 Select and Select-eV<sup>®</sup> option (Markes International Ltd, Llantrisant UK) operating in the EI mode  
298 at 70 and 12 eV. The transfer line was set at 250°C. TOF scan interval was set at  $m/z$  35-350 with  
299 50 Hz of sampling frequency for each ionization channel. The system was equipped with a two-  
300 stage KT 2004 loop thermal modulator (Zoex Corporation, Houston, TX) cooled with liquid  
301 nitrogen and controlled by Optimode™ V.2 (SRA Instruments, Cernusco sul Naviglio, MI, Italy).  
302 Hot jet pulse time was set at 250 ms, modulation time was 4s and cold-jet total flow progressively  
303 reduced with a linear function from 40% of Mass Flow Controller (MFC) at initial conditions to 8%  
304 at the end of the run. A deactivated fused silica capillary loop (1 m × 0.1 mm  $d_e$ ) was used. The  
305 column set was configured as follows: 1D SolGel-Wax column (100% polyethylene glycol) (30 m ×  
306 0.25 mm  $d_e$ , 0.25  $\mu$ m  $d_f$ ) from SGE Analytical Science (Ringwood, Australia) coupled with a 2D

307 OV1701 column (86% polydimethylsiloxane, 7% phenyl, 7% cyanopropyl) (1 m × 0.1 mm dc, 0.10  
308 μm df), from J&W (Agilent, Little Falls, DE, USA).

309 SPME thermal desorption into the GC injector port was under the following conditions:  
310 split/splitless injector in split mode, split ratio 1:20. Carrier gas was helium at a constant flow of 1.2  
311 mL/min. The oven temperature program was: from 40°C (1 min) to 200°C at 3°C/min and to 250°C  
312 at 10°C/min (5 min). The *n*-alkanes liquid sample solution for Linear Retention Indices  
313 determination ( $I^T_S$ ) was analyzed under the following conditions: split/splitless injector in split  
314 mode, split ratio 1:50, injector temperature 250°C, injection volume 1 μL.

### 315 *2.8.3 Data acquisition and data elaboration*

316 Data were acquired by Markes TOF-DS software (Markes International Ltd, Llantrisant UK) and  
317 processed by GC Image® GC×GC Edition Software, Release 2.6 (GC Image, LLC Lincoln NE,  
318 USA). Statistical analysis was performed with XLstat (Addinsoft, New York, NY USA). Targeted  
319 analysis focused on 59 compounds identified by matching their EI-MS fragmentation pattern (NIST  
320 MS Search algorithm, ver 2.2, National Institute of Standards and Technology, Gaithersburg, MD,  
321 USA, with Direct Matching threshold 900 and Reverse Matching threshold 950) with those  
322 collected in commercial (NIST2014 and Wiley 7n) and in-house databases. As a further parameter  
323 to support identification,  $I^T_S$  were considered and experimental values compared to the tabulated  
324 ones. The list of identified analytes, retention times in the two chromatographic dimensions,  
325 experimental and tabulated  $I^T_S$ , average Normalized 2D Volume and relative standard deviation (3  
326 analytical replicates)  
327 is provided as supplementary material (Supplementary Table 2S and Supplementary Figure S2)  
328 together with contour plots of volatile fractions from L-Fr, S-Fr and SD diet faecal samples.

329

## 330 **2.9 Statistical analysis**

331 The Shapiro-Wilk test was used to assess the normality of the variable distributions. One-way  
332 ANOVA followed by Bonferroni's post-hoc test was adopted for comparison among the four

333 groups of animals. Data were expressed as mean  $\pm$  standard deviation. Threshold for statistical  
334 significance was set to  $P < 0.05$ . Statistical tests were performed with GraphPad Prism 6.0 software  
335 package (GraphPad Software, San Diego, CA, USA).

336

## 337 **2.10 Materials**

338 All compounds were purchased from Sigma Chemical Co. (St. Louis, MO, USA), unless otherwise  
339 stated.

340



341 **3. Results.**

342 **3.1 General parameters.**

343 After twelve weeks of dietary intervention, the mice exposed to liquid fructose drink (L-Fr) and the  
344 mice fed with the solid fructose diet (S-Fr) showed a significant increase in plasma fasting glucose  
345 and insulin levels, while a slight increase in liver weight was recorded in the L-Fr group, when  
346 compared to the control group (Tab. 1). However, these effects were not associated with significant  
347 changes in body weight gain and serum TG levels.

348 As reported in Table 2, the L-Fr group markedly reduced solid food intake to compensate the  
349 calories introduced with the fructose syrup. Thus, the total calories intake was not different among  
350 groups. Similarly, no statistically significant differences were recorded in terms of daily intake of  
351 fructose among groups.

352

353 **3.2 Fructose-induced translocation of GLUT-2 and fructose urinary excretion.**

354 In intestine of mice exposed to S-Fr or L-Fr no differences in both mRNA expression or localization  
355 of the fructose specific transporter GLUT-5 were detected (Fig. 1A), while a stronger expression of  
356 the glucose/fructose transporter GLUT-2 in the apical membrane was observed, when compared to  
357 intestine from SD mice, with maximal effect in the S-Fr group (Fig. 1B). Also in the liver, the  
358 GLUT-2 was expressed at the level of the plasma membrane according to an active uptake of sugars  
359 by the hepatocytes, with no apparent differences between the two fructose groups (Fig. 1C).

360 Interestingly, the fructose-induced increase in intestinal GLUT-2 apical expression was associated  
361 with higher levels of urinary excretion of fructose, but not glucose, detected in both groups of  
362 fructose mice when compared to SD, thus confirming that fructose was efficiently absorbed by  
363 intestine. However, the urinary concentration of fructose was higher in the L-Fr group than in the S-  
364 Fr, indicating that fructose was more rapidly transferred by enterocytes to the plasma through  
365 basolateral transport in the liquid form (Tab. 1).

366

367 **3.3 Liquid and solid formulations of fructose differently altered microbial community profile.**

368 Concerning gut microbiota, we performed amplicon based sequencing of the 16S rRNA and  
369 shotgun metagenomic sequencing on faecal ileum content of SD and fructose-exposed mice to  
370 examine in depth the effects of the two different forms of fructose on intestinal microbiota  
371 composition and function. A total of 56.023 raw reads (2x250bp) were obtained after sequencing.  
372 After joint, a total of 54.050 reads passed the filters applied through QIIME, with an average value  
373 of 18.674 reads/sample, and a sequence length of 456 bp. The rarefaction analysis and the estimated  
374 sample coverage indicated that there was a satisfactory coverage for all the samples (ESC average  
375 99%). Moreover, alpha-diversity also showed that there was a higher level of complexity in S-Fr,  
376 when compared to L-Fr. Accordingly, the  $\beta$ -diversity through weighted UniFrac distance matrices  
377 indicated a clear separation between the diets ( $P < 0.01$ ).

378 Regarding the main operational taxonomic units (OTUs), defined at the genus or phylum level,  
379 filtered for OTUs presence  $> 0.2\%$  (Fig. 2), a remarkable individual variability of abundance was  
380 observed. S-Fr sample showed higher abundance of *Clostridium* (18% of the relative abundance),  
381 *Oscillospira* (6.2%) and *Clostridiales* phylum (32%). Mice fed with L-Fr displayed the highest  
382 abundance of *Bacteroides* (12%), *Lactobacillus* (44.8), *Lachnospiraceae* (7.25%), and *Dorea*  
383 (0.37%). Control samples were characterized by the presence of *Allobaculum* (21% of the relative  
384 abundance), *Gemella* (4%) and *Parabacteroides* (6%) (Fig. 2).

385 Regarding the minor OTUs fraction ( $< 2\%$ ), *L-Ruminococcus*, *Coprococcus* and *R-Ruminococcus*  
386 were higher in mice fed with fructose compared to standard diet. In detail, the shift in the OTUs  
387 composition resulted in an overall decrease in the Firmicutes/Bacteroidetes ratio in mice fed with  
388 fructose and the L-Fr diet showed the lowest ratio value.

389

390 **3.4 Metagenomic data: comparative analysis between solid and liquid formulations of fructose**

391 Raw reads of 29.62 Mbp were generated, which yielded 4.93 Mbp/sample. After quality trimming  
392 and host sequence removal, 1.75 Mbp of clean reads were analyzed and an average of 2.333.932

393 reads/sample were obtained. Faecal samples displayed high proportions of reads of host origin due  
394 to the higher abundance of mammalian cell and the low microbial biomass. A *de novo* assembly  
395 generated 439 contigs of more than 1000 bp in length, with an average N50 of 758 bp. To obtain the  
396 metabolic reconstruction of the mice faecal microbiota, we classified the predicted genes by  
397 aligning them to the integrated NCBI-NR database of non-redundant protein sequences. The  
398 predicted genes identified were 20,972, 40% of which were assigned to KEGG pathways by  
399 MEGAN. Rarefaction curves obtained through MEGAN were used to determine genes abundance  
400 richness, revealing that metagenomic diversity was well represented (data not shown), although  
401 mice fed with SD showed a lower diversity in genes abundance compared to fructose added diets.  
402 By performing the functional characterization and gene classification of the shotgun sequence reads  
403 against the KEGG database and the MetaHIT gene catalogue, we detected 2,629 KEGG orthologue  
404 (KO) genes and the relative abundance of each KO term was calculated based on the total read of  
405 the included catalogued reference genes, normalized to total read mapped to the whole catalogue.  
406 The L2 KEGG categories aminoacid metabolism was found most abundant in L-Fr samples. On the  
407 other hand S-Fr showed high abundance of genes related to carbohydrate and energy metabolism, in  
408 particular genes belonging to aminosugar, fructose and galactose metabolism (Fig. 3). However,  
409 genes related to glycolysis, tricarboxylic acids (TCA) and pyruvate metabolism were clearly  
410 associated with L-Fr diet.

411 The metabolic reconstruction of the faecal metagenomes displayed the complete biosynthetic  
412 pathways for leucine, isoleucine and valine, and data indicated that the main routes for the synthesis  
413 of those branched chain aminoacids (BCAAs) were from pyruvate pathways. Going more in depth  
414 into the metagenome content key enzymes responsible for the biosynthesis of BCAAs were found  
415 most abundant in L-Fr diet compared to the other diets: BCAA aminotransferase [EC:2.6.1.42] can  
416 lead to the interconversion between 4-Methyl-2-oxopentanoate to leucine and valine and it can  
417 drive the formation of isoleucine from 3-Methyl-2-oxopentanoate (Suppl Figure 1S; Suppl Table  
418 1S).

419 Regarding the *ex-novo* biosynthesis of fatty acid (SCFA and MCFA) mice fed with fructose showed  
420 the highest counts of key genes for the production of butanoate from acetyl-CoA route (butyrate  
421 kinase [EC:2.7.2.7]), propanoate from TCA route (acetate kinase [EC:2.7.2.1]) and MCFA  
422 (medium-chain acyl-hydrolase [EC:3.1.2.21]) (Suppl Figure 1S; Suppl Table 1S). In particular  
423 butyrate kinase was found most abundant in S-Fr diet and boosted the production of 1-butanol as  
424 confirmed by GC×GC-TOF-MS data. In addition, many genes related to peptidoglycan biosynthesis  
425 (ko00550) via aminosugar metabolism route were predominantly associated with fructose diet and  
426 in particular with L-Fr.

427

### 428 **3.5 Solid and liquid formulations of fructose evoke different changes in faecal volatilome** 429 **fingerprints.**

430 Faecal volatilome is influenced by several factors including the gut microbiota composition thereby  
431 its fingerprint is suggestive of metabolic changes induced and/or caused by microbial activity. The  
432 faecal volatiles here detected by GC×GC-TOF-MS are listed in the Table S4 and include:  
433 hydrocarbons, alcohols (short-chain and long-chain alcohols derived from acids reduction),  
434 carbonyl derivatives (aldehydes and ketones) short-chain fatty acids (acetic, propionic, butyric  
435 above all), branched-chain fatty acids, aromatic compounds (including heterocycles) and  
436 monoterpenoids.

437 The relative distribution of faecal volatiles between samples proved to be informative as illustrated  
438 by the heat map of Fig. 4 where clustering is clear between diet regimens (SD vs. fructose enriched  
439 diets) and for compound classes that result up- or down- regulated (blue or red spots). Above all,  
440 butyric and propanoic acid esters (butyl butanoate, 2-methylbutyl propanoate, 1-butanol-3-methyl  
441 propanoate) were up-regulated in fructose enriched diets (blue spots in the heat-map for L-Fr and S-  
442 Fr samples) while free SCFAs (acetic, propanoic and butanoic acids) were more abundant in the SD  
443 mice.

444 Analytes with a relative standard deviation higher than the analytical repeatability were submitted  
445 to pairwise t-test ( $\alpha=0.05$ ) and those with a higher informative role (marked with a star) are shown  
446 in Fig. 5 where faecal volatilome signatures of L-Fr and S-Fr diets were compared to the SD diet.  
447 Positive coefficient of variations (CV%) indicate analytes up-regulation in fructose enriched diets  
448 while negative values relate to those analyte that were more abundant in mice fed by SD diet. Red  
449 bars correspond to analytes just revealed in specific populations. Interestingly, fructose intake up-  
450 regulated the release of SCFAs esters; in particular S-Fr induced a higher production of butyl  
451 acetate and 2-methylbutyl propanoate while L-Fr concurred also to increase butyl butanoate. On the  
452 other hand, SD mice faecal signatures were connoted by higher amounts of linear and branched  
453 chain alcohols (2-propyl heptanol, hepten-3-ol, hexanol, heptanol and octanol); several carbonyl  
454 derivatives (linear saturated aldehydes - hexanal, heptanal, octanal, nonanal - and ketones -2,3-  
455 pentanedione and 2-pentanone the latter detected only in SD samples). Meaningful differences in  
456 volatiles signatures (analytes marked with the asterisk  $P<0.05$ ) suggest different microbial  
457 metabolism induced by diets.

458

### 459 **3.6 Liquid fructose evoked the highest levels of lipid synthesis/accumulation in the liver and** 460 **accelerated liver fibrosis.**

461 In order to evaluate the metabolism of fructose in the liver, we analyzed the activation of the  
462 lipogenesis regulated by the Sterol Regulatory Element Binding Protein (SREBP) 1c and the  
463 SREBP Cleavage Activating Protein (SCAP) signaling pathway. In the liver of both L-Fr and S-Fr  
464 mice, SCAP was upregulated, reaching statistical significance only in L-Fr group (Fig. 6A).  
465 Accordingly, the hepatic levels of the nuclear active form of the transcription factor SREBP1c were  
466 significantly increased only in the liver of the L-Fr group. In the liver of S-Fr mice, the cytosolic  
467 inactive form of SREBP1c was prevalent with respect to the nuclear form, indicating a limited  
468 nuclear translocation and, thus, activation of the lipogenic pathway when compared to L-Fr mice  
469 liver (Fig. 6B). In keeping with the increased SREBP1c activation, a significant up-regulation of its

470 main target genes, acetyl Coenzyme A carboxylase (ACC) and fatty acid synthase (FAS), was  
471 recorded in L-Fr mice compared to both SD and S-Fr diet mice (Fig. 6C).

472 As consequence of increased *ex novo* lipid synthesis, L-Fr mice showed a significantly higher TG  
473 liver deposition with respect to both SD and S-Fr mice (Table 1). Consistently, Oil Red O staining  
474 of liver slices revealed a marked steatosis in both groups of mice exposed to fructose, compared to  
475 SD, with widely diffused microvescicular steatosis in L-Fr mice, and more focal steatosis associated  
476 to ballooning and immune cells infiltration in S-Fr mice (Fig. 6D).

477 When we evaluated the degree of fibrosis through the expression analysis of early specific markers,  
478 we found that transforming growth factor (TGF)- $\beta$ , an inducer of fibrogenesis (Fig. 7A), small  
479 mother against decapentaplegic (SMAD), a mediator of TGF- $\beta$  intracellular signaling (Fig. 7B),  
480 fibronectin and vimentin, fibrillary components of extracellular matrix (Fig. 7C) were markedly  
481 upregulated in L-Fr, compared to SD mice, while only SMAD and fibronectin were significantly  
482 increased also in the S-Fr group (Fig. 7A-C). **Finally, NAS score on liver H&E stained sections**  
483 **indicated that both groups of mice fed the high fructose developed a relevant grade of steatosis,**  
484 **whereas the S-Fr group only presented a significant grade of inflammation and ballooning,**  
485 **compared to SD mice. Macroscopic signs of fibrosis have been observed only in few liver samples**  
486 **from the S-Fr group, indicative of a preliminary stage of fibrosis. In addition, the HIAD score**  
487 **indicated the presence of hepatocytes cytolysis induced by the fructose feeding, and confirmed the**  
488 **highest degree of inflammation in the liver of the S-Fr group (Fig. 7D).**

489

### 490 **3.7 Solid fructose induced the highest AGEs accumulation in the mouse gut**

491 Fructose-administered mice showed an increased accumulation of the major AGEs, N(epsilon)-  
492 (carboxymethyl)lysine (CML) and N(epsilon)-(carboxyethyl)lysine (CEL), in intestinal mucosa  
493 revealed by immunofluorescence. In particular, a higher accumulation of CML and CEL was  
494 detected in the villus axis and basal membranes of S-Fr mice than L-Fr groups. As consequence of  
495 AGEs accumulation, we observed an induction of AGE-receptor (RAGE) expression in the crypts

496 in correspondance to lymph nodes in fructose-fed mice, as shown by immunofluorescence analysis  
497 (Fig. 8A) and related quantification (Fig. 8B). These findings were confirmed by western blotting  
498 analysis, showing a significantly increased expression of CML-glycated proteins in the gut S-Fr  
499 mice (Fig. 5C)

500

### 501 **3.8 Solid fructose impaired gut integrity leading to increased hepatic NLRP3 inflammasome** 502 **activation.**

503 In order to evaluate whether the increased protein glycation and expression of RAGE were related  
504 to intestinal mucosa damage and inflammation, we tested the impact of different fructose  
505 formulations on key components of the tight junctions (TJ) expressed in the ileum, as well as on the  
506 portal and systemic plasma levels of LPS, a marker of loss of intestinal integrity and systemic  
507 diffusion of pro-inflammatory microbial components. Our results clearly showed that mRNA  
508 expression of the epithelial TJ markers occludin and zona occludens (ZO)-1, in the ileum regions  
509 was moderately decreased in the mice under L-Fr feedings and markedly suppressed in the mice  
510 under S-Fr feeding (Fig. 9A and 9B). **The reduced mRNA expression of ZO-1 and occluding in S-**  
511 **Fr mice was confirmed when proteins were measured by Western blot analysis (Fig. 9C and 9D).**  
512 Since TJ maintain enteral epithelial barrier, their robust defect in S-Fr mice is suggestive of gut  
513 impairment and it correlates well with the massive increase in both portal plasma and systemic  
514 levels of LPS recorded in S-Fr compared to SD. In contrast, only a slight but not significant  
515 increase in LPS concentration was detected in L-Fr (Fig. 9E and 9F). **The massive increase in LPS**  
516 **concentration in S-Fr was paralleled by a significant increase of the intestinal alkaline phosphatase**  
517 **(IAP), a brush-border protein involved in the LPS detoxifying cascade (Fig. 9G).** However, no  
518 significant alterations of mucosa morphology in mice exposed to fructose were detectable by light  
519 microscopy (Fig. S3), thus indicating an early stage of impairment of the integrity of the ileal  
520 mucosal lining.

521 We then evaluated the distal (hepatic) activation of one of the best-characterized LPS-dependent  
522 inflammatory pathway, the NLRP3 inflammasome. One of the main receptor mediating LPS-  
523 induced NLRP3 activation is the TLR-4. In the liver of the fructose-fed mice we detected increased  
524 protein levels of TLR-4, reaching highest upregulation in the S-Fr group. The involvement of  
525 TLR4 receptor was confirmed by the robust overexpression of the adapter protein myeloid  
526 differentiation response gene (MyD) 88, that cluster within TLR4 to recruit IL-1 receptor-associated  
527 kinase (IRAK) 1, whose expression was massively increased in the liver of S-Fr mice (Fig. 10A-C).  
528 Consistently, the main component of the inflammasome platform, the NLRP3 protein, was  
529 upregulated in the liver of high fructose fed mice compared to SD, reaching highest levels in S-Fr  
530 group (Fig. 10D). Also the NLRP3 downstream signaling, namely the rate of caspase-1 activation,  
531 was significantly higher in the S-Fr (Fig. 10E) than in the L-Fr mice livers. Accordingly, expression  
532 of the active IL-1 $\beta$  protein was markedly upregulated only in the S-Fr mice liver (Fig. 10F).



#### 533 4. Discussion

534 Several experimental studies have already demonstrated that diet composition plays an important  
535 role in the development of metabolic derangements [26, 27]. Besides, an increasing body of  
536 literature highlights a tight relationship between nutrients and modifications of the intestinal barrier  
537 and microbiota that can potentially interfere with systemic metabolism and health [28, 29]. Here we  
538 confirmed and further extended previous findings on the detrimental effects associated to chronic  
539 exposure to high fructose intake, leading to hyperglycemia and liver toxicity. Most notably, we  
540 performed a comparative study on the toxicological impact of different formulations (liquid versus  
541 solid forms) of the same dietary component. This is an important and topical issue, unfortunately  
542 largely unexplored. In fact, sugar sweetened beverages are thought to contribute to weight gain  
543 because beverages appear to suppress appetite and energy intake less than solid foods [30].  
544 However, most recent findings show that some high-energy snack foods may deliver the same level  
545 of satiation as a sugar-containing beverage [31], thus suggesting that the identification of the range  
546 of effects evoked by either liquid or solid foods is still controversial. **In our experimental model,**  
547 **liquid fructose intake was associated with reduced solid food consumption, resulting in no**  
548 **significant difference in the total caloric intake between the two fructose dietary manipulations.**  
549 **Thus, differences here recorded between the two fructose groups were due to formulations only not**  
550 **being affected by impairments in net energy stores and/or amount of fructose intake. Despite we did**  
551 **not highlight any behavioral and physical alterations among the groups, we cannot rule out that a**  
552 **decrease in solid food intake might affect outcomes by under nourishing of animals with essential**  
553 **micronutrients.**

554 Interestingly, here we demonstrated, for the first time, that the fructose formulation affects its  
555 absorption by the small intestine, leading to different outcomes in liver metabolism. After ingestion,  
556 fructose is absorbed in the small intestine by the apical membrane of enterocytes through the  
557 GLUT-5 facilitative transporter, and is then transferred to the blood by the GLUT-2 transporter  
558 located in the basolateral membrane [32]. High concentrations of fructose in the intestinal lumen

559 may stimulate the translocation of GLUT-2 to the apical membrane where it becomes the main  
560 sugar transporter [33-35]. Although this hypothesis is still debated [36, 37], the results here reported  
561 confirm an increased expression of GLUT-2 in the apical membranes of enterocytes, without  
562 modifying GLUT-5 expression and distribution. Interestingly, gut of mice chronically exposed to  
563 solid fructose showed a higher expression of GLUT-2 in the apical membrane when compared to  
564 gut from mice treated with liquid fructose, thus suggesting a higher fructose accumulation in the  
565 enterocytes and lower rate of blood transfer. This hypothesis is confirmed by a dramatically lower  
566 excretion of fructose in urine of solid fructose fed mice in comparison to liquid fructose fed mice.  
567 We may, thus, speculate that the liquid fructose is more rapidly absorbed in the plasma and, thus,  
568 rapidly metabolized by the liver, being the excess excreted with urine. In contrast, the solid fructose  
569 is likely to be more slowly transferred to the plasma because of the basolateral-to-apical membrane  
570 translocation of GLUT-2. Therefore, solid fructose may persist for longer time within the gut and,  
571 thus, be metabolized by enterocytes and potentially by microbiota of the large intestine when excess  
572 fructose migrates from the small intestine [38, 39]. The first evidence that fructose may affect the  
573 microbiota comes from a few recent studies in rats showing that orally administered fructose  
574 enhanced the abundance of *Enterobacteriaceae*, *Coprococcus*, and *Ruminococcus* and induced a  
575 distinct faecal metabolome profile that is associated with fructose-induced nonalcoholic fatty liver  
576 disease [40]. Here we reported, for the first time, differences in the metabolic adaptation of the  
577 intestinal microbiota to dietary fructose, with significant taxonomic differences between the two  
578 fructose formulations. Specifically, *Bacteroides*, whose increased presence has been associated to  
579 an increased risk of weight gain and insulin resistance [41], was massively detected in the liquid  
580 diet. Several studies on mouse gut microbiota obesity-related alterations reported robust changes in  
581 the Firmicutes to Bacteroidetes ratio [41, 42]. Here we found that this ratio was lowest in the  
582 intestinal microbiota of L-Fr mice. The analysis on samples from mice with SD diet was in  
583 agreement with previous data for rodents under standard diet regimens with Firmicutes much more  
584 abundant than Bacteroidetes, Proteobacteria and Tenericutes [43, 44]. On the contrary, we observed

585 an increase of *Coprococcus* and *Ruminococcus* genera and a decrease of Firmicutes and  
586 *Clostridium* genera in both the fructose experimental groups when compared to SD mice. In L-Fr  
587 mice we recorded the highest abundance of *Lactobacillus*, which could be a consequence of the  
588 increased availability of simple sugars in the intestine of these mice [45]. Our results are in  
589 agreement with the changes in the relative abundance of these taxa observed in type 2 diabetes  
590 patients when compared to healthy individuals [46].

591 Both fructose diets enriched the presence of few anaerobes like *Coprococcus* and *Ruminococcus*. It  
592 was recently shown that *Ruminococcus* produces propionate from fructose, whereas *Coprococcus*  
593 produces butyrate from fructose [47]. Interestingly, the faecal volatilome signatures confirmed the  
594 highest levels of both propionate and butyrate derivatives in mice exposed to fructose.

595 Metagenomic analysis confirmed that fructose-enriched diets could lead to *ex novo* lipogenesis with  
596 the production of SCFA and MCFA, and faecal volatilome referred higher amounts of SCFA esters  
597 when compared to SD mice (butyl acetate increase by 50% in S-Fr mice; 2-methylbutyl propanoate  
598 by 15% in S-Fr mice and butyl butanoate with by 21 and 7% in S-Fr and L-Fr mice respectively).  
599 The increased systemic bioavailability of liquid fructose and SCFA esters may account for the  
600 markedly higher activation of the lipogenic pathway in the liver of the L-Fr mice, compared to S-Fr  
601 mice. The activation of the SCAP/SREBP1c signaling pathway regulates the transcription of the  
602 enzymes involved in the *ex novo* synthesis of fatty acids and the subsequent intracellular lipid  
603 accumulation, which are peculiar aspects of fructose metabolism [13, 48]. Indeed, we found  
604 significantly higher TG levels and more diffuse hepatosteatosis in the L-Fr mice than in the S-Fr,  
605 associated to a stronger activation of early markers of the fibrogenic cascade, which has been  
606 previously demonstrated to be affected by SREBP1c activity [49-51]. **Although the histological  
607 examination and related scores confirmed the development of steatosis and focal lytic necrosis, no  
608 significant evidence of established fibrosis was documented, suggestive of a preliminary stage not  
609 yet progressed to full-blown liver scarring. These findings are in keeping with literature data  
610 reporting the appearance of macroscopic signs of fibrosis, such as collagen deposition and fibrotic**

611 septa generation, only after 16-20 weeks of high fructose intake [52]. In contrast, as previously  
612 documented, Ritze et al [16], briefer exposure time are sufficient to highlight differences in  
613 triglyceride accumulation and hepatosteatosis, confirming that that liquid sugars were more rapidly  
614 absorbed and gave greater induction of hepatic lipid accumulation compared to the solid  
615 counterparts. The lowest rate of fructose absorption when the sugar is derived from solid  
616 formulation is here suggested by the metabolic reconstruction of the mice faecal microbiota. This  
617 analysis showed that the highest increase in genes related in carbohydrate metabolism was recorded  
618 in the microbiota of mice exposed to S-Fr, suggestive of higher fructose accumulation in the gut of  
619 S-Fr than of L-Fr. In contrast, an increase in aminoacid metabolism genes was recorded in the  
620 microbiota of mice exposed to L-Fr. Besides, the most relevant impact of solid fructose on gut  
621 toxicity is confirmed by the investigation of local accumulation of fructose-derived AGEs. Fructose  
622 is a highly glycative compound [53, 54], and we have previously contributed to demonstrate that  
623 high dietary fructose intake can evoke stronger AGEs accumulation and RAGE activation than  
624 glucose [13]. Moreover, here we reported the highest levels of fructose-derived AGEs in intestinal  
625 villi of mice fed with solid formulation. AGEs ingested with highly processed foods or locally  
626 produced in the gut are slowly absorbed in the circulation and only partially excreted in urine, while  
627 they are accumulated and metabolized by enterocytes and are suggested to have distal effects on  
628 target organs [55]. Food-derived AGEs and glycated proteins can act in the intestine as substrate for  
629 colonic bacterial fermentation, driving alterations of microbiota composition and of intestinal  
630 barrier permeability [56, 57]. Accordingly, we showed here that the marked AGEs accumulation  
631 detected in gut of S-Fr mice was paralleled by a robust decrease in TJ mRNA and protein  
632 expression in the ileal mucosal lining and massive transfer of LPS in the portal vein plasma,  
633 suggestive of increased gut permeability to bacterial components [29, 58]. A higher LPS  
634 concentration was also recorded at systemic level in S-Fr mice when compared to LPS  
635 concentration measured in L-Fr mice. We also measured the IAP enzyme, which has been  
636 demonstrated to be the main LPS detoxifying system in the gut, likely thanks to its ability to induce

637 dephosphorylation of the lipid A moiety, the primary source of LPS endotoxic effects [59]. Several  
638 studies demonstrated that IAP expression and activity is altered as result of a complex interplay  
639 between dietary factors, the microbiota and the host [60]. Most notably, IAP activity has been  
640 shown to be enhanced by LPS injections [61]. Here we confirmed a parallelism between highest  
641 LPS plasma concentration and most intense ileal IAP activity in the S-Fr group. The increased IAP  
642 activity we documented was suggestive of a dysfunctional response of the intestinal detoxifying  
643 mechanisms, being insufficient to degrade the solid fructose-induced rise in LPS production, thus  
644 failing to prevent its transfer to the plasma. As very recently documented [62], the association of  
645 microbiota modifications with intestinal permeability leads to translocation of bacterial products  
646 that signal the liver through TLR4 (that recognizes LPS, a gram-negative bacteria wall component).  
647 TLR4 activation, throughout the MyD88 and IRAK-1-dependent signaling pathway, leads to  
648 secretion of mature IL1 $\beta$  by stimulating the NLRP3 inflammasome complex assembly [63]. The  
649 NLRP3 inflammasome is a pro-inflammatory complex, which senses LPS and several other stimuli  
650 related to pathogen and damage-associated molecular patterns in tissues undergoing infections, cell  
651 damage or metabolic imbalances [64]. The formation of the NLRP3 inflammasome complex leads  
652 to the activation of caspase-1, which in turn proteolytically cleaves the precursors of pro-  
653 inflammatory cytokines IL-1 $\beta$ . Very recently, we demonstrated that both LPS and microvesicles  
654 released by cells undergoing lipotoxicity may actively contribute to pro-inflammatory responses  
655 within the liver by activating in a paracrine way the multimeric protein complex NLRP3  
656 inflammasome in either hepatocytes and macrophages [65]. In this pathological context, the NLRP3  
657 inflammasome may act as key cross-talk mechanism between injured hepatocytes and macrophages.  
658 We have previously contributed to demonstrate that hepatic NLRP3 inflammasome overactivation  
659 results in a sustained release of IL-1 $\beta$ , an event supporting the lobular inflammation in diet-related  
660 metabolic diseases [66]. Here, correlations among highest LPS concentration, most intense  
661 activation of the TLR4/MyD88/IRAK1 cascade and strongest NLRP3 inflammasome  
662 expression/activity in the liver of S-Fr mice was demonstrated.

663 According to the microbiota analysis here reported and in keeping with previously published data  
664 [67, 68], we may speculate that the increased LPS translocation as well as systemic alterations of  
665 lipid metabolism and inflammatory response, are due, at least in part, to nutrient-induced  
666 modifications of the gut microbiota composition.

667 In conclusion, our results convincingly show that consumption of different fructose formulations,  
668 liquid or solid, evokes different impact on gut microbiota and integrity, thus differently affecting  
669 liver homeostasis. Our results suggest that the liquid fructose formulation is more rapidly absorbed  
670 by intestine and metabolized by the liver, leading to lipogenesis. In contrast, the solid fructose  
671 formulation is slowly absorbed by enterocytes leading to AGEs accumulation and affecting gut  
672 barrier integrity, with the following hepatic activation of the LPS-dependent TLR4/NLRP3  
673 inflammasome cascade. Overall, the combined results of the microbiota analysis, faecal volatilome  
674 profiling and molecular insights bring to the fore an original and multidisciplinary approach to  
675 determine slight, not easily detectable, differences in the toxicological impact of different dietary  
676 manipulations, including changes in nutrients formulations.

677

678

679

#### 680 **Acknowledgments.**

681 This work was supported and funded by the University of Turin (Ricerca Locale 2016 and 2017),  
682 Regione Toscana (Bando Nutraceutica 2014), Project TAGIDISFRU, ERA-HDHL-ERANET  
683 Biomarkers for Nutrition and Health Implementing the JPG HDHL objectives” - Project  
684 “SALIVAGES”.

685

686

- 688 1. Marriott BP, Cole N, Lee E: **National estimates of dietary fructose intake increased from 1977 to**  
689 **2004 in the United States.** *J Nutr* 2009, **139**:1228s-1235s.
- 690 2. Malik VS, Hu FB: **Fructose and Cardiometabolic Health: What the Evidence From Sugar-Sweetened**  
691 **Beverages Tells Us.** *J Am Coll Cardiol* 2015, **66**:1615-1624.
- 692 3. Rizkalla SW: **Health implications of fructose consumption: A review of recent data.** *Nutr Metab*  
693 *(Lond)* 2010, **7**:82.
- 694 4. Lim JS, Mietus-Snyder M, Valente A, Schwarz JM, Lustig RH: **The role of fructose in the**  
695 **pathogenesis of NAFLD and the metabolic syndrome.** *Nat Rev Gastroenterol Hepatol* 2010, **7**:251-  
696 264.
- 697 5. Teff KL, Grudziak J, Townsend RR, Dunn TN, Grant RW, Adams SH, Keim NL, Cummings BP,  
698 Stanhope KL, Havel PJ: **Endocrine and metabolic effects of consuming fructose- and glucose-**  
699 **sweetened beverages with meals in obese men and women: influence of insulin resistance on**  
700 **plasma triglyceride responses.** *J Clin Endocrinol Metab* 2009, **94**:1562-1569.
- 701 6. Stanhope KL, Schwarz JM, Keim NL, Griffen SC, Bremer AA, Graham JL, Hatcher B, Cox CL,  
702 Dyachenko A, Zhang W, et al: **Consuming fructose-sweetened, not glucose-sweetened, beverages**  
703 **increases visceral adiposity and lipids and decreases insulin sensitivity in overweight/obese**  
704 **humans.** *J Clin Invest* 2009, **119**:1322-1334.
- 705 7. Le KA, Ith M, Kreis R, Faeh D, Bortolotti M, Tran C, Boesch C, Tappy L: **Fructose overconsumption**  
706 **causes dyslipidemia and ectopic lipid deposition in healthy subjects with and without a family**  
707 **history of type 2 diabetes.** *Am J Clin Nutr* 2009, **89**:1760-1765.
- 708 8. Schwarz JM, Noworolski SM, Wen MJ, Dyachenko A, Prior JL, Weinberg ME, Herraiz LA, Tai VW,  
709 Bergeron N, Bersot TP, et al: **Effect of a High-Fructose Weight-Maintaining Diet on Lipogenesis and**  
710 **Liver Fat.** *J Clin Endocrinol Metab* 2015, **100**:2434-2442.
- 711 9. Schultz A, Neil D, Aguila MB, Mandarim-de-Lacerda CA: **Hepatic adverse effects of fructose**  
712 **consumption independent of overweight/obesity.** *Int J Mol Sci* 2013, **14**:21873-21886.
- 713 10. Manolescu AR, Witkowska K, Kinnaird A, Cessford T, Cheeseman C: **Facilitated hexose transporters:**  
714 **new perspectives on form and function.** *Physiology (Bethesda)* 2007, **22**:234-240.
- 715 11. Schalkwijk CG, Stehouwer CD, van Hinsbergh VW: **Fructose-mediated non-enzymatic glycation:**  
716 **sweet coupling or bad modification.** *Diabetes Metab Res Rev* 2004, **20**:369-382.
- 717 12. Payne AN, Chassard C, Lacroix C: **Gut microbial adaptation to dietary consumption of fructose,**  
718 **artificial sweeteners and sugar alcohols: implications for host-microbe interactions contributing**  
719 **to obesity.** *Obes Rev* 2012, **13**:799-809.
- 720 13. Mastrocola R, Collino M, Rogazzo M, Medana C, Nigro D, Boccuzzi G, Aragno M: **Advanced**  
721 **glycation end products promote hepatosteatosis by interfering with SCAP-SREBP pathway in**  
722 **fructose-drinking mice.** *Am J Physiol Gastrointest Liver Physiol* 2013, **305**:G398-407.
- 723 14. Nigro D, Menotti F, Cento AS, Serpe L, Chiazza F, Dal Bello F, Romaniello F, Medana C, Collino M,  
724 Aragno M, Mastrocola R: **Chronic administration of saturated fats and fructose differently affect**  
725 **SREBP activity resulting in different modulation of Nrf2 and Nlrp3 inflammasome pathways in**  
726 **mice liver.** *J Nutr Biochem* 2017, **42**:160-171.
- 727 15. Seiquer I, Rubio LA, Peinado MJ, Delgado-Andrade C, Navarro MP: **Maillard reaction products**  
728 **modulate gut microbiota composition in adolescents.** *Mol Nutr Food Res* 2014, **58**:1552-1560.
- 729 16. Ritze Y, Bardos G, D'Haese JG, Ernst B, Thurnheer M, Schultes B, Bischoff SC: **Effect of high sugar**  
730 **intake on glucose transporter and weight regulating hormones in mice and humans.** *PLoS One*  
731 2014, **9**:e101702.
- 732 17. Mastrocola R, Nigro D, Chiazza F, Medana C, Dal Bello F, Boccuzzi G, Collino M, Aragno M: **Fructose-**  
733 **derived advanced glycation end-products drive lipogenesis and skeletal muscle reprogramming**  
734 **via SREBP-1c dysregulation in mice.** *Free Radic Biol Med* 2016, **91**:224-235.
- 735 18. Mastrocola R, Nigro D, Cento AS, Chiazza F, Collino M, Aragno M: **High-fructose intake as risk**  
736 **factor for neurodegeneration: Key role for carboxy methyllysine accumulation in mice**  
737 **hippocampal neurons.** *Neurobiol Dis* 2016, **89**:65-75.

- 738 19. Chan EC, Pasikanti KK, Nicholson JK: **Global urinary metabolic profiling procedures using gas**  
739 **chromatography-mass spectrometry.** *Nat Protoc* 2011, **6**:1483-1499.
- 740 20. Reichenbach SE, Rempe DW, Tao Q, Bressanello D, Liberto E, Bicchi C, Balducci S, Cordero C:  
741 **Alignment for comprehensive two-dimensional gas chromatography with dual secondary**  
742 **columns and detectors.** *Anal Chem* 2015, **87**:10056-10063.
- 743 21. Kleiner DE, Brunt EM, Van Natta M, Behling C, Contos MJ, Cummings OW, Ferrell LD, Liu YC,  
744 Torbenson MS, Unalp-Arida A, et al: **Design and validation of a histological scoring system for**  
745 **nonalcoholic fatty liver disease.** *Hepatology* 2005, **41**:1313-1321.
- 746 22. Knodell RG, Ishak KG, Black WC, Chen TS, Craig R, Kaplowitz N, Kiernan TW, Wollman J: **Formulation**  
747 **and application of a numerical scoring system for assessing histological activity in asymptomatic**  
748 **chronic active hepatitis.** *Hepatology* 1981, **1**:431-435.
- 749 23. Collino M, Aragno M, Castiglia S, Miglio G, Tomasinelli C, Boccuzzi G, Thiemermann C, Fantozzi R:  
750 **Pioglitazone improves lipid and insulin levels in overweight rats on a high cholesterol and**  
751 **fructose diet by decreasing hepatic inflammation.** *Br J Pharmacol* 2010, **160**:1892-1902.
- 752 24. Nurk S, Bankevich A, Antipov D, Gurevich AA, Korobeynikov A, Lapidus A, Prjibelski AD, Pyskhin A,  
753 Sirotkin A, Sirotkin Y, et al: **Assembling single-cell genomes and mini-metagenomes from chimeric**  
754 **MDA products.** *J Comput Biol* 2013, **20**:714-737.
- 755 25. Gurevich A, Saveliev V, Vyahhi N, Tesler G: **QUAST: quality assessment tool for genome**  
756 **assemblies.** *Bioinformatics* 2013, **29**:1072-1075.
- 757 26. Bessesen DH: **The role of carbohydrates in insulin resistance.** *J Nutr* 2001, **131**:2782s-2786s.
- 758 27. Axen KV, Dikeakos A, Sclafani A: **High dietary fat promotes syndrome X in nonobese rats.** *J Nutr*  
759 2003, **133**:2244-2249.
- 760 28. Conlon MA, Bird AR: **The impact of diet and lifestyle on gut microbiota and human health.**  
761 *Nutrients* 2014, **7**:17-44.
- 762 29. Bischoff SC, Barbara G, Buurman W, Ockhuizen T, Schulzke JD, Serino M, Tilg H, Watson A, Wells  
763 JM: **Intestinal permeability--a new target for disease prevention and therapy.** *BMC Gastroenterol*  
764 2014, **14**:189.
- 765 30. de Graaf C: **Trustworthy satiety claims are good for science and society. Comment on 'Satiety. No**  
766 **way to slim'.** *Appetite* 2011, **57**:778-783; discussion 784-790.
- 767 31. Martin AA, Hamill LR, Davies S, Rogers PJ, Brunstrom JM: **Energy-dense snacks can have the same**  
768 **expected satiation as sugar-containing beverages.** *Appetite* 2015, **95**:81-88.
- 769 32. Douard V, Ferraris RP: **The role of fructose transporters in diseases linked to excessive fructose**  
770 **intake.** *J Physiol* 2013, **591**:401-414.
- 771 33. Le Gall M, Tobin V, Stolarczyk E, Dalet V, Leturque A, Brot-Laroche E: **Sugar sensing by enterocytes**  
772 **combines polarity, membrane bound detectors and sugar metabolism.** *J Cell Physiol* 2007,  
773 **213**:834-843.
- 774 34. Kellett GL, Brot-Laroche E, Mace OJ, Leturque A: **Sugar absorption in the intestine: the role of**  
775 **GLUT2.** *Annu Rev Nutr* 2008, **28**:35-54.
- 776 35. Chaudhry RM, Scow JS, Madhavan S, Duenes JA, Sarr MG: **Acute enterocyte adaptation to luminal**  
777 **glucose: a posttranslational mechanism for rapid apical recruitment of the transporter GLUT2.** *J*  
778 *Gastrointest Surg* 2012, **16**:312-319; discussion 319.
- 779 36. Moran AW, Al-Rammahi MA, Arora DK, Batchelor DJ, Coulter EA, Ionescu C, Bravo D, Shirazi-  
780 Beechey SP: **Expression of Na<sup>+</sup>/glucose co-transporter 1 (SGLT1) in the intestine of piglets**  
781 **weaned to different concentrations of dietary carbohydrate.** *Br J Nutr* 2010, **104**:647-655.
- 782 37. Gorboulev V, Schurmann A, Vallon V, Kipp H, Jaschke A, Klessen D, Friedrich A, Scherneck S, Rieg T,  
783 Cunard R, et al: **Na<sup>(+)</sup>-D-glucose cotransporter SGLT1 is pivotal for intestinal glucose absorption**  
784 **and glucose-dependent incretin secretion.** *Diabetes* 2012, **61**:187-196.
- 785 38. Ait-Omar A, Monteiro-Sepulveda M, Poitou C, Le Gall M, Cotillard A, Gilet J, Garbin K, Houllier A,  
786 Chateau D, Lacombe A, et al: **GLUT2 accumulation in enterocyte apical and intracellular**  
787 **membranes: a study in morbidly obese human subjects and ob/ob and high fat-fed mice.**  
788 *Diabetes* 2011, **60**:2598-2607.
- 789 39. Naftalin RJ: **Does apical membrane GLUT2 have a role in intestinal glucose uptake?** *F1000Res*  
790 2014, **3**:304.



- 791 40. Jena PK, Singh S, Prajapati B, Nareshkumar G, Mehta T, Seshadri S: **Impact of targeted specific**  
792 **antibiotic delivery for gut microbiota modulation on high-fructose-fed rats.** *Appl Biochem*  
793 *Biotechnol* 2014, **172**:3810-3826.
- 794 41. Le Chatelier E, Nielsen T, Qin J, Prifti E, Hildebrand F, Falony G, Almeida M, Arumugam M, Batto JM,  
795 Kennedy S, et al: **Richness of human gut microbiome correlates with metabolic markers.** *Nature*  
796 2013, **500**:541-546.
- 797 42. Schwartz A, Taras D, Schafer K, Beijer S, Bos NA, Donus C, Hardt PD: **Microbiota and SCFA in lean**  
798 **and overweight healthy subjects.** *Obesity (Silver Spring)* 2010, **18**:190-195.
- 799 43. Di Luccia B, Crescenzo R, Mazzoli A, Cigliano L, Venditti P, Walser JC, Widmer A, Baccigalupi L, Ricca  
800 E, Iossa S: **Rescue of Fructose-Induced Metabolic Syndrome by Antibiotics or Faecal**  
801 **Transplantation in a Rat Model of Obesity.** *PLoS One* 2015, **10**:e0134893.
- 802 44. Manichanh C, Reeder J, Gibert P, Varela E, Llopis M, Antolin M, Guigo R, Knight R, Guarner F:  
803 **Reshaping the gut microbiome with bacterial transplantation and antibiotic intake.** *Genome Res*  
804 2010, **20**:1411-1419.
- 805 45. Karlsson FH, Tremaroli V, Nookaew I, Bergstrom G, Behre CJ, Fagerberg B, Nielsen J, Backhed F: **Gut**  
806 **metagenome in European women with normal, impaired and diabetic glucose control.** *Nature*  
807 2013, **498**:99-103.
- 808 46. Larsen N, Vogensen FK, van den Berg FW, Nielsen DS, Andreasen AS, Pedersen BK, Al-Soud WA,  
809 Sorensen SJ, Hansen LH, Jakobsen M: **Gut microbiota in human adults with type 2 diabetes differs**  
810 **from non-diabetic adults.** *PLoS One* 2010, **5**:e9085.
- 811 47. Reichardt N, Duncan SH, Young P, Belenguer A, McWilliam Leitch C, Scott KP, Flint HJ, Louis P:  
812 **Phylogenetic distribution of three pathways for propionate production within the human gut**  
813 **microbiota.** *ISME J* 2014, **8**:1323-1335.
- 814 48. Koo HY, Miyashita M, Cho BH, Nakamura MT: **Replacing dietary glucose with fructose increases**  
815 **ChREBP activity and SREBP-1 protein in rat liver nucleus.** *Biochem Biophys Res Commun* 2009,  
816 **390**:285-289.
- 817 49. Chen G, Wang T, Uttarwar L, vanKrieken R, Li R, Chen X, Gao B, Ghayur A, Margetts P, Krepinsky JC:  
818 **SREBP-1 is a novel mediator of TGFbeta1 signaling in mesangial cells.** *J Mol Cell Biol* 2014, **6**:516-  
819 530.
- 820 50. Uttarwar L, Gao B, Ingram AJ, Krepinsky JC: **SREBP-1 activation by glucose mediates TGF-beta**  
821 **upregulation in mesangial cells.** *Am J Physiol Renal Physiol* 2012, **302**:F329-341.
- 822 51. Wang TN, Chen X, Li R, Gao B, Mohammed-Ali Z, Lu C, Yum V, Dickhout JG, Krepinsky JC: **SREBP-1**  
823 **Mediates Angiotensin II-Induced TGF-beta1 Upregulation and Glomerular Fibrosis.** *J Am Soc*  
824 *Nephrol* 2015, **26**:1839-1854.
- 825 52. Sodhi K, Puri N, Favero G, Stevens S, Meadows C, Abraham NG, Rezzani R, Ansinelli H, Lebovics E,  
826 Shapiro JL: **Fructose Mediated Non-Alcoholic Fatty Liver Is Attenuated by HO-1-SIRT1 Module in**  
827 **Murine Hepatocytes and Mice Fed a High Fructose Diet.** *PLoS One* 2015, **10**:e0128648.
- 828 53. Luers L, Rysiewski K, Dumpitak C, Birkmann E: **Kinetics of advanced glycation end products**  
829 **formation on bovine serum albumin with various reducing sugars and dicarbonyl compounds in**  
830 **equimolar ratios.** *Rejuvenation Res* 2012, **15**:201-205.
- 831 54. Sadowska-Bartosz I, Galiniak S, Bartosz G: **Kinetics of glycooxidation of bovine serum albumin by**  
832 **methylglyoxal and glyoxal and its prevention by various compounds.** *Molecules* 2014, **19**:4880-  
833 4896.
- 834 55. Rapin JR, Wiernsperger N: **Possible links between intestinal permeability and food processing: A**  
835 **potential therapeutic niche for glutamine.** *Clinics (Sao Paulo)* 2010, **65**:635-643.
- 836 56. Tuohy KM, Hinton DJ, Davies SJ, Crabbe MJ, Gibson GR, Ames JM: **Metabolism of Maillard reaction**  
837 **products by the human gut microbiota--implications for health.** *Mol Nutr Food Res* 2006, **50**:847-  
838 857.
- 839 57. Zhong Y, Nyman M, Fak F: **Modulation of gut microbiota in rats fed high-fat diets by processing**  
840 **whole-grain barley to barley malt.** *Mol Nutr Food Res* 2015, **59**:2066-2076.
- 841 58. Yang B, Bostick RM, Tran HQ, Gewirtz AT, Campbell PT, Fedirko V: **Circulating Biomarkers of Gut**  
842 **Barrier Function: Correlates and Nonresponse to Calcium Supplementation among Colon**  
843 **Adenoma Patients.** *Cancer Epidemiol Biomarkers Prev* 2016, **25**:318-326.

- 844 59. Beumer C, Wulferink M, Raaben W, Fiechter D, Brands R, Seinen W: **Calf intestinal alkaline**  
845 **phosphatase, a novel therapeutic drug for lipopolysaccharide (LPS)-mediated diseases,**  
846 **attenuates LPS toxicity in mice and piglets.** *J Pharmacol Exp Ther* 2003, **307**:737-744.
- 847 60. Estaki M, DeCoffe D, Gibson DL: **Interplay between intestinal alkaline phosphatase, diet, gut**  
848 **microbes and immunity.** *World J Gastroenterol* 2014, **20**:15650-15656.
- 849 61. Tuin A, Huizinga-Van der Vlag A, van Loenen-Weemaes AM, Meijer DK, Poelstra K: **On the role and**  
850 **fate of LPS-dephosphorylating activity in the rat liver.** *Am J Physiol Gastrointest Liver Physiol* 2006,  
851 **290**:G377-385.
- 852 62. Pierantonelli I, Rychlicki C, Agostinelli L, Giordano DM, Gaggini M, Fraumene C, Saponaro C,  
853 Manghina V, Sartini L, Mingarelli E, et al: **Lack of NLRP3-inflammasome leads to gut-liver axis**  
854 **derangement, gut dysbiosis and a worsened phenotype in a mouse model of NAFLD.** *Sci Rep*  
855 2017, **7**:12200.
- 856 63. Lin KM, Hu W, Troutman TD, Jennings M, Brewer T, Li X, Nanda S, Cohen P, Thomas JA, Pasare C:  
857 **IRAK-1 bypasses priming and directly links TLRs to rapid NLRP3 inflammasome activation.** *Proc*  
858 *Natl Acad Sci U S A* 2014, **111**:775-780.
- 859 64. Henao-Mejia J, Elinav E, Thaïss CA, Flavell RA: **Inflammasomes and metabolic disease.** *Annu Rev*  
860 *Physiol* 2014, **76**:57-78.
- 861 65. Cannito S, Morello E, Bocca C, Foglia B, Benetti E, Novo E, Chiazza F, Rogazzo M, Fantozzi R, Povero  
862 D, et al: **Microvesicles released from fat-laden cells promote activation of hepatocellular NLRP3**  
863 **inflammasome: A pro-inflammatory link between lipotoxicity and non-alcoholic steatohepatitis.**  
864 *PLoS One* 2017, **12**:e0172575.
- 865 66. Chiazza F, Couturier-Maillard A, Benetti E, Mastrocola R, Nigro D, Cutrin JC, Serpe L, Aragno M,  
866 Fantozzi R, Ryffel B, et al: **Targeting the NLRP3 inflammasome to reduce diet-induced metabolic**  
867 **abnormalities in mice.** *Mol Med* 2015.
- 868 67. Moreira AP, Texeira TF, Ferreira AB, Peluzio Mdo C, Alfenas Rde C: **Influence of a high-fat diet on**  
869 **gut microbiota, intestinal permeability and metabolic endotoxaemia.** *Br J Nutr* 2012, **108**:801-809.
- 870 68. Pendyala S, Walker JM, Holt PR: **A high-fat diet is associated with endotoxemia that originates**  
871 **from the gut.** *Gastroenterology* 2012, **142**:1100-1101.e1102.
- 872
- 873

874 **Table 1. General parameters.** Physical characteristics, plasma glucose, insulin and triglyceride,  
 875 and liver triglycerides of mice exposed for 12 weeks to standard diet (SD) or 60% fructose  
 876 administered in liquid (L-Fr) or solid (S-Fr) formulation. Data are means  $\pm$  s.e.m. of 6-10 mice per  
 877 group. Statistical significance: \*P<0.05, \*\*P<0.01, vs SD; §P<0.05, §§§P<0.001, vs L-Fr.

	<b>SD</b>	<b>L-Fr</b>	<b>S-Fr</b>
<b>Starting body weight</b> (g)	16.17 $\pm$ 1.60	16.88 $\pm$ 2.39	15.99 $\pm$ 2.38
<b>Ending body weight</b> (g)	29.48 $\pm$ 1.72	28.42 $\pm$ 1.44	27.70 $\pm$ 2.71
<b>Liver-to-body weight ratio</b> (% of body weight)	3.21 $\pm$ 0.05	3.95 $\pm$ 0.12**	2.98 $\pm$ 0.21 <sup>§§§</sup>
<b>Fasting glycaemia</b> (mg/dL)	114.5 $\pm$ 3.5	142.6 $\pm$ 6.7*	149.0 $\pm$ 5.7**
<b>Insulinemia</b> (ng/dL)	59.1 $\pm$ 9.2	49.0 $\pm$ 3.0	51.8 $\pm$ 7.9
<b>TG</b> (mg/dL)	26.3 $\pm$ 4.8	23.1 $\pm$ 1.6	28.5 $\pm$ 2.7
<b>Hepatic TG</b> (mg/g tissue)	24.8 $\pm$ 2.1	40.5 $\pm$ 5.5*	26.6 $\pm$ 1.2 <sup>§</sup>
<b>Urinary Glucose</b> (mg/dL)	120.3 $\pm$ 25.4	1417.0 $\pm$ 424.5**	520.7 $\pm$ 259.4 <sup>§</sup>
<b>Urinary Fructose</b> (mg/dL)	415.2 $\pm$ 122.6	453.9 $\pm$ 133.0	311.0 $\pm$ 55.0

878

879

880

881

882

883

884

885

886

887 **Table 2. Characteristics of dietary intervention.** Daily food and drink consumption and calories  
888 intake of mice exposed for 12 weeks to standard diet (SD) or 60% fructose administered in liquid  
889 (L-Fr) or solid (S-Fr) formulation. Data are means  $\pm$  s.e.m. of 6-10 mice per group. Statistical  
890 significance: \*P<0.05, \*\*\*P<0.001, vs SD; §P<0.05, §§§P<0.001, vs L-Fr.

	<b>SD</b>	<b>L-Fr</b>	<b>S-Fr</b>
<b>Food intake</b> (g/die)	2.95 $\pm$ 0.07	1.76 $\pm$ 0.03***	3.25 $\pm$ 0.15§§§
<b>Drink intake</b> (ml/die)	2.73 $\pm$ 0.07	2.78 $\pm$ 0.18	3.59 $\pm$ 0.25*§
<b>Calories intake</b> (Kcal/die)	11.34 $\pm$ 0.33	12.46 $\pm$ 0.36	12.63 $\pm$ 0.43
<b>Fructose intake</b> (g/die)	-	1.67 $\pm$ 0.11	1.88 $\pm$ 0.09

891

892

893

894

895

896

897

898

899

900

901

902

903 **Figure Legends**

904 **Figure 1. GLUT-5 and GLUT-2 localization in intestine and liver.** Representative  
905 photomicrographs showing expression and tissue distribution of GLUT-5 and GLUT-2 evaluated by  
906 indirect immunofluorescence on cryostatic sections of ileum (A and B, respectively) and GLUT-2  
907 evaluated in liver (C) from mice exposed to SD and liquid and solid fructose. Data are means  $\pm$   
908 s.e.m. of 6-10 mice per group. Statistical significance: \*\*\*P<0.001, vs SD; §§§P<0.001, vs L-Fr.

909

910 **Figure 2. Taxonomy analysis of mice gut microbiota.** Relative abundance of the major taxonomic  
911 groups detected by 16S rRNA sequencing. Only OTUs with an incidence above 0.2% are shown.

912

913 **Figure 3. Functional classification of mice gut metagenome.** Functional classes were determined  
914 according to the second level of the KEGG annotations.

915

916 **Figure 4. Faecal volatiles distribution.** Heat map based on analytes relative abundance (mean of  
917 three analytical replicates) between mice faecal samples from S-Fr, L-Fr, and SD diets. Features  
918 (analytes detected) and diet groups dendrograms are shown to make easier the location of signature  
919 similitudes-differences as a function of diet manipulation. Data were centered and normalized  
920 against row standard deviation. Color scale varies between red (low abundance) to blue (high  
921 abundance).

922

923 **Figure 5. Faecal volatilome signatures.** Histogram referring to Coefficients of Variation (CV%)  
924 for informative analytes detected in L-Fr, S-Fr and SD diets (data were based on analytes relative  
925 abundance). Positive CV% values indicate analytes more abundant in fructose enriched diets while  
926 negative values indicate those more abundant in the SD diet. Red bars are for analytes exclusively  
927 detected in one population while asterisk is for those that reported statistically relevant changes  
928 (p<0.05).

929

930 **Figure 6. Hepatic activation of the SCAP/SREBP1c lipogenic pathway.** Representative  
931 immunoblotting showing the expression of the activating protein SCAP (A), the cytosol-to-nuclear  
932 translocation of SREBP1c (B), and the protein expression of the SREBP1c target genes ACC and  
933 FAS (C) on liver protein extracts. Histograms report the densitometric analysis for each protein  
934 normalized for the corresponding tubulin or histone H3 content, for cytosolic or nuclear extracts,  
935 respectively, and expressed as fold of SD value. Data are means  $\pm$  s.e.m. of 6-10 mice per group.  
936 Statistical significance: \*P<0.05, \*\*P<0.01, \*\*\*P<0.001, vs SD; §§§P<0.001, vs L-Fr. (D)  
937 Representative photomicrographs of Oil red O staining performed on liver cryostatic sections for  
938 the evaluation of steatosis. Ballooning of hepatocytes and inflammatory foci can be observed in the  
939 20X magnification micrographs of S-Fr sample.

940

941 **Figure 7. Hepatic activation of fibrosis.** Representative immunoblotting showing the expression  
942 of TGF- $\beta$  (A), total and phosphorylated SMAD (B), fibronectin and vimentin (C) on liver protein  
943 extracts. Histograms report the densitometric analysis for each protein normalized for the  
944 corresponding tubulin content and expressed as fold of SD value. (D) **Representative**  
945 **photomicrographs at 200x magnification of H&E staining performed on liver dewaxed sections for**  
946 **the evaluation of histology scoring. Histograms report the single components of NAS score and**  
947 **fibrosis staging (left graph), and the HIAD score for necro-inflammatory grading (right graph),**  
948 **evaluated on 10 fields per liver section.** Data are means  $\pm$  s.e.m. of 4-6 mice per group. Statistical  
949 significance: \*P<0.05, \*\*P<0.01, \*\*\*P<0.001, vs SD; §P<0.05, vs L-Fr.

950

951 **Figure 8. AGEs accumulation and RAGE expression in the intestine.** (A) Representative  
952 photomicrographs showing expression and tissue distribution of CML, CEL and RAGE evaluated  
953 by indirect immunofluorescence on cryostatic sections of ileum from mice exposed to SD and liquid  
954 and solid fructose. Enlarged squares show details of CML distribution in the intestinal villi axis. (B)

955 Analysis of immunoreactivity expressed as fluorescence intensity evaluated by Image J in the entire  
956 ileum section. Data are means  $\pm$  s.e.m. of 5-6 mice per group. (C) Representative immunoblotting  
957 showing the CML-glycated proteins on liver protein extracts. Histograms report the densitometric  
958 analysis expressed as fold of SD value. Data are means  $\pm$  s.e.m. of 6-10 mice per group. Statistical  
959 significance: \*P<0.05, \*\*P<0.01, \*\*\*P<0.001, vs SD; §P<0.05, §§P<0.01, vs L-Fr.

960

961 **Figure 9. Tight junctions markers, plasma LPS and IAP activity.** Gene expression of TJ  
962 proteins occludin (A) and ZO-1 (B) evaluated by RT-PCR analysis on mRNA samples from ileum  
963 tract and related protein levels (C and D). LPS concentration evaluated in portal (E) and systemic  
964 (F) plasma by biochemical technique represents an index of intestinal permeability. **Intestinal**  
965 **alkaline phosphatase activity evaluated in ileum extracts by kinetic assay (G).** Data are means  $\pm$   
966 s.e.m. of 6-10 mice per group. Statistical significance: \*P<0.05, \*\*P<0.01, vs SD; §P<0.05,  
967 §§P<0.01, vs L-Fr.

968

969 **Figure 10. TLR4 and NLRP3 inflammatory pathways activation.** **The signaling pathway**  
970 **activated by TLR4, the major receptor involved in LPS-induced NLRP3 activation in liver, has been**  
971 **evaluated by western blotting analysis for the protein expression of TLR4 (A), MyD88 (B), and**  
972 **IRAK1 (C).** Activation of liver inflammatory signaling has been evaluated by protein amount of  
973 NLRP3 (D), of pro-caspase and cleaved active caspase-1 (E), and of IL-1 $\beta$  (F) evaluated by western  
974 blotting on liver extracts. Data are means  $\pm$  s.e.m. of 6-10 mice per group. Statistical significance:  
975 \*P<0.05, \*\*P<0.01, \*\*\*P<0.001, vs SD; §P<0.05, §§P<0.01, §§§P<0.001, vs L-Fr.

976

977

978

979

**Figure 1**

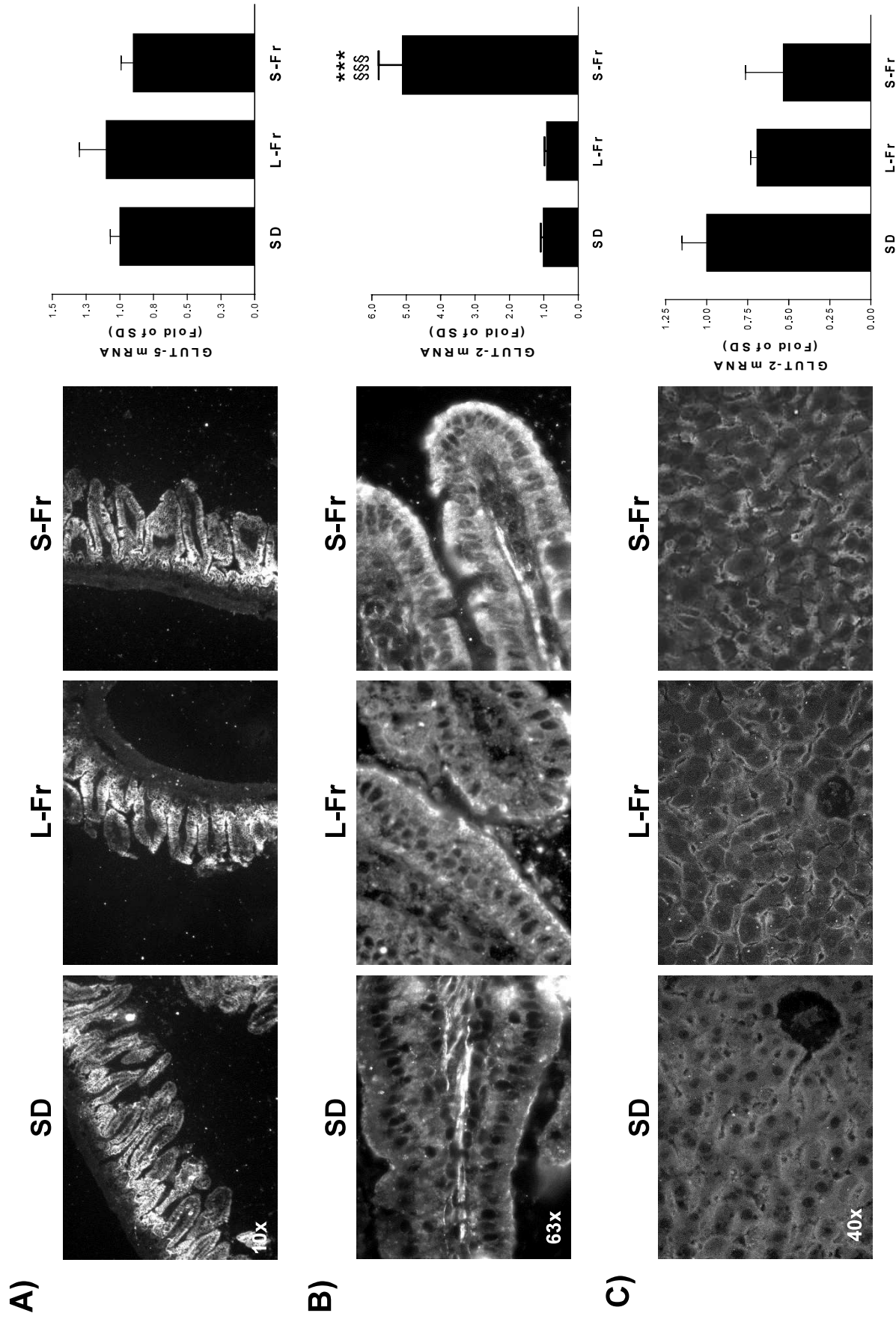




**Figure 2**

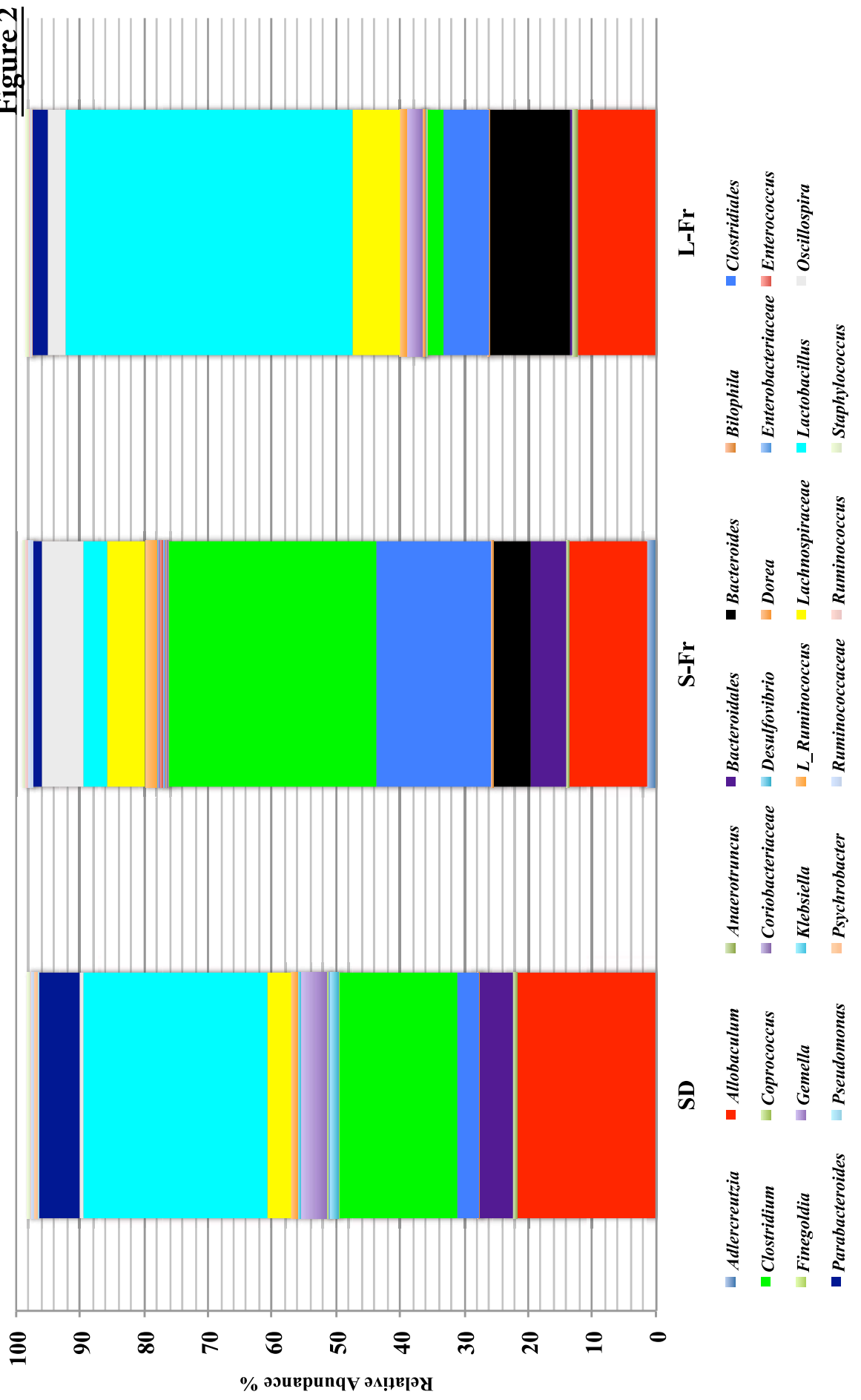


**Figure 3**

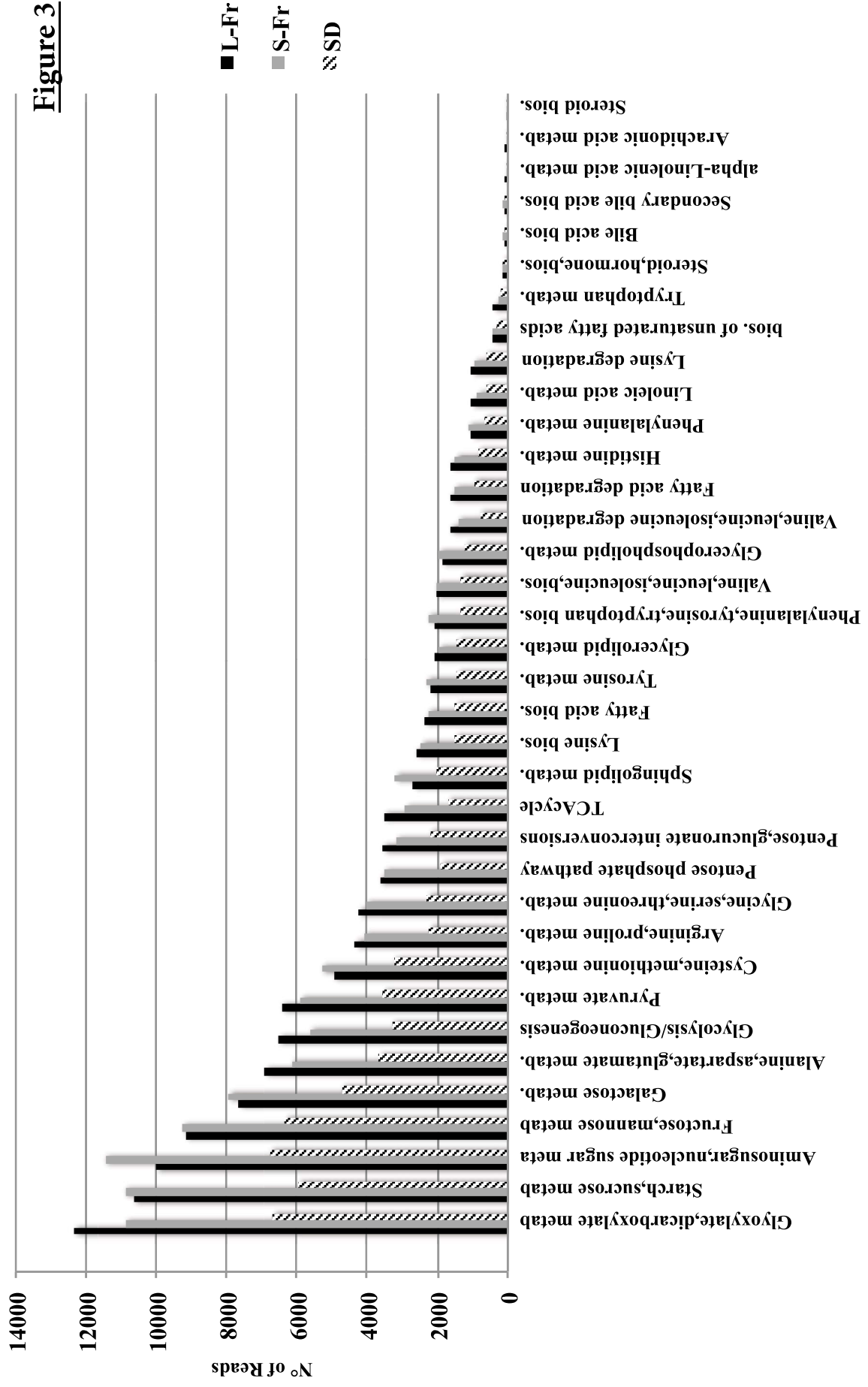


**Figure 4**

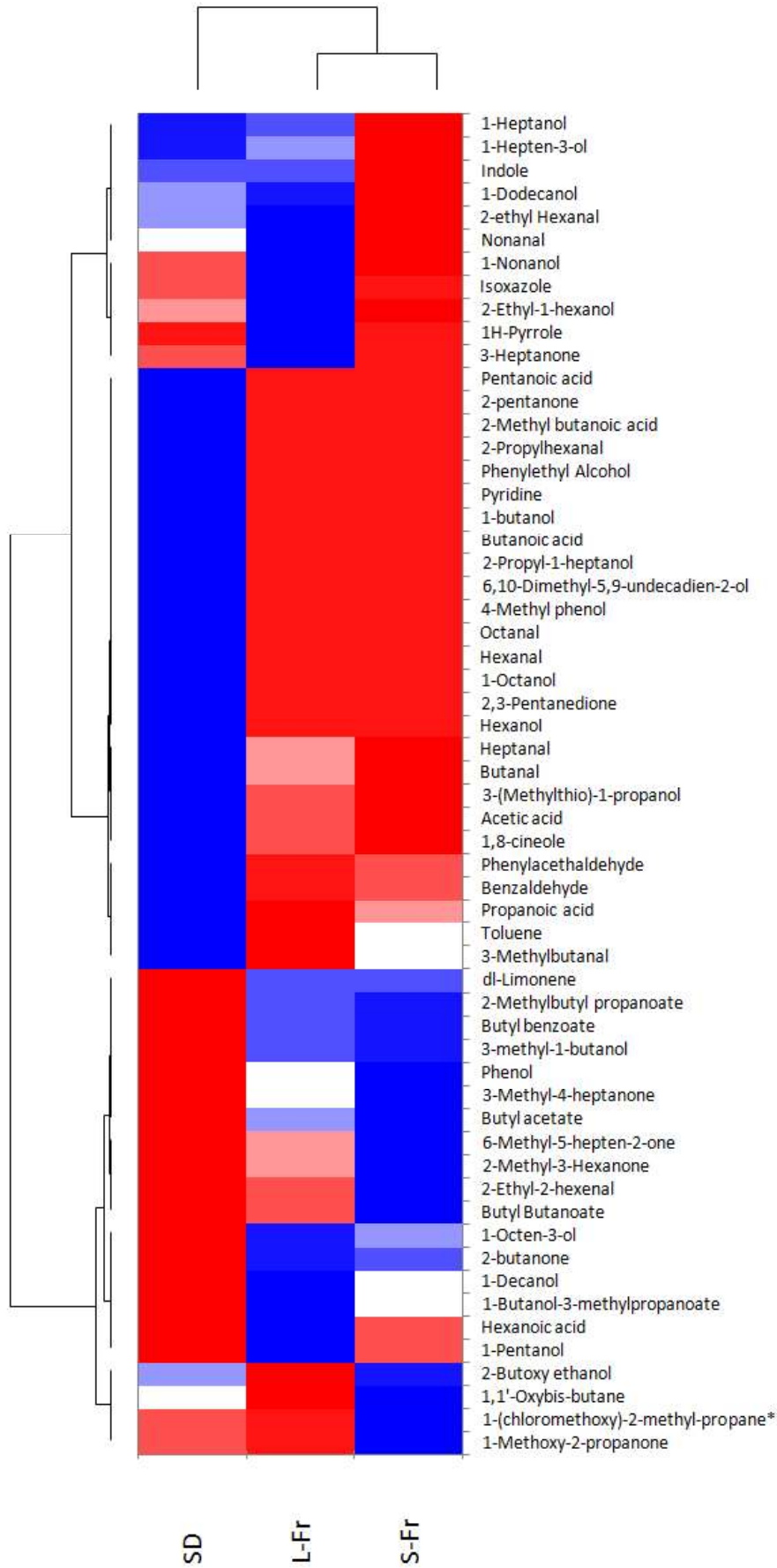


**Figure 5**

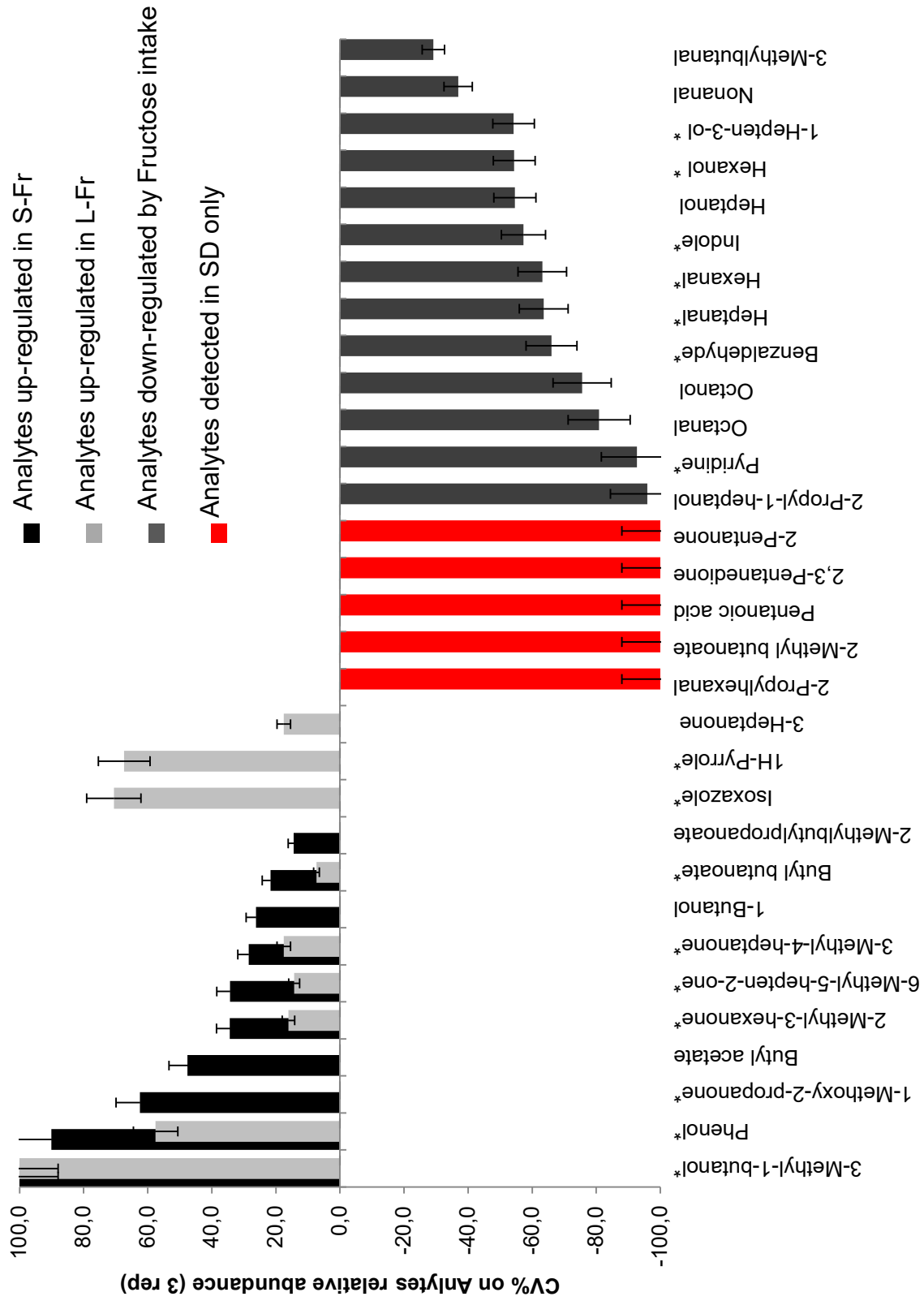


**Figure 6**

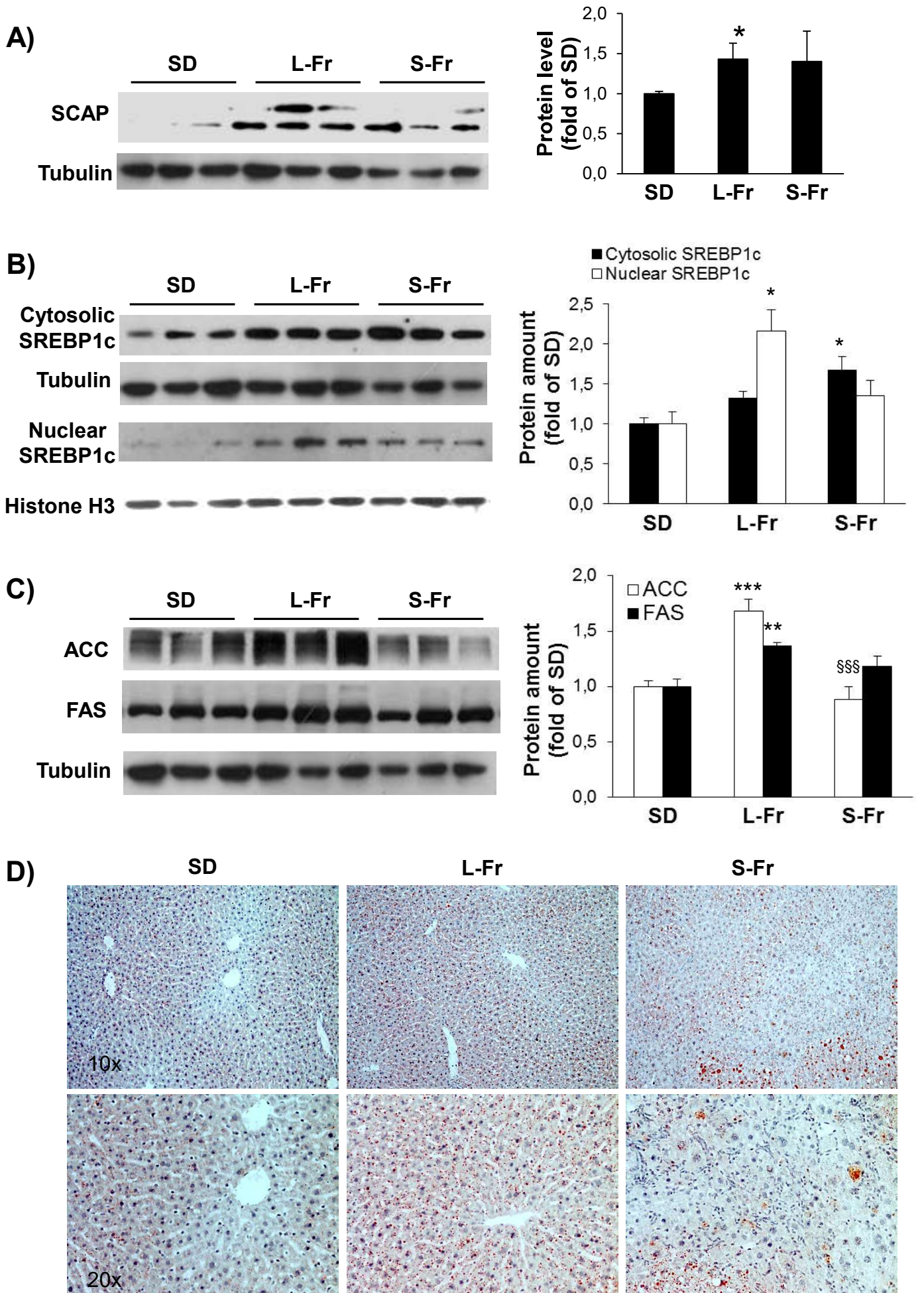




**Figure 7**

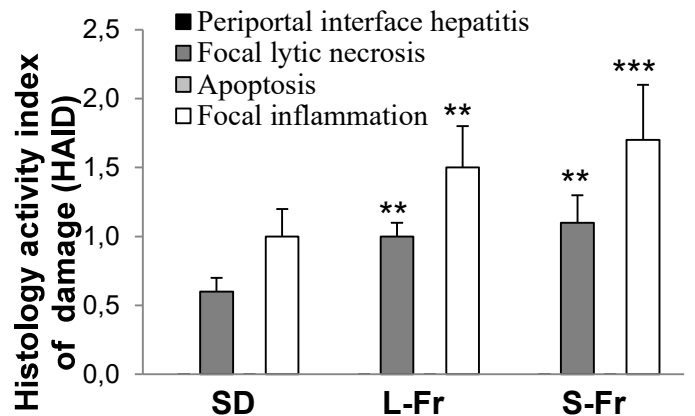
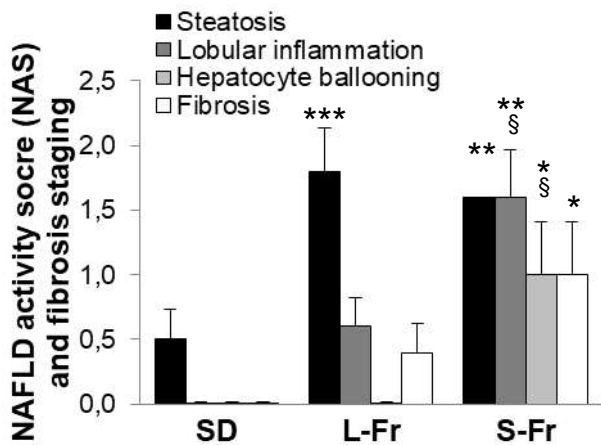
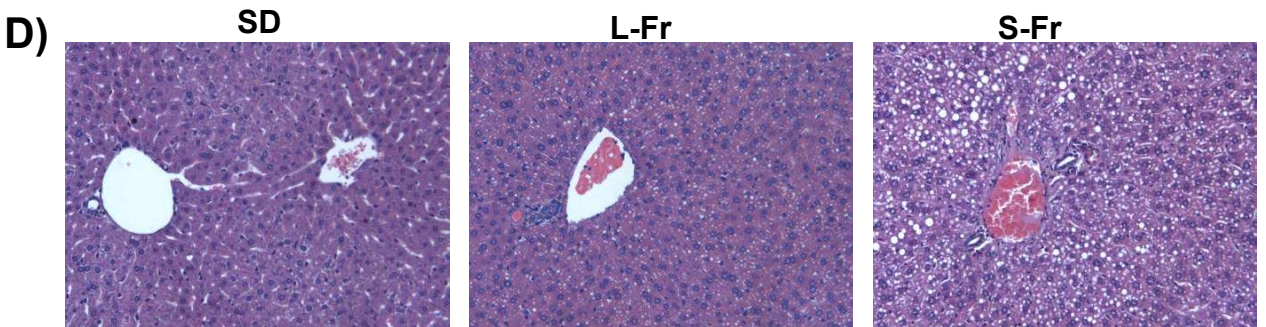
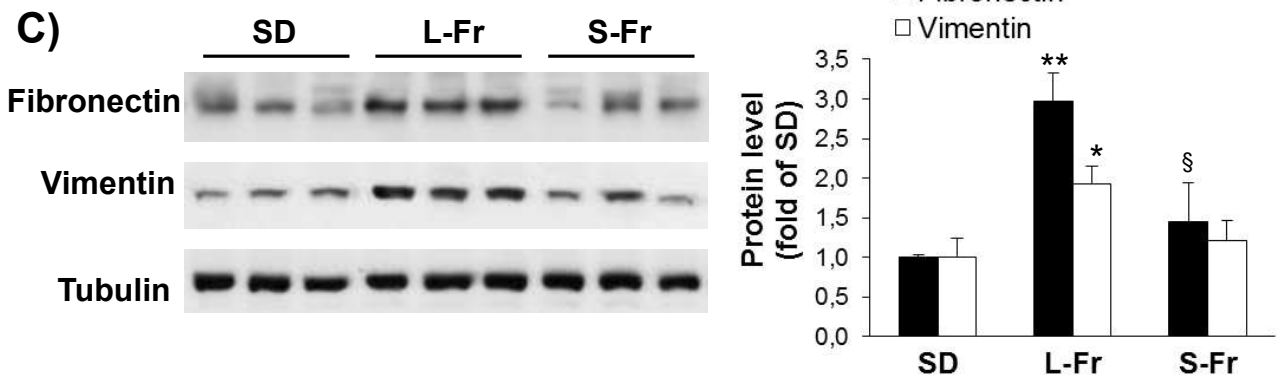
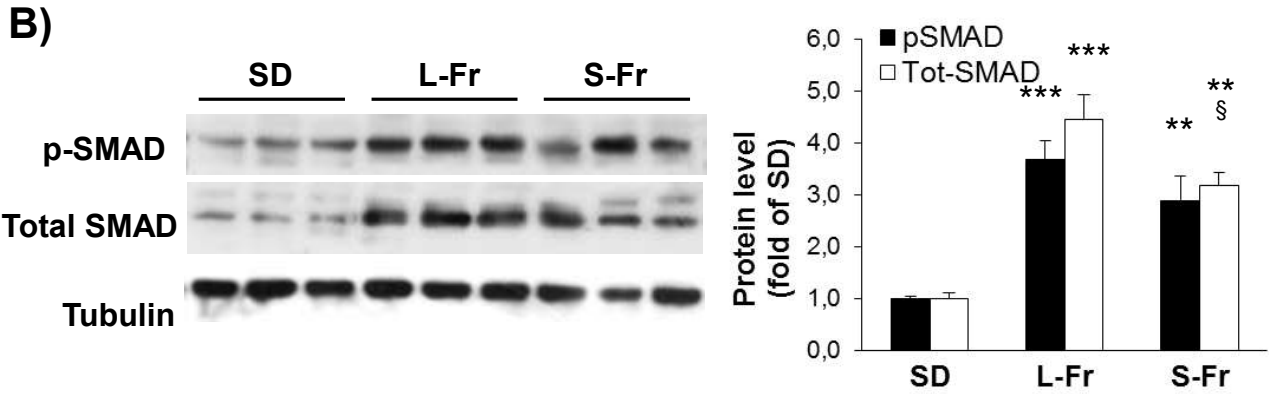
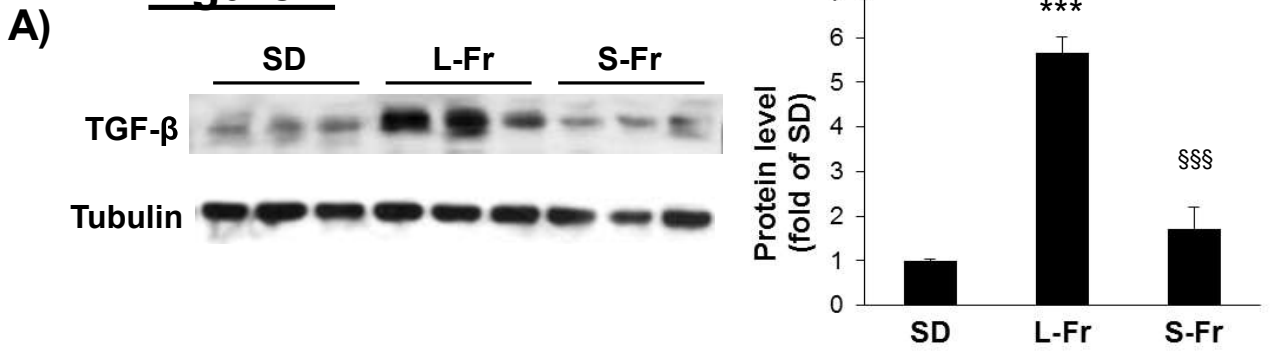


**Figure 8**

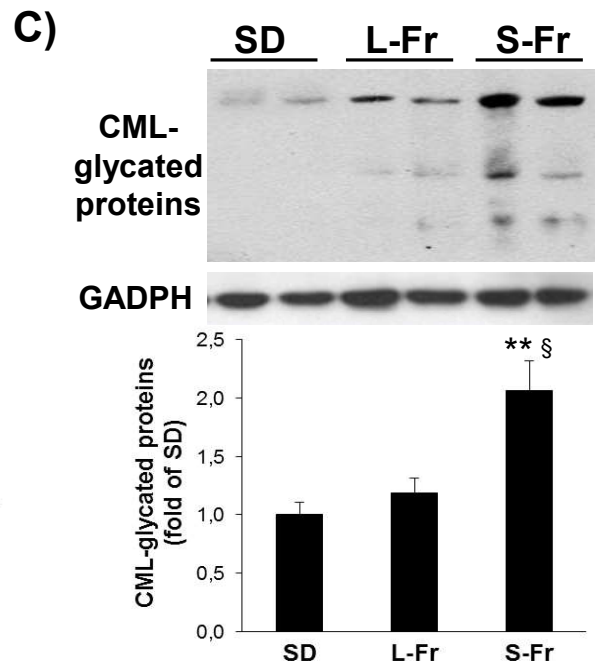
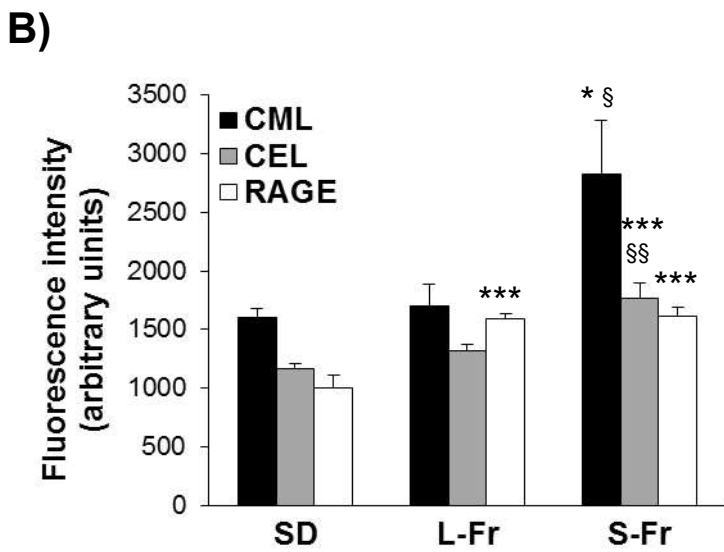
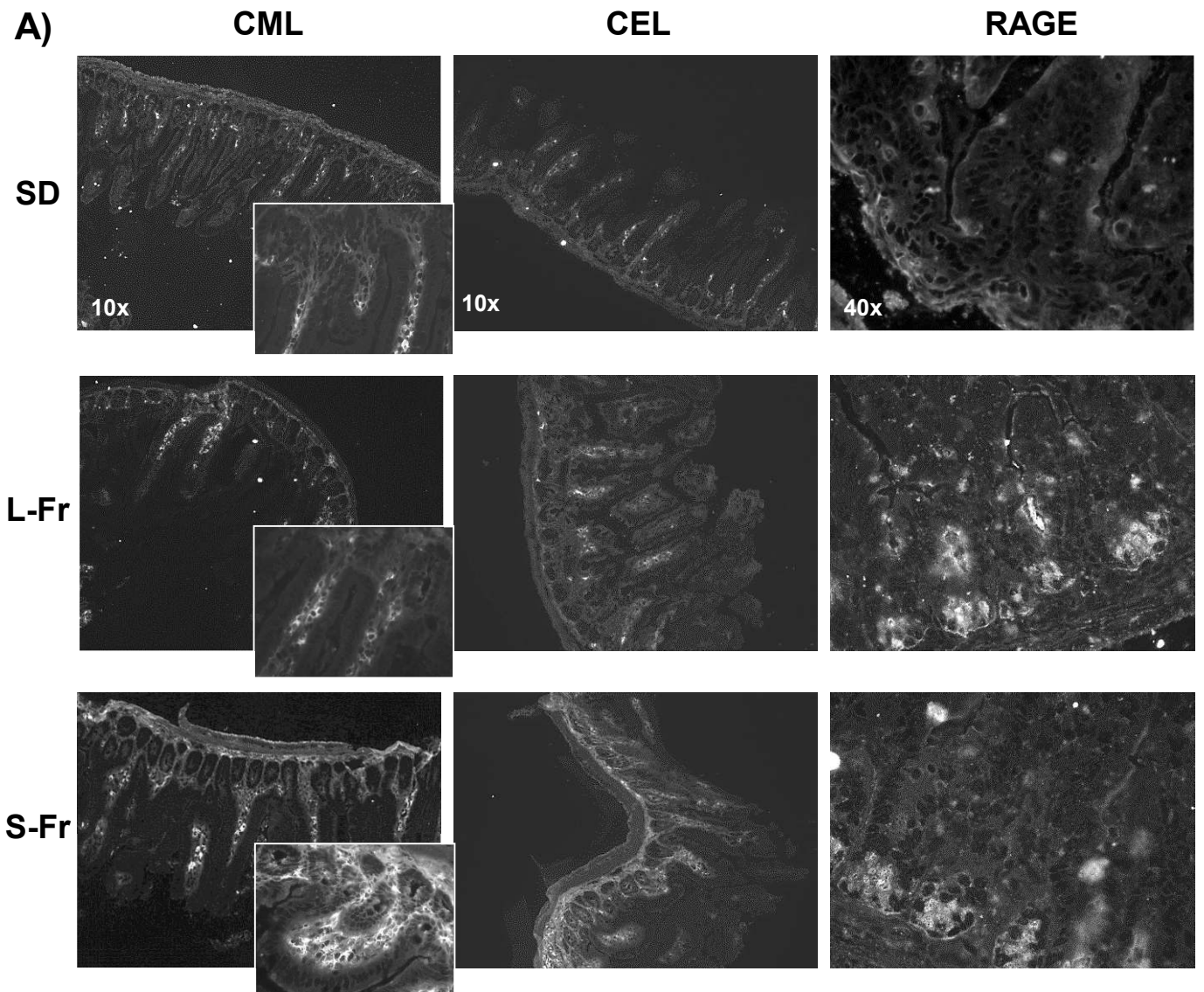


**Figure 9**

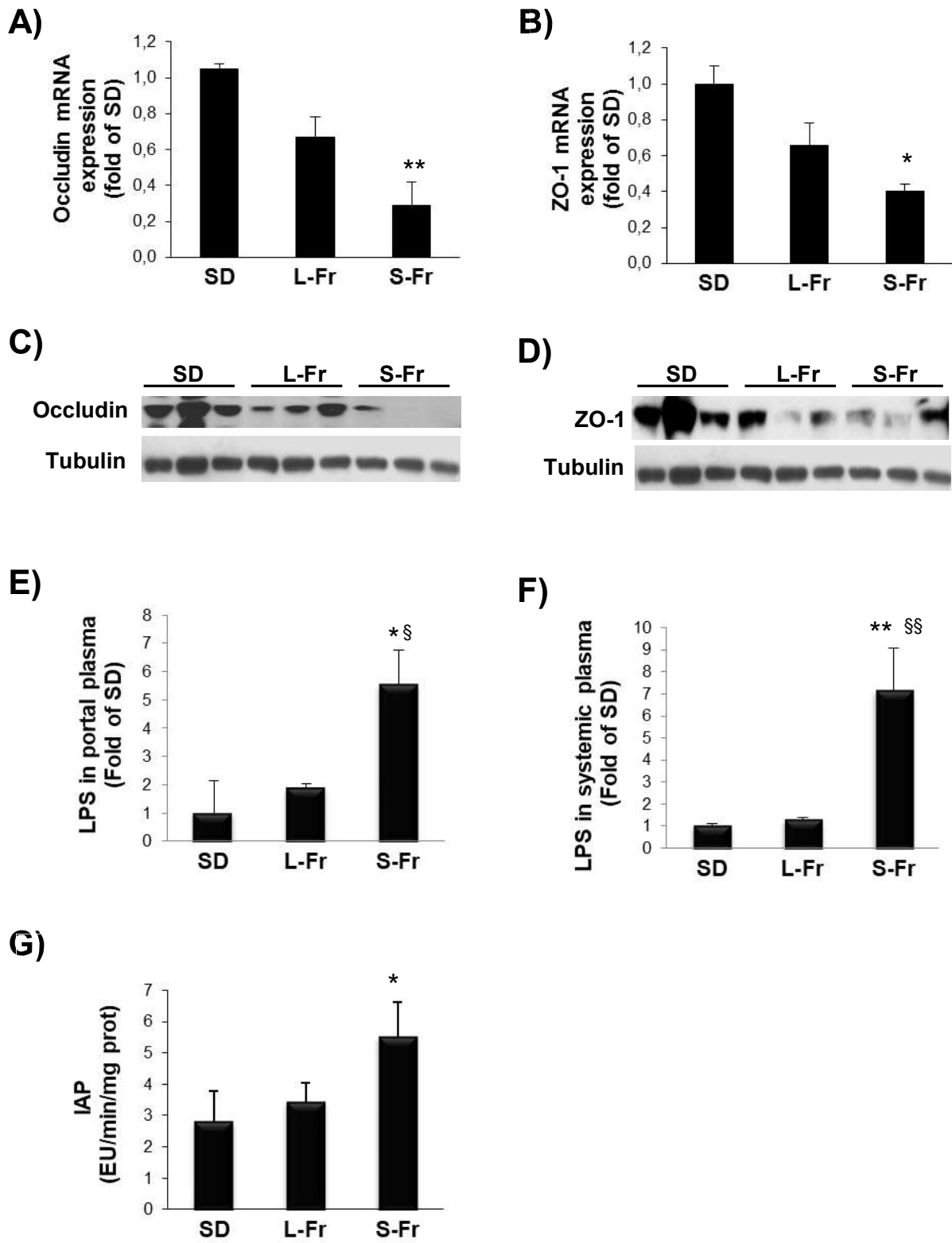
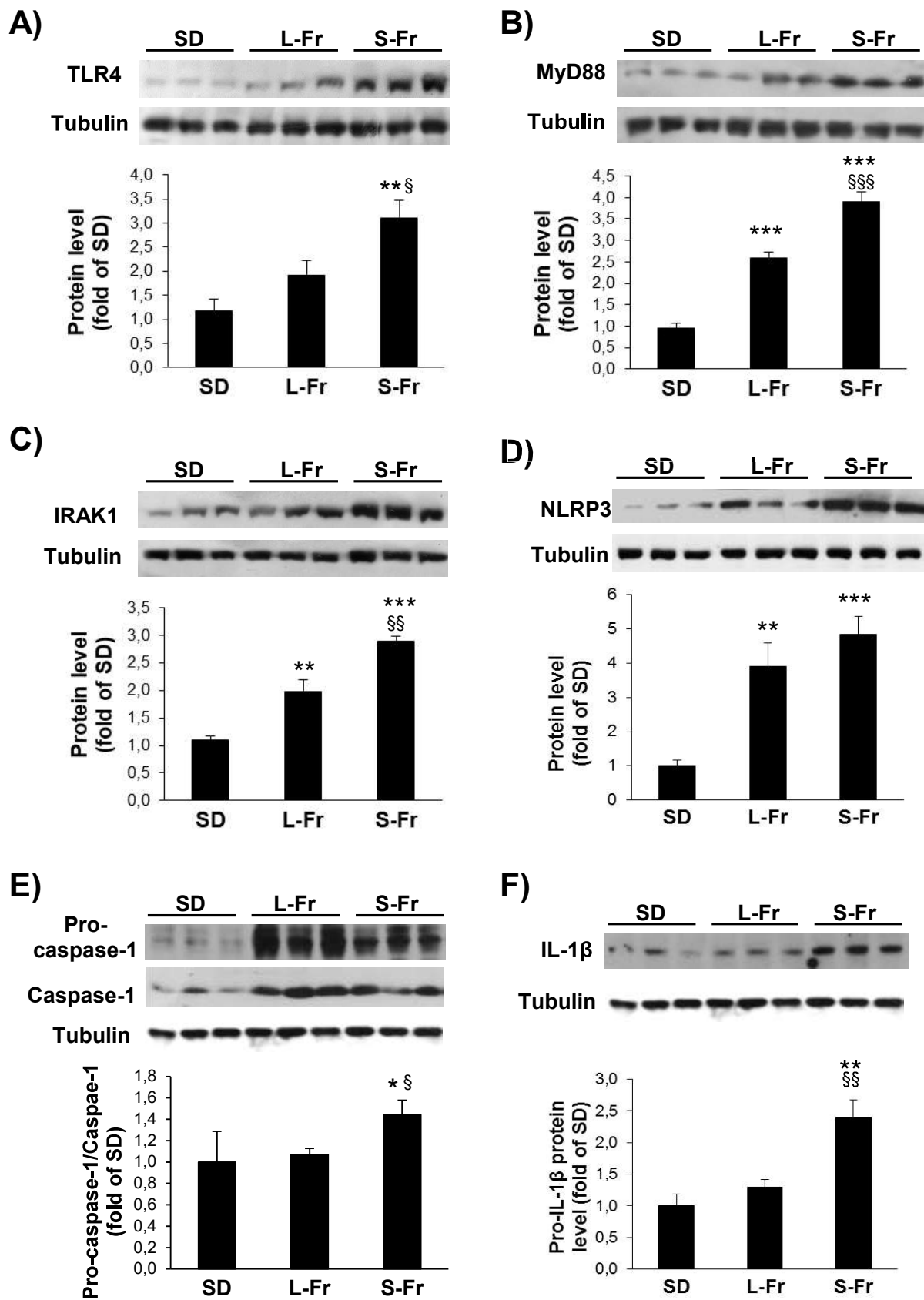


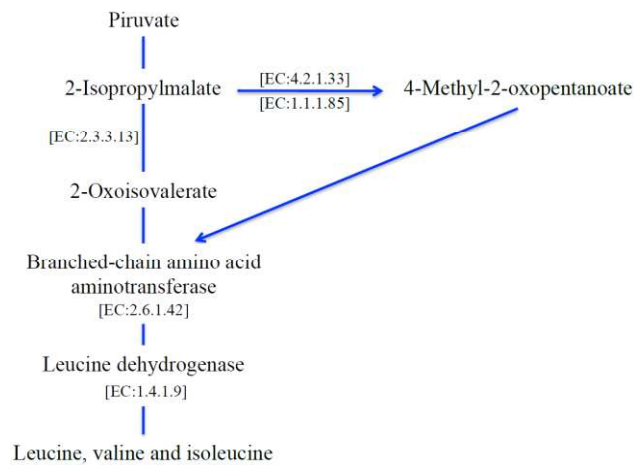


**Figure 10**

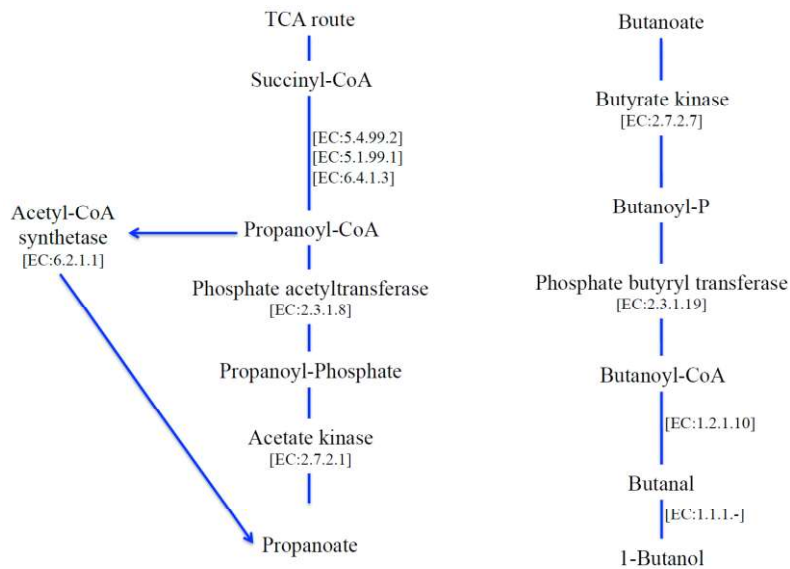


# Supplementary Figure1

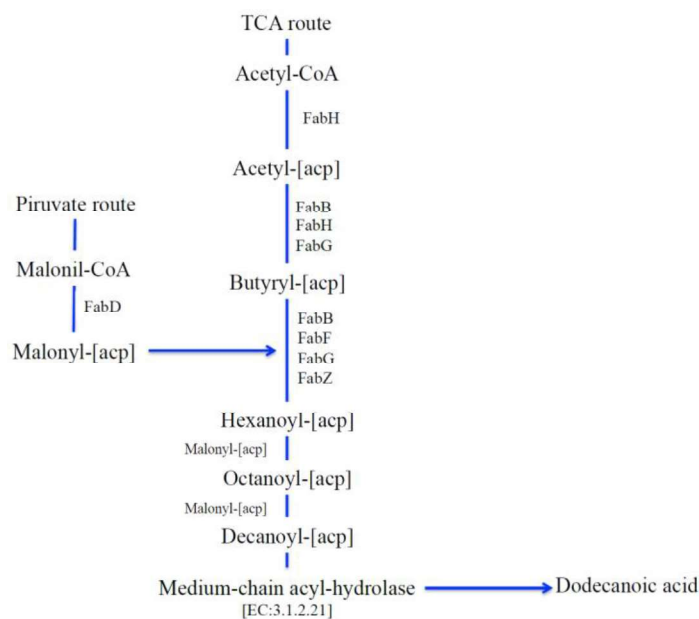
(A)



(B)



(C)



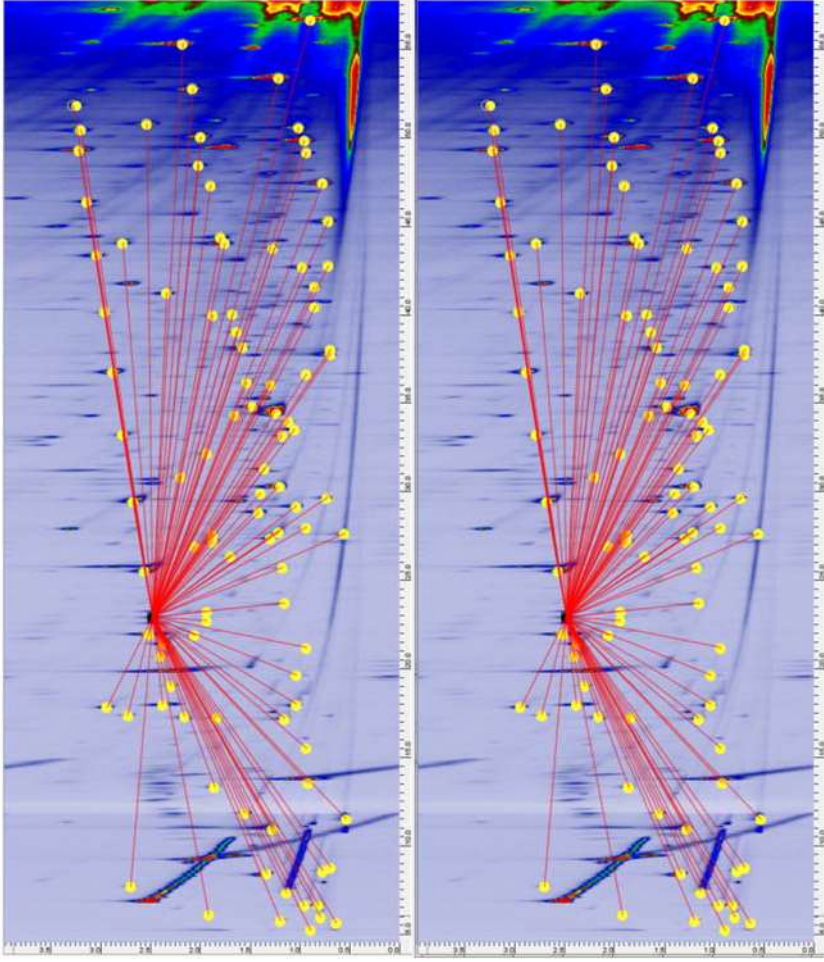


**Figure S2a**

**S-Fr diet volatiles fingerprint**

Averaged 2D plot of faeces volatiles.

Yellow circles indicate target analytes and their relative position over the chromatographic plane. Red connection lines converge to the Internal Standard ( $\alpha$ -Tujone) position (black circle).

**Figure S2b**

**L-Fr diet volatiles fingerprint**

Averaged 2D plot of faeces volatiles.

Yellow circles indicate target analytes and their relative position over the chromatographic plane. Red connection lines converge to the Internal Standard ( $\alpha$ -Tujone) position (black circle).

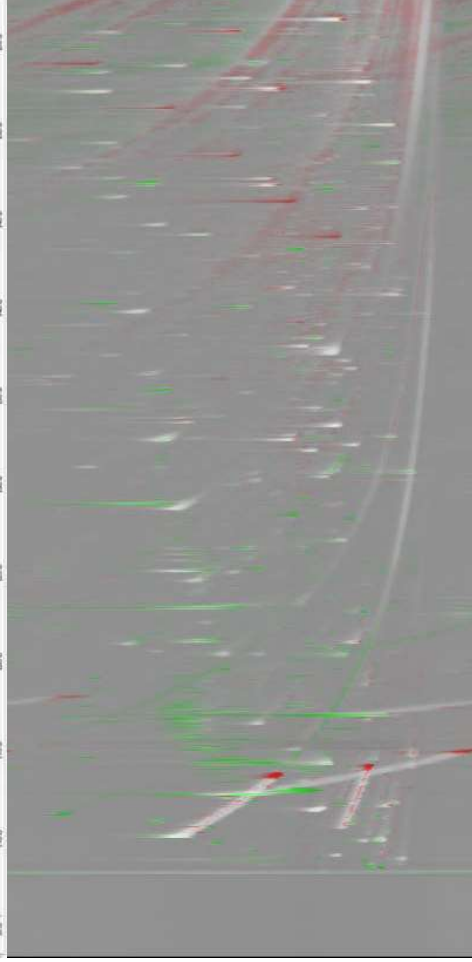
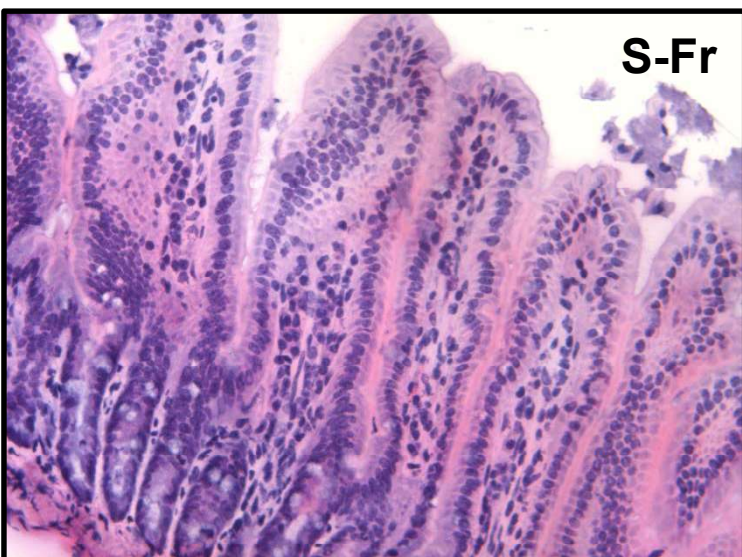


**Figure S2c -Comparative visualization between S-Fr (reference) and L-Fr (analyzed) 2D patterns -Colorized fuzzy ratio rendering.**

Visualization uses the Hue-Intensity-Saturation (HIS) color space to color each pixel in the retention-times plane. The method first computes the difference at each data point. The pixel hue is set to green if the difference is positive and red if it is negative (i.e., green if the value in the L-Fr chromatogram is smaller than the value in the S-Fr chromatogram and red if the value is greater). The pixel intensity is set to the larger of the two values (scaled by the largest intensity value in the chromatogram) and the pixel saturation is set to the magnitude of the difference between the data points (scaled by the magnitude of the largest difference in the chromatogram). Peaks are visible because large-valued data points yield bright pixels and small-valued data points yield dark pixels. If the difference is relatively large, the color is saturated with red or green (depending on the largest data point); if the difference is relatively small, the color saturation is low, producing a grey level from black to white depending on intensity. Peaks with large differences therefore appear red or green and peaks with small differences appear white or grey. The fuzzy difference is computed as the difference between a data point and a small region of data points in the other chromatogram (scaled by the largest fuzzy difference in the chromatogram). Thus, the colors are saturated with red or green only when the relative difference is large.



### Supplementary Figure 3



















K10847_k003420	NucleoidXioninProcessing_GeneticInformationProcessing_ReplicationandRepair_XPA-DNA-repairproteincomplementingXP-Acellis	2,07452E-05	1.5286E-05	8.30037E-06
K03688_k001130	Ubiquitineandotherpenoid-quinonebiosynthesis_Metabolism_Metabolismofcofactorsandvitamins_ubib_arF_ubiquitinubiquitinbiosynthesisprotein	0.00014003	0.000366864	0.0001382047
K01910_k002020	Two-componentsystem_EnvironmentalInformationProcessing_Signaltransduction_cIc(E)tracitor-35)_(yaeJ)ase[EC:2.1.2.2]	6.74218E-05	0.000101907	0.000182718
K01615_k00650	Glyoxylateanddicarboxylatemetabolism_Metabolism_Carbohydratemetabolism_E4.1.1.70(Lutococcus)_(yaeJ)ase[EC:2.1.2.2]	0.00014003	0.000163051	0.000148487
K0681_k00946	Cyanoaminoacidmetabolism_Metabolism_Metabolismofotheraminoacids_3pg_gamma-amino-glutarimyl-enzyme[glutathionethionylase][EC:2.2.2.3.4.13.13](K00681_k000480_Glutathionethionylase)Metabolism_Metabolismofotheraminoacids_Bi	0.000119285	0.000347765	0.000182718
K0627_k02171	SynaptotagminIII_Cyanoaminoacidmetabolism_Metabolism_Metabolismofotheraminoacids_3pg_gamma-amino-glutarimyl-enzyme[glutathionethionylase][EC:2.2.2.3.4.13.13](K00681_k000480_Glutathionethionylase)Metabolism_Metabolismofotheraminoacids_Bi	0.000276081	0.000300625	0.000038843
K13889_k002010	Transposons_EnvironmentalInformationProcessing_Membranetransport_g3bB_glycylationtransposonsustrate_bindingprotein	3.1117E-05	0	0
K0278	Alanine-aspartateandL-glutamatemetabolism_Metabolism_Aminoacidmetabolism_nadE1_aspartatease[EC:1.4.3.16](K00278_k0012078_Nicotinateandnicotinamidemetabolism_Metabolism_Metabolismofcofactorsandvitamins_nadE1-aspartate	0.002020474	0.001895464	0.001866043
K01893_k00970	Aminoacyl-HRNABiosynthesis_GeneticInformationProcessing_Transcription_WARS_sansaparajiryl-HRNAsynthetase[EC:6.1.1.22]	0.000200109	0.001963909	0.000199639
K03150_k00730	Thiaminemetabolism_Metabolism_Metabolismofcofactorsandvitamins_thiH2_4-iminoacetate[EC:4.1.99.19]	0.0001960418	0.001441979	0.0001594631
K10542_k002010	Transposons_EnvironmentalInformationProcessing_Membranetransport_mgA_methyl-galactosyltransferase[EC:3.6.1.37]	0.000342295	0.000274077	0.000274077
K11444_k002020	Two-componentsystem_EnvironmentalInformationProcessing_Signaltransduction_wspR_two-componentsystem,chemotaxisfamily,responderegulatorWspR[EC:2.7.7.65]	3.1117E-05	0.000326101	0.000326101
K02471_k002010	Transposons_EnvironmentalInformationProcessing_Membranetransport_ydA(yup)ATP-bindingcasasetransferase	2.03813E-05	9.13591E-05	9.13591E-05
K00356_k00530	Oxidativephosphorylation_Metabolism_HumanDiseases_Cancers_PK_pyk_pyruvatekinase[EC:2.7.1.40](K00873_k005203_	8.29817E-05	4.5813E-05	2.49161E-05
K00873_k005203	Oxidativephosphorylation_Metabolism_HumanDiseases_Cancers_PK_pyk_pyruvatekinase[EC:2.7.1.40](K00873_k005203_	0.000145216	0.000137574	0.00010797
K01091_k00630	Glyoxylateanddicarboxylatemetabolism_Metabolism_Carbohydratemetabolism_E3.1.1.38	0.0001327691	0.000117702	0.0001254111
K01867_k00970	Aminoacyl-HRNABiosynthesis_GeneticInformationProcessing_Transcription_WARS_TpRS_TpR(yup)thioaminoacyl-HRNAsynthetase[EC:6.1.1.2]	0.000909582	0.001080211	0.000149467
K00680_k00350	Transposons_EnvironmentalInformationProcessing_Membranetransport_pnA_spermidine(poly)acetyltransferase[EC:3.1.1.2]	0.001405485	0.000147551	0.0001215284
K1072_k002010	Transposons_EnvironmentalInformationProcessing_Membranetransport_pnA_spermidine(poly)acetyltransferase[EC:3.1.1.2]	0.006861464	0.00679175	0.007299117
K1072_k002010	Transposons_EnvironmentalInformationProcessing_Membranetransport_pnA_spermidine(poly)acetyltransferase[EC:3.1.1.2]	0.001109866	0.000953827	0.000747483
K01735_k00040	Phenylalanine,tyrosineandtryptophanbiosynthesis_Metabolism_Aminoacidmetabolism_arbD3_3-dehydroquinate[EC:4.2.3.4](K01735_k00230_Biosynthesisofaminoacids_Metabolism_Overview_arbD3_3-dehydroquinate[EC:4.2.3.4]	0.001021699	0.001029237	0.001295638
K01834_k005200	Centralcarboxymethyltransferase_HumanDiseases_Cancers_PGAM2.3_bisphosphoglycerate-dependentphosphoglycerate[EC:5.4.2.11](K01834_k00280_Glycine,serineandthreoninemetabolism_Metabolism_Aminoacidmetabolism	0.000184383	0.002585866	0.002585866
K02405_k002040	Flagellarassembly_Organismsystem_Cellmobility_fliH_flagellarM-ringproteinHfl	0.000114098	0.000122288	8.3037E-05
K12340_k002010	Transposons_EnvironmentalInformationProcessing_Membranetransport_tolC_outermembranechannelprotein;K12340_k005133_P	0.000580865	0.000973209	0.001054782
K03544_k004112	Celastrolide_Caulobacter_CellularProcesses_Cellgrowthanddeath_cIpx_CLPX-ATP-dependentCIPtransferaseATP-bindingubiquitinCIPX	0.002427184	0.002211565	0.002084648
K07309_k00450	Selenocompoundmetabolism_Metabolism_Metabolismofotheraminoacids_yHcE_Tar-targetedethionyltransferaseubiquitinYHcE[EC:1.97.1.9]	1.5589E-05	1.56607E-05	1.66107E-05
K00602_k00670	Oncarboxymethyltransferase_Metabolism_Metabolismofcofactorsandvitamins_purH_phosphoribosylaminonucleotidesubunit[EC:1.97.1.9]	0.001146975	0.001391026	0.001204279
K02536_k00540	Lipopolysaccharidebiosynthesis_Metabolism_Glycanbiosynthesisandmetabolism_lpxD_UDP-3-O-β-D-hydroxybutyryl]glucosamine-acyltransferase[EC:2.3.1.191]	0.0005233815	0.000402531	0.000597987
K02844_k00540	Lipopolysaccharidebiosynthesis_Metabolism_Glycanbiosynthesisandmetabolism_waaG_HgC-UDP-glucose:(heptose)yl]P-α-1,3-galactosyltransferase[EC:2.4.1.1]	0.000233383	0.000275148	0.000440185
K01438_k00330	Arginineandprolinecatabolism_Metabolism_Aminoacidmetabolism_argE_acylornithineacetylase[EC:3.5.1.16](K01438_ko	0.000320625	0.000300625	0.000270764
K00257_k002010	Arginineandprolinecatabolism_Metabolism_Aminoacidmetabolism_argE_acylornithineacetylase[EC:3.5.1.16](K01438_ko	0.00012862	0.000942637	0.000880369
K10012_k00520	Amino sugarandnucleosidecatabolism_Metabolism_Carbohydratemetabolism_aNC_pmp_undecapentosephosphate4-deoxy-4-formamide-L-arabinosetransferase[EC:2.4.2.53]	9.85395E-05	5.60487E-05	9.13591E-05
K01854_k00050	Galactosemetabolism_Metabolism_Carbohydratemetabolism_eff_UDP_galactopyranosemutase[EC:5.4.99.9]	0.0001758153	0.000986885	0.000164464
K01897_k00330	Arginineandprolinecatabolism_Metabolism_Aminoacidmetabolism_E4.1.1.19_argininecatabolase[EC:4.1.1.19]	0.000134844	4.07627E-05	0.000134581
K13497_k00040	Phenylalanine,tyrosineandtryptophanbiosynthesis_Metabolism_Aminoacidmetabolism_trpGD_antI	9.85395E-05	4.07627E-05	0
K02141_k00930	Neomycinbiosynthesis_Metabolism_Metabolismofcofactorsandvitamins_BLVpA_bvA_BiVernindolizyltransferase[EC:1.3.1.24]	4.14903E-05	8.66207E-05	1.66107E-05
K01815_k002010	Pentoseandgluconateinterconversions_Metabolism_Carbohydratemetabolism_kduJ_4-deoxy-L-threo-5-hexoseulose-uronateketol-isomerase[EC:5.3.1.17]	0.000274873	0.000224195	0.000174413
K02063_k00040	Transposons_EnvironmentalInformationProcessing_Membranetransport_tHP_thiaminetransposonemergease[EC:5.3.1.17]	3.6304E-05	2.54767E-05	2.49161E-05
K01924_k002010	Transposons_EnvironmentalInformationProcessing_Membranetransport_ABC_NGC-SN-acyetylglucosaminetransposonsubstrate-bindingprotein	0.00067169	0.000636917	0.0001445135
K01924_k002010	Transposons_EnvironmentalInformationProcessing_Membranetransport_ABC_NGC-SN-acyetylglucosaminetransposonsubstrate-bindingprotein	0.001275828	0.001294215	0.001254111
K01913_k00960	Tropone,perindolinediethylalcoholbiosynthesis_Metabolism_Glycanbiosynthesisandmetabolism_murCD_UDP-N-acetylmuramate-alminalinase[EC:3.2.2.8](K01924_k000471_D-GlutamineandD-glutamatemetabolism_Metabolism_Metabolismofotheramir	5.18629E-05	5.81376E-05	5.81376E-05
K00325_k00760	Nicotinamideandnicotinamidebiosynthesis_Metabolism_Biosynthesisofothercoenzymesubunit[EC:1.10.3.1](K00325_k000903_Limoneneandgeranienedegradation_Metabolism_Metabolismofotherpenoisandubiquitin[EC:1.8.98.1]	0.000129657	5.09533E-06	6.6443E-05
K13834_k005144	Malaria_HumanDiseases_SPECT2_sporozoitocromoneprotein2	1.03726E-05	0	0
K01657_k00400	Phenylalanine,tyrosineandtryptophanbiosynthesis_Metabolism_Aminoacidmetabolism_trpE_anthranilate[EC:2.3.1.27](K01657_k00230_Biosynthesisofaminoacids_Metabolism_Overview_trpE_anthranilate[EC:2.3.1.27]	0.00032155	0.000463675	0.000390352
K07775_k002020	Two-componentsystem_EnvironmentalInformationProcessing_Signaltransduction_resD_two-componentsystem,OmpRfamily,responderegulatorResD	0.001472907	0.001115378	0.001362081
K00425_k001200	Carbonmetabolism_Metabolism_Overview_hdrD_heterodisulfide[EC:2.4.2.17](K00765_k001230_Biosynthesisofaminoacids_Metabolism_Overview_hisG_ATP-phosphoribosyltransferase[EC:2.4.2.17]	0.000809061	0.000662393	0.00055646
K00765_k001200	Carbonmetabolism_Metabolism_Overview_hdrD_heterodisulfide[EC:2.4.2.17](K00765_k001230_Biosynthesisofaminoacids_Metabolism_Overview_hisG_ATP-phosphoribosyltransferase[EC:2.4.2.17]	0.000165961	1.5286E-05	0.00010797
K00765_k001200	Carbonmetabolism_Metabolism_Overview_hdrD_heterodisulfide[EC:2.4.2.17](K00765_k001230_Biosynthesisofaminoacids_Metabolism_Overview_hisG_ATP-phosphoribosyltransferase[EC:2.4.2.17]	0.000451207	0.000417817	0.00034052
K13533_k00200	Two-componentsystem_EnvironmentalInformationProcessing_Signaltransduction_kinE_two-componentsystem,sporulationensorkinase[EC:2.7.13.3]	0	5.09533E-06	2.49161E-05
K02195_k00930	Neomycinbiosynthesis_Metabolism_Metabolismofcofactorsandvitamins_henM_henZ_oxygen-independentprotoporphyrinogenoxidase[EC:1.3.1.99.22]	0.001519383	0.001498028	0.001644464
K00789_k002020	Oxidativephosphorylation_Metabolism_Aminoacidmetabolism_mekK5_adenosylmethioninesynthetase[EC:2.5.1.6](K00789_k001789_k001230_Biosynthesisofaminoacids_Metabolism_Overview_mekK5_adenosylmethioninesynthetase[EC:2.5.1.6]	0.001773712	0.001701841	0.001602937
K00342_k00350	Oxidativephosphorylation_Metabolism_Energymetabolism_nuoM_NADH-quinoneoxidoreductaseubiquin[EC:1.6.5.3]	0.000115063	0.000975304	0.000622903
K07715_k002020	Two-componentsystem_EnvironmentalInformationProcessing_Signaltransduction_gRR_gseF_two-componentsystem,NtrCfamily,responderegulatorGRR	0.000124471	0.000142669	9.13591E-05
K07152_k00320	Cysteineandmethioninemetabolism_Metabolism_Aminoacidmetabolism_E4.3.1.17_sdbA_L-serinehydratase[EC:4.3.1.17](K07152_k00260_Glycine,serineandthreoninemetabolism_Metabolism_Aminoacidmetabolism_E4.3.1.17_sdbA_L-serine	0.00097601	0.000856016	0.000830537
K02803_k002010	Transposons_EnvironmentalInformationProcessing_Membranetransport_PTS-Nag-ElB_nagE_PTSsystem_N-acetylglucosamine-specificoligomer[EC:7.1.6.9](K02803_k000520_Aminoglycosidicantibioticdegradatemetabolism_Metabolism_Carbo	0.000165961	0.000112097	0.000116275
K01232_k000260	Glycine,serineandthreoninemetabolism_Metabolism_Aminoacidmetabolism_trecThreoninesynthase[EC:2.3.1.3](K01733_k00750_VitaminB6metabolism_Metabolismofcofactorsandvitamins_thrC_threoninesynthase[EC:2.3.1.3](K01	0.000978304	0.000978304	0.000978304
K01232_k00050	Starchandsucrosemetabolism_Metabolism_Carbohydratemetabolism_trecThreoninesynthase[EC:2.3.1.3](K01733_k00750_VitaminB6metabolism_Metabolismofcofactorsandvitamins_thrC_threoninesynthase[EC:2.3.1.3](K01	0.000207452	0.000168146	0.000157802
K01845_k00040	Pentoseandgluconateinterconversions_Metabolism_Carbohydratemetabolism_usaA_altronatehydrolyase[EC:3.2.1.193]	0.000331923	0.000387245	0.000440185
K09815_k002010	Transposons_EnvironmentalInformationProcessing_Membranetransport_znuA_zinctransposonsubstrate-bindingprotein	0.000554933	0.000562393	0.000780705
K01042_k005143	Africantrypanosiasis_HumanDiseases_infectiousdiseases_pRR_oligopeptidase[EC:3.4.21.83](K01554_k005142_Chagasdisease(Americantrypanosomiasis)_HumanDiseases_infectiousdiseases_pRR_oligopeptidase[EC:3.4.21.83]	9.85395E-05	0.000193623	0.000257467
K0137E-05	Phenylalanine,tyrosineandtryptophanbiosynthesis_Metabolism_Aminoacidmetabolism_murCD_UDP-N-acetylmuramate-alminalinase[EC:3.2.2.8](K01924_k000471_D-GlutamineandD-glutamatemetabolism_Metabolism_Metabolismofotheramir	3.1117E-05	5.09533E-06	4.15269E-05
K0106_k002010	Transposons_EnvironmentalInformationProcessing_Membranetransport_SRPS4_Fts_splincapnicaptilin[EC:3.4.3.10](K0106_k004120_Ubiquitinmediatedproteolysis_GeneticInformationProcessing_Folding_sortinganddegradation_SRPS4)	0.000330206	0.000191075	0.000107075
K09011_k000390	Villine,leucineandisoleucinebiosynthesis_Metabolism_Aminoacidmetabolism_cimA-D_ε-aminoacyltransferase[EC:2.3.1.182](K09011_k001210_Oxocarboxylicacidmetabolism_Metabolism_Overview_cimA-D_citramalatesynthase[EC:2.3.1.182](K09011	0.000171148	0.000293481	0.000207634
K0684_k00050	Starchandsucrosemetabolism_Metabolism_Carbohydratemetabolism_kcsA_cellobiosynthase[EC:4.1.1.2]	7.77944E-05	0.000137574	0.000116275
K01804_k00940	Pentoseandgluconateinterconversions_Metabolism_Carbohydratemetabolism_arA_L-arabinosidaseubiquitin[EC:1.99.4.4]	0.01099894	0.000850563	0.000830537
K00782_k00930	Neomycinbiosynthesis_Metabolism_Energymetabolism_nsaX_ssimilatorylactate reductase catalytic subunit[EC:1.7.99.4]	3.6304E-05	0.000112097	0.00010797
K00366_k00910	Nitrogenmetabolism_Metabolism_Energymetabolism_nirA_Ferredoxin-nitrite reductase[EC:1.7.1.1]	7.77944E-05	0.000321006	0.000207634
K02642_k002020	Two-componentsystem_EnvironmentalInformationProcessing_Signaltransduction_baeS_baeT_two-componentsystem,OmpRfamily,ensorhisidkinaseBase[EC:2.7.13.3]	0.000230011	0.00032479	0.000141191
K00245_k002020	Two-componentsystem_EnvironmentalInformationProcessing_Signaltransduction_rFB_fumarate reductase-sulfur subunit[EC:1.3.5.4](K00245_k000020_Citratecycle(TCA cycle)_Metabolism_Carbohydratemetabolism_rFB_fumarate reductase	7.26081E-05	0.000157802	0.000137241
K01026_k00630	Glyoxylateanddicarboxylatemetabolism_Metabolism_Carbohydratemetabolism_pct_pronotateCoA-transferase[EC:2.8.3.1](K01026_k001026_PyruvateCoA-transferase[EC:2.8.3.1]	0.000254128	0.000157955	0.000191024
K00104_k00630	Glyoxylateanddicarboxylatemetabolism_Metabolism_Carbohydratemetabolism_β(kD)γ-cyolite oxidase[EC:1.3.1.15]	0.000394158	0.000270053	0.000351544













K00900	Terpenoidbackbonebiosynthesis	Metabolism	Lipidmetabolism	Terpenoidbackbonebiosynthesis	Metabolism	0.000897228	0.000032446	0.000647819
K12506	Terpenoidbackbonebiosynthesis	Metabolism	Metabolism	Terpenoidbackbonebiosynthesis	Metabolism	7.13347E-05	0.000116275	0.000116275
K13498	Phenylalanine, tyrosine and tryptophan biosynthesis	Metabolism	Metabolism	Phenylalanine, tyrosine and tryptophan biosynthesis	Metabolism	2.59315E-05	0.0001907E-05	0
K02563	Cellulose Catabolism	CellularProcess	CellularProcess	Cellulose Catabolism	CellularProcess	0.000938719	0.000122288	0.0001079688
K00132	Glucosyl-Lipid metabolism	Metabolism	Lipid metabolism	Glucosyl-Lipid metabolism	Metabolism	4.6766E-05	1.5286E-05	1.66107E-05
K04000	Glucosyl-Lipid metabolism	Metabolism	Lipid metabolism	Glucosyl-Lipid metabolism	Metabolism	0.000233383	0.0002339481	0.000199329
K02491	Two-component system	EnvironmentalInformationProcessing	SignalTransduction	Two-component system	EnvironmentalInformationProcessing	5.18629E-06	0	2.49161E-05
K07015	Two-component system	EnvironmentalInformationProcessing	SignalTransduction	Two-component system	EnvironmentalInformationProcessing	2.07452E-05	1.01907E-05	0
K00002	Glucose homeostasis	Metabolism	Carbohydrate metabolism	Glucose homeostasis	Metabolism	5.60487E-05	4.15269E-05	4.15269E-05
K13529	Basexcretion pathway	GeneticInformationProcessing	ReplicationandRepair	Basexcretion pathway	GeneticInformationProcessing	2.59315E-05	2.54767E-05	0
K01613	Glucosyl-Lipid metabolism	Metabolism	Lipid metabolism	Glucosyl-Lipid metabolism	Metabolism	0.000438786	0.000438588	0.000448489
K01684	Glucosyl-Lipid metabolism	Metabolism	Lipid metabolism	Glucosyl-Lipid metabolism	Metabolism	0.000145216	8.15253E-05	0.000207634
K00164	Glucosyl-Lipid metabolism	Metabolism	Lipid metabolism	Glucosyl-Lipid metabolism	Metabolism	2.59315E-05	1.5286E-05	1.66107E-05
K00826	Valine, leucine and isoleucine biosynthesis	Metabolism	Amino acid metabolism	Valine, leucine and isoleucine biosynthesis	Metabolism	0.000299967	0.000089698	0.000089698
K00145	Glucosyl-Lipid metabolism	Metabolism	Lipid metabolism	Glucosyl-Lipid metabolism	Metabolism	0.000234337	0.000514629	0.000373742
K00250	Arginine and ornithine biosynthesis	Metabolism	Amino acid metabolism	Arginine and ornithine biosynthesis	Metabolism	4.6766E-05	2.54767E-05	1.66107E-05
K07250	Alanine, aspartate and glutamate metabolism	Metabolism	Amino acid metabolism	Alanine, aspartate and glutamate metabolism	Metabolism	7.26081E-05	0.000101907	0.000132886
K03430	Phosphatidylethanolamine metabolism	Metabolism	Lipid metabolism	Phosphatidylethanolamine metabolism	Metabolism	0.0001052817	0.000166831	0.000838843
K01711	Two-component system	EnvironmentalInformationProcessing	SignalTransduction	Two-component system	EnvironmentalInformationProcessing	0.000497884	0.000394488	0.000408693
K00259	Two-component system	EnvironmentalInformationProcessing	SignalTransduction	Two-component system	EnvironmentalInformationProcessing	0.000954278	0.0001054734	0.000921896
K00133	Glucosyl-Lipid metabolism	Metabolism	Lipid metabolism	Glucosyl-Lipid metabolism	Metabolism	0.000430662	0.000351578	0.00023255
K08478	Arginine and ornithine metabolism	Metabolism	Amino acid metabolism	Arginine and ornithine metabolism	Metabolism	8.29807E-05	8.15253E-05	0.000132886
K00325	Two-component system	EnvironmentalInformationProcessing	SignalTransduction	Two-component system	EnvironmentalInformationProcessing	3.1117E-05	7.643E-05	3.32215E-05
K01103	Tryptophan metabolism	Metabolism	Carbohydrate metabolism	Tryptophan metabolism	Metabolism	5.18629E-06	0	3.32215E-05
K01259	Basexcretion pathway	GeneticInformationProcessing	ReplicationandRepair	Basexcretion pathway	GeneticInformationProcessing	5.18629E-05	0.000132479	0.000191024
K00818	Arginine and ornithine metabolism	Metabolism	Amino acid metabolism	Arginine and ornithine metabolism	Metabolism	0.000414903	0.000478961	0.000465101
K03271	Glucosyl-Lipid metabolism	Metabolism	Lipid metabolism	Glucosyl-Lipid metabolism	Metabolism	0.000186706	0.00015286	0.000373742
K00847	Glucosyl-Lipid metabolism	Metabolism	Lipid metabolism	Glucosyl-Lipid metabolism	Metabolism	0.000731267	0.001182117	0.000838843
K07796	Two-component system	EnvironmentalInformationProcessing	SignalTransduction	Two-component system	EnvironmentalInformationProcessing	0.000116033	0.000203813	0.000274077
K11688	Two-component system	EnvironmentalInformationProcessing	SignalTransduction	Two-component system	EnvironmentalInformationProcessing	0.001021469	0.000692965	0.000863759
K00640	Two-component system	EnvironmentalInformationProcessing	SignalTransduction	Two-component system	EnvironmentalInformationProcessing	0.00145217	0.001295638	0.001295638
K13787	Terpenoidbackbonebiosynthesis	Metabolism	Lipid metabolism	Terpenoidbackbonebiosynthesis	Metabolism	6.1144E-05	2.49161E-05	2.49161E-05
K00785	Biosynthesis of porphyrin and heme	Metabolism	Metabolism	Biosynthesis of porphyrin and heme	Metabolism	1.01907E-05	1.66107E-05	1.66107E-05
K01736	Two-component system	EnvironmentalInformationProcessing	SignalTransduction	Two-component system	EnvironmentalInformationProcessing	0.000647107	0.000531544	0.000531544
K02936	Two-component system	EnvironmentalInformationProcessing	SignalTransduction	Two-component system	EnvironmentalInformationProcessing	0.000426898	0.000369533	0.000568765
K13985	Retinol metabolism	Metabolism	Lipid metabolism	Retinol metabolism	Metabolism	4.6766E-05	9.68113E-05	0.000157802
K03382	Two-component system	EnvironmentalInformationProcessing	SignalTransduction	Two-component system	EnvironmentalInformationProcessing	4.9832E-05	4.9832E-05	4.9832E-05
K00575	Two-component system	EnvironmentalInformationProcessing	SignalTransduction	Two-component system	EnvironmentalInformationProcessing	5.60487E-05	9.13591E-05	9.13591E-05
K03524	Two-component system	EnvironmentalInformationProcessing	SignalTransduction	Two-component system	EnvironmentalInformationProcessing	0.000466766	0.00043544	0.000531544
K13280	Ubiquitin-mediated proteolysis	GeneticInformationProcessing	Folding, sorting and degradation	Ubiquitin-mediated proteolysis	GeneticInformationProcessing	0.000689777	0.000738823	0.000917129
K02401	Glucosyl-Lipid metabolism	Metabolism	Lipid metabolism	Glucosyl-Lipid metabolism	Metabolism	0.000186706	0.000122288	4.9832E-05
K04517	Phenylalanine, tyrosine and tryptophan biosynthesis	Metabolism	Amino acid metabolism	Phenylalanine, tyrosine and tryptophan biosynthesis	Metabolism	0.000285246	0.000203813	0.000274077
K00249	Valine, leucine and isoleucine degradation	Metabolism	Carbohydrate metabolism	Valine, leucine and isoleucine degradation	Metabolism	7.26081E-05	2.54767E-05	9.13591E-05
K13017	Two-component system	EnvironmentalInformationProcessing	SignalTransduction	Two-component system	EnvironmentalInformationProcessing	0.000103726	0.000443294	0.000166107
K00748	Two-component system	EnvironmentalInformationProcessing	SignalTransduction	Two-component system	EnvironmentalInformationProcessing	0.00031923	0.000443294	0.000332215
K02108	Glucosyl-Lipid metabolism	Metabolism	Lipid metabolism	Glucosyl-Lipid metabolism	Metabolism	0.00068459	0.000668787	0.000838843
K00946	Two-component system	EnvironmentalInformationProcessing	SignalTransduction	Two-component system	EnvironmentalInformationProcessing	0.000352668	0.000361769	0.000408693
K07645	Two-component system	EnvironmentalInformationProcessing	SignalTransduction	Two-component system	EnvironmentalInformationProcessing	2.59315E-05	2.03813E-05	0
K02845	Glucosyl-Lipid metabolism	Metabolism	Lipid metabolism	Glucosyl-Lipid metabolism	Metabolism	4.14903E-05	2.03813E-05	3.32215E-05
K02364	Two-component system	EnvironmentalInformationProcessing	SignalTransduction	Two-component system	EnvironmentalInformationProcessing	0.000103726	0.000132479	4.9832E-05
K02492	Retinol metabolism	Metabolism	Lipid metabolism	Retinol metabolism	Metabolism	0.000165961	0.00098215	0.000373742
K03462	Two-component system	EnvironmentalInformationProcessing	SignalTransduction	Two-component system	EnvironmentalInformationProcessing	4.14903E-05	4.07627E-05	2.49161E-05
K00095	Fructose and mannose metabolism	Metabolism	Carbohydrate metabolism	Fructose and mannose metabolism	Metabolism	7.26081E-05	8.15253E-05	0.000116275
K03856	Glucosyl-Lipid metabolism	Metabolism	Lipid metabolism	Glucosyl-Lipid metabolism	Metabolism	0.000285246	0.000270053	0.000498322
K03816	Phenylalanine, tyrosine and tryptophan biosynthesis	Metabolism	Amino acid metabolism	Phenylalanine, tyrosine and tryptophan biosynthesis	Metabolism	0.00037109	0.000428008	0.000207634
K04566	Glucosyl-Lipid metabolism	Metabolism	Lipid metabolism	Glucosyl-Lipid metabolism	Metabolism	5.18629E-05	1.01907E-05	5.81376E-05
K05131	Glucosyl-Lipid metabolism	Metabolism	Lipid metabolism	Glucosyl-Lipid metabolism	Metabolism	3.6304E-05	4.07627E-05	4.15269E-05
K03280	Glucosyl-Lipid metabolism	Metabolism	Lipid metabolism	Glucosyl-Lipid metabolism	Metabolism	3.1117E-05	5.60487E-05	7.47483E-05
K03390	Glucosyl-Lipid metabolism	Metabolism	Lipid metabolism	Glucosyl-Lipid metabolism	Metabolism	3.1117E-05	1.5286E-05	8.30537E-05
K00939	Glucosyl-Lipid metabolism	Metabolism	Lipid metabolism	Glucosyl-Lipid metabolism	Metabolism	7.26081E-05	5.60487E-05	2.49161E-05
K00938	Glucosyl-Lipid metabolism	Metabolism	Lipid metabolism	Glucosyl-Lipid metabolism	Metabolism	0.000803875	5.60487E-05	4.15269E-05
K00721	Two-component system	EnvironmentalInformationProcessing	SignalTransduction	Two-component system	EnvironmentalInformationProcessing	0.00127683	0.001472551	0.001544799
K00886	Glucosyl-Lipid metabolism	Metabolism	Lipid metabolism	Glucosyl-Lipid metabolism	Metabolism	0.000114698	8.15253E-05	0.000149497
K00931	Two-component system	EnvironmentalInformationProcessing	SignalTransduction	Two-component system	EnvironmentalInformationProcessing	0.000191893	0.000331197	0.000274077
K00932	Two-component system	EnvironmentalInformationProcessing	SignalTransduction	Two-component system	EnvironmentalInformationProcessing	0.000436448	0.000489152	0.000332215
K00215	Glucosyl-Lipid metabolism	Metabolism	Lipid metabolism	Glucosyl-Lipid metabolism	Metabolism	0.000166766	0.000264957	0.000307299
K01046	Glucosyl-Lipid metabolism	Metabolism	Lipid metabolism	Glucosyl-Lipid metabolism	Metabolism	0.00015708	0.000820349	0.000805621
K00261	Alanine, aspartate and glutamate metabolism	Metabolism	Amino acid metabolism	Alanine, aspartate and glutamate metabolism	Metabolism	0.000171448	0.000472669	0.000166107
K00259	Two-component system	EnvironmentalInformationProcessing	SignalTransduction	Two-component system	EnvironmentalInformationProcessing	0.000215708	0.00012586	0.000290688



K02048	ko00920_Sulfurmetabolism_Metabolism_Energymetabolism_cyP_sbp_sulfate transport systems substrat	4,66766E-05	3,56673E-05	8,30537E-05
K10561	ko02010_Transporters_EnvironmentalInformationProcessing_Membranetransport_rhO_chromosom transport systems permease/protein	0	5,09533E-06	8,30537E-06
K10942	ko02020_Two-componentsystem_EnvironmentalInformationProcessing_Signals transduction_fibB/fus_two-componentsystem_sensoryhistidinekinase/respE[EC:2.7.13.3];k10942_ko05111_Vibriocholeeraepathogeniccycle_HumanDiseases_infectiousdiseases_fibB_f	2,58915E-05	5,09533E-06	4,15269E-05
K01639	ko00530_Amino-sugar-and-nucleotide-sugarmetabolism_Metabolism_Carbohydratemetabolism_E4.1.3.3.narXa,NPL-N-acetylneuraminicase[EC:4.1.3.3]	0,000539374	0,000468199	0,000548155
K01599	ko00930_Nonmetabolism_Metabolismof cofactors and vitamins_hemE/URD_uncoupling_inorganic_catabolism/oxalate[EC:4.1.1.37]	0,000549747	0,000713347	0,001386997
K02044	ko00920_Cysteineandmethioninemetabolism_Metabolism_Aminoacidmetabolism_mdh_malatedehydrogenase[EC:1.1.1.37];k00024	0,000710522	0,000307002	0,00066443
K13771	ko00530_VitaminB6metabolism_Metabolismof cofactors and vitamins_E1.1.65.pyridoxal-dehydrogenase[EC:1.1.1.65]	4,14903E-05	3,0572E-05	2,49161E-05
K09459	ko02010_Transporters_EnvironmentalInformationProcessing_Membranetransport_cBM_cobal/nickel transport systems permease/protein	6,23255E-05	5,60487E-05	7,47483E-05
K09459	ko02010_Transporters_EnvironmentalInformationProcessing_Membranetransport_cBM_cobal/nickel transport systems permease/protein	0,000124471	0,000102288	0,00010797
K09487	ko04151_PIK-Akt signaling pathway_EnvironmentalInformationProcessing_Signals transduction_HSP90B,TRAI1,Hechtshockprotein90B,bea,KO9487_ko04141_Protein processing in the endoplasmic reticulum_GeneticInformationProcessing_Foldingsortinganddeg	8,15253E-05	0,000212957	0,000207634
K09352	ko00760_Nicotinateandnicotinamidetabolism_Metabolism_Metabolismof cofactors and vitamins_nadM_nicotinate-nucleotideadenylate transferase[EC:2.7.1.7]	0	1,5286E-05	0
K11473	ko00630_Glyoxylateanddicarboxylatemetabolism_Metabolism_Glyoxylateanddicarboxylatemetabolism_glxF_glyoxylatease/iron-sulfurubiquitin	1,03726E-05	0	0
K01997	ko02010_Two-componentsystem_EnvironmentalInformationProcessing_Signals transduction_wspE_two-componentsystem_chemotaxisfamily_sensoryhistidinekinase/respense/respase/protein	3,56673E-05	8,30537E-06	8,30537E-06
K03841	ko04151_PIK-Akt signaling pathway_EnvironmentalInformationProcessing_Signals transduction_FBP_fbp_fructose-1,6-bisphosphatase[EC:3.1.3.11];k03841_ko00051_Fructoseandmannosemetabolism_Metabolism_Carbohydratemetabolism_FBP_fbp_fructose	0,000117193	0,000124581	0,000135731
K02548	ko00130_Ubiquinoneandubiquinonemetabolism_Metabolism_Metabolismof cofactors and vitamins_meaA_1,4-dihydroxy-2-naphtholacetate pyruvate transferase[EC:2.5.1.742.5.1.1]	0,00037482	0,001037258	0,001287333
K1738	ko00220_Cysteineandmethioninemetabolism_Metabolism_Aminoacidmetabolism_cysK_cysteine synthase[EC:2.5.1.47];k01738_ko00920_Sulfurmetabolism_cysK_cysteine synthase[EC:2.5.1.47];k01738_ko01230_Biosynth	0,000373413	0,00053501	0,000382047
K02597	ko00670_Oxocarboxylatemetabolism_Metabolismof cofactors and vitamins_mefM_MTHFR_methyltetrahydrofolate reductase[NA0P][EC:1.5.1.20];k02597_ko01200_Carbonmetabolism_Metabolism_Overview_mefM_MTHFR_methyltetrahydr	5,70492E-05	1,01907E-05	8,30537E-06
K03230	ko02010_Transporters_EnvironmentalInformationProcessing_Membranetransport_yscV_sctV/hcrY/yellisecretin/protein	0,000771944	0,000718442	0,000103871
K10440	ko02010_Transporters_EnvironmentalInformationProcessing_Membranetransport_rbcS_ribosome transport systems permease/protein	0,000254128	0,000215099	0,000141191
K07109	ko00530_Amino-sugar-and-nucleotide-sugarmetabolism_Metabolism_Carbohydratemetabolism_rfG_CDP-glucose-4-dehydrogenase[EC:4.2.1.45]	5,70492E-05	5,60487E-05	2,49161E-05
K02319	ko00230_Purinemetabolism_Metabolism_Nucleotidemetabolism_DPA_poiB1_DNA polymerase[EC:2.7.7.7];k02319_ko00240_Pyrimidinemetabolism_Metabolism_Nucleotidemetabolism_DPA_poiB1_DNA polymerase[EC:2.7.7.7]	2,59315E-05	2,03813E-05	7,47483E-05
K11480	ko00330_Arginineandprolinemetabolism_Metabolism_Aminoacidmetabolism_E3.5.3.1.spbA arginase[EC:3.5.3.11]	0,000150402	0,000182718	0,000182718
K01517	ko00760_Nicotinateandnicotinamidetabolism_Metabolism_Metabolismof cofactors and vitamins_nadA quinolinate/nicotinate synthase[EC:2.5.1.72]	0,000746826	0,000888675	0,000888675
K13789	ko00900_Terpenoidandcarotenoidmetabolism_Metabolism_Metabolismof terpenoids and polyketides_GGPs_geranylgeranylphosphatase[EC:2.5.1.202.5.1.20]	0,000591237	0,000545201	0,000390532
K08878	ko00190_Oxidativephosphorylation_Metabolism_Energymetabolism_ndh_MADH dehydrogenase[EC:1.6.99.3]	0,000280243	0,000315604	0,000315604
K01781	ko00622_Aminobenzoate degradation_Metabolism_Lipidmetabolism_dhK_dihydroxycarboxylatemetabolism_nidA_mandelate acenase[EC:5.1.2.2]	0,000134844	0,000157955	0,000174443
K09692	ko02010_Transporters_EnvironmentalInformationProcessing_Membranetransport_nidA_mandelate acenase[EC:5.1.2.2]	6,23255E-05	5,60487E-05	2,49161E-05
K02843	ko00540_Uroporphyrinogen III biosynthesis_Metabolism_Glycambiosynthesis and heme metabolism_warF_PfPR_hepatitis virus transferase[EC:2.4.1.7]	0,000264501	0,000351578	0,000532391
K01865	ko00960_Traupane,piperidineandpyridinemetabolism_Metabolism_Biosynthesis of secondary metabolites_E3.1.1.1.esterase/lipase[EC:3.1.1.1];k01865_ko00963_Bisphenolide degradation_Metabolism_Xenobiotics biodegradation and metabolism_E3	0,00053501	0,00053501	0,00053501
K03851	ko00490_Traupane,piperidineandpyridinemetabolism_Metabolism_Metabolismof terpenoids and polyketides_tpa_taurine pyruvate transferase[EC:2.6.1.71]	7,26008E-05	5,09533E-06	0
K02591	ko00910_Pentoseandgluconatemetabolism_Metabolism_Energymetabolism_nfk_nitrogenase/lysozyme/nitroreductase[EC:1.38.6.1];k02591_ko00625_Chloroalkaneandchloroalkenedegradation_Metabolism_Xenobiotics biodegradation and metabolism_nfk_n	5,18629E-05	4,07627E-05	8,30537E-06
K06920	ko00785_Lipopolysaccharide synthesis_Metabolism_Carbohydratemetabolism_DHDH_dihydrodihydroxyacetone phosphate dehydrogenase[EC:3.8.6.1];k06920_ko00980_Metabolismof ketenolitecs by x-chromop450_Metabo	6,62393E-05	0,000116275	0,000116275
K07031	ko00540_Lipopolysaccharide synthesis_Metabolism_Glycambiosynthesis and heme metabolism_HdaD_glycero-alpha-D-manno-heptose-7-phosphatase[EC:2.7.1.168]	0,000372425	0,000372425	0,000315604
K12615	ko03018_RNA degradation_GeneticInformationProcessing_Folding sorting and degradation_EDC3_enhancer of RNA-decapping protein3	0,000212638	0,000210702	0,000240856
K03336	ko00630_Glyoxylateanddicarboxylatemetabolism_Metabolism_Carbohydratemetabolism_iold_3D-(3,5,4)-trihydroxycyclohexane-1,2-dione acylhydratase[EC:3.7.1.22]	5,18629E-05	7,643E-05	5,81376E-05
K05284	ko00563_Glyoxylateanddicarboxylatemetabolism_Metabolism_Glycambiosynthesis and heme metabolism_PiGM_phosphatidylinositol glycan, class M[EC:2.4.1.1]	1,03726E-05	1,01907E-05	1,66107E-05
K01995	ko02010_Transporters_EnvironmentalInformationProcessing_Membranetransport_jvg_branched-chain amino acid transport system ATP-binding protein	0,000611982	0,000504438	0,000498322
K03474	ko00750_VitaminB6metabolism_Metabolismof cofactors and vitamins_nrkX_pyridoxine-5-phosphatase[EC:2.5.4.3.3]	0,00018152	0,000244576	0,000116275
K02446	ko00951_Fructose and mannose metabolism_KanD_beta_hsl_nps_6-aminocaproate phosphatase[EC:5.4.3.3]	5,18629E-05	4,5858E-05	3,3215E-05
K01844	ko00350_Glycerophospholipidmetabolism_Metabolism_Lipidmetabolism_kanD_beta_hsl_nps_6-aminocaproate phosphatase[EC:5.4.3.3]	6,23255E-05	2,54767E-05	8,30537E-06
K01777	ko02020_Two-componentsystem_EnvironmentalInformationProcessing_Signals transduction_degS_two-componentsystem_Nar/family_sensoryhistidinekinase/DegS[EC:2.7.13.3]	0,000342295	0,000356673	0,0004849
K08882	ko00951_Fructose and mannose metabolism_Metabolism_Carbohydratemetabolism_Truk_1-phosphotransferase[EC:2.7.1.56]	3,1117E-05	5,09533E-06	5,81376E-05
K08239	ko04142_Zeatinome, Cellular Processes_Transport and metabolism_GNP7AB_UDP-N-acetylglucosamine-lysozyme-enzyme[EC:2.7.8.17]	0,000285246	0,000295529	0,000240856
K07091	ko00908_Zeatinbiosynthesis_Metabolismof terpenoids and polyketides_misA_TRIT1_RNAi methyltransferase[EC:2.5.1.79]	8,29807E-05	0,000122288	9,96645E-05
K07096	ko00785_Lipopolysaccharide synthesis_Metabolism_Metabolismof cofactors and vitamins_foP_dihydroxyacetone synthase[EC:2.5.1.15]	0,000985395	0,001263643	0,000968423
K01485	ko00330_Arginineandprolinemetabolism_Metabolism_Aminoacidmetabolism_codA_cytosine deaminase[EC:3.5.4.1];k01485_ko0240_Pyrimidinemetabolism_Nucleotidemetabolism_codA_cytosine deaminase[EC:3.5.4.1]	0,00037109	0,000519724	0,000390352
K01643	ko02020_Two-componentsystem_EnvironmentalInformationProcessing_Signals transduction_cifE_citr latease/substrate utilization/CoA-transferase[EC:2.8.3.10]	0,000119285	0,000224195	0,000166107
K03786	ko00400_Phenylalanine, tyrosine and tryptophan metabolism_Metabolism_Aminoacidmetabolism_arocQueE_3-dehydroquinate dehydratase[EC:4.2.1.10];k03786_ko01230_Biosynthesis of amino acids_Metabolism_Overview_arocQueE_3-dehydroquinate de	0,000259315	0,000208909	0,000147765
K01625	ko00630_Glyoxylateanddicarboxylatemetabolism_Metabolism_Carbohydratemetabolism_edb_2-dehydro-3-deoxyphosphogluconate aldolase[EC:4.2.1.14.1.3.42];k01625_ko0030_Pentose phosphate pathway_Metab	0,00046021	0,000438199	0,000415269
K02793	ko02010_Transporters_EnvironmentalInformationProcessing_Membranetransport_PTS_Nar-Xna-PTSsystem_mannose-specific amino acid transport system ATP-binding protein	0,000308005	0,000183432	0,000207634
K07095	ko00900_Terpenoidandcarotenoidmetabolism_Metabolism_Metabolismof terpenoids and polyketides_narX_pyridoxine-5-phosphatase[EC:2.5.1.12.5.1.10]	3,6304E-05	1,01907E-05	4,00526E-05
K01761	ko00270_Cysteineandmethioninemetabolism_Metabolism_Aminoacidmetabolism_E4.4.1.11.methionine-gamma-lyase[EC:4.4.1.11];k01761_ko00450_Selenocompoundmetabolism_Metabolism_Metabolismof selenoamino acids_E4.4.1.11.methionine-gamm	7,7994E-05	8,66207E-05	3,3215E-05
K00426	ko02020_Two-componentsystem_EnvironmentalInformationProcessing_Signals transduction_cyH7_cytochrome b/hydroquinone deacetylase[EC:1.10.3.1];k00426_ko00980_Oxidative phosphorylation_Metabolism_Energymetabolism_cyH8_cytochrome b/hydroquin	0,000560119	0,000331197	0,00065772
K14982	ko02020_Two-componentsystem_EnvironmentalInformationProcessing_Signals transduction_cyH7_cytochrome b/hydroquinone deacetylase[EC:2.7.13.3]	5,18629E-06	2,03813E-05	6,6443E-05
K0257	ko00300_Bacterialchemotaxis_Metabolism_Cellmobility_mob_chemotaxis protein Mob8_K0257_k00300_Flagellar assembly_Organism analysis_Cellmobility_mob8_chemotaxis protein Mob8	0,000468286	0,000468771	0,000490017
K00150	ko00010_Glyceraldehyde-3-phosphate dehydrogenase_Metabolism_Overview_gap2_glyceraldehyde-3-phosphate	1,55989E-05	2,54767E-05	0
K110707	ko02010_Transporters_EnvironmentalInformationProcessing_Membranetransport_ompR_family_sensoryhistidinekinase/ompR[EC:1.2.1.59];k0150_ko01230_Pentose phosphate pathway_Metabolism_Overview_gap2_glyceraldehyde-3-phosphate	3,1117E-05	5,09533E-06	2,49161E-05
K10336	ko02010_Transporters_EnvironmentalInformationProcessing_Membranetransport_ompR_family_sensoryhistidinekinase/ompR[EC:1.2.1.59];k00892_ko00040_Pentoseandgluconatemetabolism_Metabolism_Carbohydratemetabolism_djgD_3-dehydro-L-gulo	0,000193623	0,000193623	1,66107E-05
K00975	ko00052_Galactosemetabolism_Metabolism_Carbohydratemetabolism_djgD_3-dehydro-L-gulonate-2-dehydrogenase[EC:1.1.1.130];k00975_ko00194_Phototransduction_Metabolism_Energymetabolism	4,07627E-05	3,6304E-05	0,00066443
K00175	ko00020_Citrate cycle (TCA cycle)_Metabolism_Carbohydratemetabolism_K00175_ko01200_Carbonmetabolism_Metabolism_Overview_mefM_MTHFR_methyltetrahydrofolate reductase[NA0P][EC:1.5.1.20];k00175_ko02030_Bacterialchemotaxis_Organism analysis_Cellmobility_CheV;two-compo	0,000111327	0,000111327	9,96645E-05
K03415	ko02020_Two-componentsystem_EnvironmentalInformationProcessing_Signals transduction_chemotaxis family response regulator CheV;K03415_ko02030_Pentose phosphate pathway_Metabolism_Overview_gap2_glyceraldehyde-3-phosphate	0,000124471	0,000112097	0,000124471















K07659	ko02020	Two-componentsystem	Environmentalinformationprocessing_Signaltransduction_ompR	Two-componentsystem_ompR	Two-componentsystem_ompRfamilyphosphateregulationresponse	regulatorOmpR	3.1117E-05	1.5286E-05	1.66107E-05
K11689	ko02020	Two-componentsystem	Environmentalinformationprocessing_Signaltransduction_dtrC	Two-componentsystem_dtrC	Two-componentsystem_dtrCfamilyphosphatetransporter	DtrCsubunit	0.000197079	0.000254767	0.000265772
K10979	ko03040	Non-homologousrecombination	GenetinformatioProcessing_ReplicationandRepair_kuDNAend-bindingproteinku	Non-homologousrecombination_GeneticinformationProcessing_ReplicationandRepair_kuDNAend-bindingproteinku	Non-homologousrecombination_GeneticinformationProcessing_ReplicationandRepair_kuDNAend-bindingproteinku	ku	4.14903E-05	1.5286E-05	6.6443E-05
K12848	ko03040	Spliceosome	GeneticinformationProcessing_Transcription_DDX23	Spliceosome_GeneticinformationProcessing_Transcription_DDX23	Spliceosome_GeneticinformationProcessing_Transcription_DDX23	DDX23	2.0745E-05	0	0
K00483	ko00350	Yrosinome	Environmentalinformationprocessing_Signaltransduction	Yrosinome_Environmentalinformationprocessing_Signaltransduction	Yrosinome_Environmentalinformationprocessing_Signaltransduction	Yrosinome	2.59315E-05	0	1.66107E-05
K00579	ko05200	Thermodilactobacilliosis	Environmentalinformationprocessing_Signaltransduction	Thermodilactobacilliosis_Environmentalinformationprocessing_Signaltransduction	Thermodilactobacilliosis_Environmentalinformationprocessing_Signaltransduction	Thermodilactobacilliosis	1.58929E-06	1.01907E-05	0.000116275
K00587	ko00900	Chemicalcommunication	Environmentalinformationprocessing_Signaltransduction	Chemicalcommunication_Environmentalinformationprocessing_Signaltransduction	Chemicalcommunication_Environmentalinformationprocessing_Signaltransduction	Chemicalcommunication	3.32215E-05	2.54767E-05	4.9832E-05
K07694	ko02020	Two-componentsystem	Environmentalinformationprocessing_Signaltransduction	Two-componentsystem_ompR	Two-componentsystem_ompRfamilyphosphateregulationresponse	regulatorVraR	4.66766E-05	6.62393E-05	4.9832E-05
K03519	ko02020	Two-componentsystem	Environmentalinformationprocessing_Signaltransduction	Two-componentsystem	Two-componentsystem	Two-componentsystem	4.14903E-05	3.56673E-05	4.9832E-05
K10218	ko00630	Glyoxylateanddicarboxylatemetabolism	Environmentalinformationprocessing_Signaltransduction	Glyoxylateanddicarboxylatemetabolism	Glyoxylateanddicarboxylatemetabolism	Glyoxylateanddicarboxylatemetabolism	4.66766E-05	2.54767E-05	3.32215E-05
K11175	ko00630	Oxalateanddicarboxylatemetabolism	Environmentalinformationprocessing_Signaltransduction	Oxalateanddicarboxylatemetabolism	Oxalateanddicarboxylatemetabolism	Oxalateanddicarboxylatemetabolism	9.89359E-05	8.66207E-05	0.0004438
K02045	ko02010	Oncarboxylatemetabolism	Environmentalinformationprocessing_Signaltransduction	Oncarboxylatemetabolism	Oncarboxylatemetabolism	Oncarboxylatemetabolism	0.00034295	0.000504438	0.000406963
K03873	ko00230	Purinetriazinemetabolism	Environmentalinformationprocessing_Signaltransduction	Purinetriazinemetabolism	Purinetriazinemetabolism	Purinetriazinemetabolism	7.7794E-05	4.5858E-05	0.000157802
K01087	ko00500	Starchanddisaccharidemetabolism	Environmentalinformationprocessing_Signaltransduction	Starchanddisaccharidemetabolism	Starchanddisaccharidemetabolism	Starchanddisaccharidemetabolism	1.03726E-05	8.30537E-05	8.30537E-05
K03816	ko00230	Purinetriazinemetabolism	Environmentalinformationprocessing_Signaltransduction	Purinetriazinemetabolism	Purinetriazinemetabolism	Purinetriazinemetabolism	0.000244576	0.000244576	0.000290688
K13566	ko00250	Alanine	Environmentalinformationprocessing_Signaltransduction	Alanine	Alanine	Alanine	3.0572E-05	8.30537E-05	8.30537E-05
K02635	ko00195	Photosynthesis	Environmentalinformationprocessing_Signaltransduction	Photosynthesis	Photosynthesis	Photosynthesis	0	0	4.15269E-05
K00292	ko02010	Carboxylatemetabolism	Environmentalinformationprocessing_Signaltransduction	Carboxylatemetabolism	Carboxylatemetabolism	Carboxylatemetabolism	4.14903E-05	2.54767E-05	1.66107E-05
K10040	ko02010	Carboxylatemetabolism	Environmentalinformationprocessing_Signaltransduction	Carboxylatemetabolism	Carboxylatemetabolism	Carboxylatemetabolism	7.7794E-05	3.0572E-05	4.9832E-05
K01783	ko00910	Nitrogenmetabolism	Environmentalinformationprocessing_Signaltransduction	Nitrogenmetabolism	Nitrogenmetabolism	Nitrogenmetabolism	0.00034295	0.000224195	0.000298993
K01783	ko00910	Nitrogenmetabolism	Environmentalinformationprocessing_Signaltransduction	Nitrogenmetabolism	Nitrogenmetabolism	Nitrogenmetabolism	0	0.000682775	0.000606292
K01016	ko00910	Nitrogenmetabolism	Environmentalinformationprocessing_Signaltransduction	Nitrogenmetabolism	Nitrogenmetabolism	Nitrogenmetabolism	0	2.03833E-05	8.30537E-06
K09970	ko02010	Carboxylatemetabolism	Environmentalinformationprocessing_Signaltransduction	Carboxylatemetabolism	Carboxylatemetabolism	Carboxylatemetabolism	2.0745E-05	1.01907E-05	3.32215E-05
K02424	ko02010	Carboxylatemetabolism	Environmentalinformationprocessing_Signaltransduction	Carboxylatemetabolism	Carboxylatemetabolism	Carboxylatemetabolism	2.0745E-05	5.09533E-06	2.49161E-05
K14084	ko01200	Carbonylmetabolism	Environmentalinformationprocessing_Signaltransduction	Carbonylmetabolism	Carbonylmetabolism	Carbonylmetabolism	2.59315E-05	4.5858E-05	3.32215E-05
K07794	ko02020	Two-componentsystem	Environmentalinformationprocessing_Signaltransduction	Two-componentsystem	Two-componentsystem	Two-componentsystem	9.68113E-05	9.68113E-05	3.32215E-05
K03077	ko00052	Galactosemetabolism	Environmentalinformationprocessing_Signaltransduction	Galactosemetabolism	Galactosemetabolism	Galactosemetabolism	0.000243756	0.000243756	8.30537E-05
K07703	ko02020	Two-componentsystem	Environmentalinformationprocessing_Signaltransduction	Two-componentsystem	Two-componentsystem	Two-componentsystem	1.03726E-05	0	0
K06209	ko00400	Phenylalanine	Environmentalinformationprocessing_Signaltransduction	Phenylalanine	Phenylalanine	Phenylalanine	0.000112097	4.15269E-05	4.15269E-05
K05822	ko03010	Ribosome	Environmentalinformationprocessing_Signaltransduction	Ribosome	Ribosome	Ribosome	3.1117E-05	5.09533E-06	2.49161E-05
K02948	ko03010	Ribosome	Environmentalinformationprocessing_Signaltransduction	Ribosome	Ribosome	Ribosome	0.000845366	0.000682775	0.000631544
K07813	ko02020	Two-componentsystem	Environmentalinformationprocessing_Signaltransduction	Two-componentsystem	Two-componentsystem	Two-componentsystem	0.000243756	0.000280243	0.000686681
K10194	ko02020	Two-componentsystem	Environmentalinformationprocessing_Signaltransduction	Two-componentsystem	Two-componentsystem	Two-componentsystem	1.55589E-05	1.5286E-05	1.66107E-05
K00587	ko00900	Chemicalcommunication	Environmentalinformationprocessing_Signaltransduction	Chemicalcommunication	Chemicalcommunication	Chemicalcommunication	3.1117E-05	2.54767E-05	1.66107E-05
K00755	ko02020	Two-componentsystem	Environmentalinformationprocessing_Signaltransduction	Two-componentsystem	Two-componentsystem	Two-componentsystem	0.00035648	0.00068277	0.000597987
K05814	ko02010	Carboxylatemetabolism	Environmentalinformationprocessing_Signaltransduction	Carboxylatemetabolism	Carboxylatemetabolism	Carboxylatemetabolism	6.22355E-05	7.13347E-05	6.6443E-05
K03270	ko00540	Uroporphyrin	Environmentalinformationprocessing_Signaltransduction	Uroporphyrin	Uroporphyrin	Uroporphyrin	8.8167E-05	0.000168146	0.000116275
K02535	ko00540	Uroporphyrin	Environmentalinformationprocessing_Signaltransduction	Uroporphyrin	Uroporphyrin	Uroporphyrin	1.55589E-05	3.0572E-05	6.6443E-05
K12815	ko03040	Spliceosome	GeneticinformationProcessing_Transcription_DHX38	Spliceosome_GeneticinformationProcessing_Transcription_DHX38	Spliceosome_GeneticinformationProcessing_Transcription_DHX38	Spliceosome	1.55589E-05	1.01907E-05	0
K07789	ko02020	Two-componentsystem	Environmentalinformationprocessing_Signaltransduction	Two-componentsystem	Two-componentsystem	Two-componentsystem	6.304E-05	0	0
K07173	ko05111	Vibrio	Environmentalinformationprocessing_Signaltransduction	Vibrio	Vibrio	Vibrio	0.000448389	0.000448389	0.000182718
K15024	ko00630	Glyoxylateanddicarboxylatemetabolism	Environmentalinformationprocessing_Signaltransduction	Glyoxylateanddicarboxylatemetabolism	Glyoxylateanddicarboxylatemetabolism	Glyoxylateanddicarboxylatemetabolism	0.000264957	0.000132886	0.000264957
K02959	ko03010	Ribosome	Environmentalinformationprocessing_Signaltransduction	Ribosome	Ribosome	Ribosome	0.000985395	0.001655983	0.001926846
K08679	ko00500	Starchanddisaccharidemetabolism	Environmentalinformationprocessing_Signaltransduction	Starchanddisaccharidemetabolism	Starchanddisaccharidemetabolism	Starchanddisaccharidemetabolism	1.03726E-05	3.0572E-05	8.30537E-06
K06446	ko00930	Caprolactamdegradation	Environmentalinformationprocessing_Signaltransduction	Caprolactamdegradation	Caprolactamdegradation	Caprolactamdegradation	1.55589E-05	1.01907E-05	0
K02393	ko02040	Flagellin	Environmentalinformationprocessing_Signaltransduction	Flagellin	Flagellin	Flagellin	0.000395619	0.000395619	0.000395619
K10495	ko00785	Histidinemetabolism	Environmentalinformationprocessing_Signaltransduction	Histidinemetabolism	Histidinemetabolism	Histidinemetabolism	0.00014098	0.00014098	0.000207634
K00492	ko00340	Histidinemetabolism	Environmentalinformationprocessing_Signaltransduction	Histidinemetabolism	Histidinemetabolism	Histidinemetabolism	4.66766E-05	2.54767E-05	5.81376E-05
K02941	ko03010	Ribosome	Environmentalinformationprocessing_Signaltransduction	Ribosome	Ribosome	Ribosome	2.59315E-05	5.09533E-06	3.32215E-05
K00287	ko00785	Histidinemetabolism	Environmentalinformationprocessing_Signaltransduction	Histidinemetabolism	Histidinemetabolism	Histidinemetabolism	0.000425276	0.000425276	0.000498322
K03101	ko03010	Ribosome	Environmentalinformationprocessing_Signaltransduction	Ribosome	Ribosome	Ribosome	0.000106141	0.000178442	0.000722567
K02988	ko03010	Ribosome	Environmentalinformationprocessing_Signaltransduction	Ribosome	Ribosome	Ribosome	2.0745E-05	0.000601249	0.00082232
K01678	ko00630	Glyoxylateanddicarboxylatemetabolism	Environmentalinformationprocessing_Signaltransduction	Glyoxylateanddicarboxylatemetabolism	Glyoxylateanddicarboxylatemetabolism	Glyoxylateanddicarboxylatemetabolism	0.001085306	0.000647819	0.000647819
K02986	ko02010	Carboxylatemetabolism	Environmentalinformationprocessing_Signaltransduction	Carboxylatemetabolism	Carboxylatemetabolism	Carboxylatemetabolism	0.000456394	0.000257467	0.000257467
K00331	ko00190	Oxidativetransport	Environmentalinformationprocessing_Signaltransduction	Oxidativetransport	Oxidativetransport	Oxidativetransport	3.6304E-05	2.03813E-05	2.49161E-05
K03779	ko00630	Glyoxylateanddicarboxylatemetabolism	Environmentalinformationprocessing_Signaltransduction	Glyoxylateanddicarboxylatemetabolism	Glyoxylateanddicarboxylatemetabolism	Glyoxylateanddicarboxylatemetabolism	1.66107E-05	1.66107E-05	0.000124581
K02756	ko02020	Two-componentsystem	Environmentalinformationprocessing_Signaltransduction	Two-componentsystem	Two-componentsystem	Two-componentsystem	5.09533E-05	0.000244576	0.000124581
K01769	ko00630	Glyoxylateanddicarboxylatemetabolism	Environmentalinformationprocessing_Signaltransduction	Glyoxylateanddicarboxylatemetabolism	Glyoxylateanddicarboxylatemetabolism	Glyoxylateanddicarboxylatemetabolism	0.000331923	0.000244576	0.000249161
K10196	ko00564	Glyoxylateanddicarboxylatemetabolism	Environmentalinformationprocessing_Signaltransduction	Glyoxylateanddicarboxylatemetabolism	Glyoxylateanddicarboxylatemetabolism	Glyoxylateanddicarboxylatemetabolism	3.1117E-05	5.81376E-05	5.81376E-05
K01704	ko00630	Glyoxylateanddicarboxylatemetabolism	Environmentalinformationprocessing_Signaltransduction	Glyoxylateanddicarboxylatemetabolism	Glyoxylateanddicarboxylatemetabolism	Glyoxylateanddicarboxylatemetabolism	0.000432669	0.000432669	0.000116275
K02926	ko03010	Ribosome	Environmentalinformationprocessing_Signaltransduction	Ribosome	Ribosome	Ribosome	0.000242576	0.000310815	0.000240856
K03649	ko03410	Bax	Environmentalinformationprocessing_Signaltransduction	Bax	Bax	Bax	0.00073685	0.000749014	0.00055646
K03649	ko03410	Bax	Environmentalinformationprocessing_Signaltransduction	Bax	Bax	Bax	0.000160775	0.000249671	0.000298993
K03204	ko02010	Carboxylatemetabolism	Environmentalinformationprocessing_Signaltransduction	Carboxylatemetabolism	Carboxylatemetabolism	Carboxylatemetabolism	4.07627E-05	2.49161E-05	4.07627E-05
K14977	ko00230	Purinetriazinemetabolism	Environmentalinformationprocessing_Signaltransduction	Purinetriazinemetabolism	Purinetriazinemetabolism	Purinetriazinemetabolism	6.74218E-05	2.54767E-05	7.4783E-05
K00995	ko00564	Glyoxylateanddicarboxylatemetabolism	Environmentalinformationprocessing_Signaltransduction	Glyoxylateanddicarboxylatemetabolism	Glyoxylateanddicarboxylatemetabolism	Glyoxylateanddicarboxylatemetabolism	2.49161E-05	1.5286E-05	2.49161E-05
K00995	ko00564	Glyoxylateanddicarboxylatemetabolism	Environmentalinformationprocessing_Signaltransduction	Glyoxylateanddicarboxylatemetabolism	Glyoxylateanddicarboxylatemetabolism	Glyoxylateanddicarboxylatemetabolism	0.00043062	0.000550296	0.000597987







K01444	ko04142	Lysosome	CellularProcesses	Transportandataabolism	AGA_spgN4_(beta-N-acetylglucosaminyl)-L-asparaginase[EC:3.5.1.26];K01444_K000511_Otherglycandegradation_Metabolism_Glycanbiosynthesisandmetabolism_AGA_spgN4_(beta-Na	1,5589E-05	0,000219099	7,47483E-05	0
K0368	ko00910	Nitrogenmetabolism	Metabolism	Energymetabolism	nitr_nitritereductase(NO-forming)[EC:1.7.2.1]	5,18629E-06	0	0	0
K03126	ko00450	Selenocompoundmetabolism	Metabolism	Energymetabolism	metabolism_of_selenocompounds	1,01907E-05	0	1,66107E-05	0
K14941	ko00194	Phenolsynthesisproteins	Metabolism	Energymetabolism	cofC2_phospho-L-tyrosineyltransferase[EC:2.7.6.8]	1,03726E-05	0	3,32215E-05	0
K0718	ko00240	Pyrimidinemetabolism	Metabolism	Nucleotidemetabolism	F4_2.1.70_pseudouridylyltransferase[EC:2.7.1.70]	1,01907E-05	0	1,66107E-05	0
K02946	ko03010	Ribosome	GeneticInformationProcessing	Transcription	RP-S10_MRP510_rpsJ_smallsubunitribosomalproteinS10	0,000663845	0,000560487	0,000560487	0,000398658
K02952	ko03010	Ribosome	GeneticInformationProcessing	Transcription	RP-S13_rpsM_smallsubunitribosomalproteinS13	0,00078313	0,000642012	0,000642012	0,000398658
K02793	ko00930	Argininedeaminemetabolism	Metabolism	Aminoacidmetabolism	prdD_prolineindependentdHAP[EC:1.2.1.41]	4,14903E-05	0	0	0
K0773	ko02010	Citrateandprolineinterconversion	Membranetransport	PTS-Gat-EIaGatA_PTSsystem_glatcit-specificAkoComponent[EC:2.7.1.69];K02773_ko00052_Galactosemetabolism_Metabolism_Carbohydratemetabolism_PTS-Gat-EIaI	9,1716E-05	0,000141191	0,000141191	0	0
K10126	ko02020	Citrateandprolineinterconversion	Membranetransport	PTS-Gat-EIaGatA_PTSsystem_glatcit-specificAkoComponent[EC:2.7.1.69];K02773_ko00052_Galactosemetabolism_Metabolism_Carbohydratemetabolism_PTS-Gat-EIaI	7,13347E-05	4,15269E-05	4,15269E-05	0	0
K02618	ko00360	Phenylalaninemetabolism	Metabolism	Aminoacidmetabolism	Signaltransduction_dtdD_two-componentsystem,NtrCFamily_Co-dicarboxylatedehydrogenase[EC:3.2.3.21.17.1]	2,59315E-05	0	2,03813E-05	8,30537E-06
K00940	ko00230	Purinemetabolism	Metabolism	Nucleotidemetabolism	paaz_xoepin_CoAhydrolyase/3-oxo-5-6-dehydroxyl-CoA-dicarboxylatedehydrogenase[EC:3.2.3.21.17.1]	0,000160775	9,1716E-05	4,15269E-05	0
K03743	ko00760	Nicotinateandnicotinametabolism	Metabolism	Nucleotidemetabolism	ndk,NME,nucleoside-diphosphatekinase[EC:2.7.4.6]	6,22355E-05	0	6,6443E-05	0
K08730	ko00564	Glycerolphospholipidmetabolism	Metabolism	Metabolism	metabolism_of_glycerolphospholipids	1,01907E-05	0	1,66107E-05	0
K08730	ko00564	Glycerolphospholipidmetabolism	Metabolism	Metabolism	PTD552_phosphatidylserinesynthase[EC:3.5.1.42]	5,18629E-06	0	1,66107E-05	8,30537E-06
K02194	ko02010	Citrateandprolineinterconversion	Membranetransport	PTS-Gat-EIaGatA_PTSsystem_glatcit-specificAkoComponent[EC:2.7.1.69];K02773_ko00052_Galactosemetabolism_Metabolism_Carbohydratemetabolism_PTS-Gat-EIaI	1,03726E-05	0	1,03726E-05	0	0
K02456	ko02010	Citrateandprolineinterconversion	Membranetransport	PTS-Gat-EIaGatA_PTSsystem_glatcit-specificAkoComponent[EC:2.7.1.69];K02773_ko00052_Galactosemetabolism_Metabolism_Carbohydratemetabolism_PTS-Gat-EIaI	2,07452E-05	0	1,01907E-05	0	0
K07168	ko00340	Basexclusionrepair	GeneticInformationProcessing	Replicationandrepair	alkA,DNA-3-methyladenineglycosylase[EC:3.2.2.21]	2,07452E-05	1,5286E-05	4,15269E-05	0
K02472	ko00340	Basexclusionrepair	GeneticInformationProcessing	Replicationandrepair	alkA,DNA-3-methyladenineglycosylase[EC:3.2.2.21]	3,1117E-05	8,66207E-05	8,30537E-05	0
K06821	ko00520	Aminoacidnucleotidesugarmetabolism	Metabolism	Carbohydratemetabolism	GNPNA11_GNA11_guanylatecyclohydrolase[EC:3.2.3.14]	1,55589E-05	1,01907E-05	0	0
K0324	ko00760	Nicotinateandnicotinametabolism	Metabolism	Carbohydratemetabolism	paaz_xoepin_CoAhydrolyase/3-oxo-5-6-dehydroxyl-CoA-dicarboxylatedehydrogenase[EC:3.2.3.21.17.1]	0,000191893	0,000203813	0,00021594	0,00021594
K0324	ko00760	Nicotinateandnicotinametabolism	Metabolism	Carbohydratemetabolism	paaz_xoepin_CoAhydrolyase/3-oxo-5-6-dehydroxyl-CoA-dicarboxylatedehydrogenase[EC:3.2.3.21.17.1]	6,74218E-05	5,09533E-06	1,66107E-05	0
K02650	ko02020	Two-componentsystem	EnvironmentalInformationProcessing	Signaltransduction	nrdB,nrdE,MFStransporter,NREfamily_putativenickelresistanceprotein	0	5,60487E-05	0,000132886	0
K12371	ko02010	Citrateandprolineinterconversion	Membranetransport	PTS-Gat-EIaGatA_PTSsystem_glatcit-specificAkoComponent[EC:2.7.1.69];K02773_ko00052_Galactosemetabolism_Metabolism_Carbohydratemetabolism_PTS-Gat-EIaI	5,18629E-06	0	1,66107E-05	0	0
K02204	ko00260	Glycine,serineandthreoninemetabolism	Metabolism	Aminoacidmetabolism	dppD_dipeptidyltransferase[EC:2.7.1.39]	2,07452E-05	5,60487E-05	5,81376E-05	0
K02388	ko02040	Flagellarassembly	Organismsystem	Cellmotility	flgC,flagellarbasal-bodyproteinflgC	5,70492E-05	5,60487E-05	4,15269E-05	0
K01911	ko00130	Ubiquinoneandubiquinolmetabolism	Metabolism	Metabolism	metabolism_of_ubiquinoneandubiquinol	0,000108912	0,000116275	0,000116275	0
K06114	ko00561	Glycerolphospholipidmetabolism	Metabolism	Metabolism	SDQ2_sulfoglycosyltransferase[EC:3.1.2.26]	2,54767E-05	3,32215E-05	3,32215E-05	0
K02619	ko00360	Phenylalaninemetabolism	Metabolism	Aminoacidmetabolism	paalacyl-CoAhydroxylase[EC:3.1.2.2]	8,28007E-05	0,000127383	0,000141191	0
K07772	ko02020	Two-componentsystem	EnvironmentalInformationProcessing	Signaltransduction	torR_two-componentsystem,OmpRfamily_torCADoperonregulatortorR	1,55589E-05	0	1,66107E-05	0
K03782	ko00360	Phenylalaninemetabolism	Metabolism	Aminoacidmetabolism	katG_catalase-peroxidase[EC:1.11.1.21];K03782_ko00940_Ph	5,18629E-06	0	1,66107E-05	0
K13710	ko02010	Citrateandprolineinterconversion	Membranetransport	PTS-Gat-EIaGatA_PTSsystem_glatcit-specificAkoComponent[EC:2.7.1.69];K02773_ko00052_Galactosemetabolism_Metabolism_Carbohydratemetabolism_PTS-Gat-EIaI	1,58629E-06	0	0	0	0
K02935	ko03010	Ribosome	GeneticInformationProcessing	Transcription	RP-L7_MRP12_rplJ_largesubunitribosomalproteinL7/L12	0,000834993	0,000606345	0,000606345	0,00056628
K13940	ko00785	Uptakeandmetabolism	Metabolism	Metabolism	metabolism_of_uptakeandmetabolism	0,000176334	7,6433E-06	1,66107E-05	0
K02461	ko02020	Two-componentsystem	EnvironmentalInformationProcessing	Signaltransduction	rimM,rmsA,transcriptionfactor	5,18629E-06	0,000710522	0,000601249	0,000603208
K02887	ko03010	Ribosome	GeneticInformationProcessing	Transcription	RP-L20_MRP20_rplI_largesubunitribosomalproteinL20	0,000601249	0,000601249	0,000601249	0,000603208
K02887	ko03010	Ribosome	GeneticInformationProcessing	Transcription	RP-L20_MRP20_rplI_largesubunitribosomalproteinL20	0,000601249	0,000601249	0,000601249	0,000603208
K02887	ko03010	Ribosome	GeneticInformationProcessing	Transcription	RP-L20_MRP20_rplI_largesubunitribosomalproteinL20	0,000601249	0,000601249	0,000601249	0,000603208
K02887	ko03010	Ribosome	GeneticInformationProcessing	Transcription	RP-L20_MRP20_rplI_largesubunitribosomalproteinL20	0,000601249	0,000601249	0,000601249	0,000603208
K02887	ko03010	Ribosome	GeneticInformationProcessing	Transcription	RP-L20_MRP20_rplI_largesubunitribosomalproteinL20	0,000601249	0,000601249	0,000601249	0,000603208
K02887	ko03010	Ribosome	GeneticInformationProcessing	Transcription	RP-L20_MRP20_rplI_largesubunitribosomalproteinL20	0,000601249	0,000601249	0,000601249	0,000603208
K02887	ko03010	Ribosome	GeneticInformationProcessing	Transcription	RP-L20_MRP20_rplI_largesubunitribosomalproteinL20	0,000601249	0,000601249	0,000601249	0,000603208
K02887	ko03010	Ribosome	GeneticInformationProcessing	Transcription	RP-L20_MRP20_rplI_largesubunitribosomalproteinL20	0,000601249	0,000601249	0,000601249	0,000603208
K02887	ko03010	Ribosome	GeneticInformationProcessing	Transcription	RP-L20_MRP20_rplI_largesubunitribosomalproteinL20	0,000601249	0,000601249	0,000601249	0,000603208
K02887	ko03010	Ribosome	GeneticInformationProcessing	Transcription	RP-L20_MRP20_rplI_largesubunitribosomalproteinL20	0,000601249	0,000601249	0,000601249	0,000603208
K02887	ko03010	Ribosome	GeneticInformationProcessing	Transcription	RP-L20_MRP20_rplI_largesubunitribosomalproteinL20	0,000601249	0,000601249	0,000601249	0,000603208
K02887	ko03010	Ribosome	GeneticInformationProcessing	Transcription	RP-L20_MRP20_rplI_largesubunitribosomalproteinL20	0,000601249	0,000601249	0,000601249	0,000603208
K02887	ko03010	Ribosome	GeneticInformationProcessing	Transcription	RP-L20_MRP20_rplI_largesubunitribosomalproteinL20	0,000601249	0,000601249	0,000601249	0,000603208
K02887	ko03010	Ribosome	GeneticInformationProcessing	Transcription	RP-L20_MRP20_rplI_largesubunitribosomalproteinL20	0,000601249	0,000601249	0,000601249	0,000603208
K02887	ko03010	Ribosome	GeneticInformationProcessing	Transcription	RP-L20_MRP20_rplI_largesubunitribosomalproteinL20	0,000601249	0,000601249	0,000601249	0,000603208
K02887	ko03010	Ribosome	GeneticInformationProcessing	Transcription	RP-L20_MRP20_rplI_largesubunitribosomalproteinL20	0,000601249	0,000601249	0,000601249	0,000603208
K02887	ko03010	Ribosome	GeneticInformationProcessing	Transcription	RP-L20_MRP20_rplI_largesubunitribosomalproteinL20	0,000601249	0,000601249	0,000601249	0,000603208
K02887	ko03010	Ribosome	GeneticInformationProcessing	Transcription	RP-L20_MRP20_rplI_largesubunitribosomalproteinL20	0,000601249	0,000601249	0,000601249	0,000603208
K02887	ko03010	Ribosome	GeneticInformationProcessing	Transcription	RP-L20_MRP20_rplI_largesubunitribosomalproteinL20	0,000601249	0,000601249	0,000601249	0,000603208
K02887	ko03010	Ribosome	GeneticInformationProcessing	Transcription	RP-L20_MRP20_rplI_largesubunitribosomalproteinL20	0,000601249	0,000601249	0,000601249	0,000603208
K02887	ko03010	Ribosome	GeneticInformationProcessing	Transcription	RP-L20_MRP20_rplI_largesubunitribosomalproteinL20	0,000601249	0,000601249	0,000601249	0,000603208
K02887	ko03010	Ribosome	GeneticInformationProcessing	Transcription	RP-L20_MRP20_rplI_largesubunitribosomalproteinL20	0,000601249	0,000601249	0,000601249	0,000603208
K02887	ko03010	Ribosome	GeneticInformationProcessing	Transcription	RP-L20_MRP20_rplI_largesubunitribosomalproteinL20	0,000601249	0,000601249	0,000601249	0,000603208
K02887	ko03010	Ribosome	GeneticInformationProcessing	Transcription	RP-L20_MRP20_rplI_largesubunitribosomalproteinL20	0,000601249	0,000601249	0,000601249	0,000603208
K02887	ko03010	Ribosome	GeneticInformationProcessing	Transcription	RP-L20_MRP20_rplI_largesubunitribosomalproteinL20	0,000601249	0,000601249	0,000601249	0,000603208
K02887	ko03010	Ribosome	GeneticInformationProcessing	Transcription	RP-L20_MRP20_rplI_largesubunitribosomalproteinL20	0,000601249	0,000601249	0,000601249	0,000603208
K02887	ko03010	Ribosome	GeneticInformationProcessing	Transcription	RP-L20_MRP20_rplI_largesubunitribosomalproteinL20	0,000601249	0,000601249	0,000601249	0,000603208
K02887	ko03010	Ribosome	GeneticInformationProcessing	Transcription	RP-L20_MRP20_rplI_largesubunitribosomalproteinL20	0,000601249	0,000601249	0,000601249	0,000603208
K02887	ko03010	Ribosome	GeneticInformationProcessing	Transcription	RP-L20_MRP20_rplI_largesubunitribosomalproteinL20	0,000601249	0,000601249	0,000601249	0,000603208
K02887	ko03010	Ribosome	GeneticInformationProcessing	Transcription	RP-L20_MRP20_rplI_largesubunitribosomalproteinL20	0,000601249	0,000601249	0,000601249	0,000603208
K02887	ko03010	Ribosome	GeneticInformationProcessing	Transcription	RP-L20_MRP20_rplI_largesubunitribosomalproteinL20	0,000601249	0,000601249	0,000601249	0,000603208
K02887	ko03010	Ribosome	GeneticInformationProcessing	Transcription	RP-L20_MRP20_rplI_largesubunitribosomalproteinL20	0,000601249	0,000601249	0,000601249	0,000603208
K02887	ko03010	Ribosome	GeneticInformationProcessing	Transcription	RP-L20_MRP20_rplI_largesubunitribosomalproteinL20	0,000601249	0,000601249	0,000601249	0,000603208
K02887	ko03010	Ribosome	GeneticInformationProcessing	Transcription	RP-L20_MRP20_rplI_largesubunitribosomalproteinL20	0,000601249	0,000601249	0,000601249	0,000603208
K02887	ko03010	Ribosome	GeneticInformationProcessing	Transcription	RP-L20_MRP20_rplI_largesubunitribosomalproteinL20	0,000601249	0,000601249	0,000601249	0,000603208
K02887	ko03010	Ribosome	GeneticInformationProcessing	Transcription	RP-L20_MRP20_rplI_largesubunitribosomalproteinL20	0,000601249	0,000601249	0,000601249	0,000603208
K02887	ko03010	Ribosome	GeneticInformationProcessing	Transcription	RP-L20_MRP20_rplI_largesubunitribosomalproteinL20	0,000601249	0,000601249	0,000601249	0,000603208
K02887	ko03010	Ribosome	GeneticInformationProcessing	Transcription	RP-L20_MRP20_rplI_largesubunitribosomalproteinL20	0,000601249	0,000601249	0,000601249	0,000603208
K02887	ko03010	Ribosome	GeneticInformationProcessing	Transcription	RP-L20_MRP20_rplI_largesubunitribosomalproteinL20	0,000601249	0,000601249	0,000601249	0,000603208
K02887	ko03010	Ribosome	GeneticInformationProcessing	Transcription	RP-L20_MRP20_rplI_largesubunitribosomalproteinL20	0,000601249	0,000601249	0,000601249	0,000603208
K02887	ko03010	Ribosome	GeneticInformationProcessing	Transcription	RP-L20_MRP20_rplI_largesubunitribosomalproteinL20	0,000601249	0,000601249	0,000601249	0,000603208
K02887	ko03010	Ribosome	GeneticInformationProcessing	Transcription	RP-L20_MRP20_rplI_largesubunitribosomalproteinL20	0,000601249	0,000601249	0,000601249	0,000603208
K02887	ko03010	Ribosome	GeneticInformationProcessing	Transcription	RP-L20_MRP20_rplI_largesubunitribosomalproteinL20	0,000601249	0,000601249	0,000601249	0,000603208
K02887	ko03010	Ribosome	GeneticInformationProcessing	Transcription	RP-L20_MRP20_rplI_largesubunitribosomalproteinL20	0,000601249	0,000601249	0,000601249	0,000603208
K02887	ko03010	Ribosome	GeneticInformationProcessing	Transcription	RP-L20_MRP20_rplI_largesubunitribosomalproteinL20	0,000601249	0,000601249	0,000601249	0,000603208
K02887	ko03010	Ribosome	GeneticInformationProcessing	Transcription	RP-L20_MRP20_rplI_largesubunitribosomalproteinL20	0,000601249	0,000601249	0,000601249	0,000603208
K02887	ko03010	Ribosome	GeneticInformationProcessing	Transcription	RP-L20_MRP20_rplI_largesubunitribosomalproteinL20	0,000601249	0,000601249	0,000601249	0,000603208
K02887	ko03010	Ribosome	GeneticInformationProcessing	Transcription	RP-L20_MRP20_rplI_largesubunitribosomalproteinL20	0,000601249	0,000601249	0,000601249	0,000603208
K02887	ko03010	Ribosome	GeneticInformationProcessing	Transcription	RP-L20_MRP20_rplI_largesubunitribosomalproteinL20	0,000601249	0,000601249	0,000601249	0,000603208
K02887	ko03010	Ribosome	GeneticInformationProcessing	Transcription	RP-L20_MRP20_rplI_largesubunitribosomalproteinL20	0,000601249	0,000601249	0,000601249	0,000603208
K02887	ko03010	Ribosome	GeneticInformationProcessing	Transcription	RP-L20_MRP20_rplI_largesubunitribosomalproteinL20	0,000601249	0,000601249	0,000601249	0,000603208
K02887	ko03010	Ribosome	GeneticInformationProcessing	Transcription	RP-L20_MRP20_rplI_largesubunitribosomalproteinL20	0,000601249	0,000601249	0,000601249	0,000603208
K02887	ko03010	Ribosome	GeneticInformationProcessing	Transcription	RP-L20_MRP20_rplI_largesubunitribosomalproteinL20	0,000601249	0,000601249	0,000601249	0,000603208
K02887	ko03010	Ribosome	GeneticInformationProcessing						



















K11631_ko02010	Transporters	EnvironmentalInformationProcessing	Membranetransport_bceA	bac	tracrIntr	1,03726E-05	5,09533E-06	0	0
K11721_ko00540	Lipopolysaccharidebiosynthesis	Metabolism	Glycylglycylserinehydrolase	Metabolism	glyA	1,01907E-05	1,01907E-05	0	0
K1906_ko00780	Biotinmetabolism	Metabolism	6-carboxybiotinamide	Metabolism	bioW_6-carboxybiotinamide-CoA ligase	8,30537E-06	8,30537E-06	0	0
K12852_ko03040	Spliceosome	GeneticInformationProcessing	Transcription_LFTU02	L18	Ou5	5,18629E-06	0	0	0
K0881_ko00960	Tropone	lipidmetabolism	lipidbiosynthesis	Metabolism	biosynthesisofsteroidmetabolites_TyL	1,55589E-05	3,0572E-05	0	0
K05975_ko00154	Photosynthesisproteins	Metabolism	Energy	metabolism	EC:3.1.3.71	1,66307E-05	6,6443E-05	0	0
K00596_ko02020	Two-componentsystem	EnvironmentalInformationProcessing	Signaltransduction	Two-componentsystem	OmpKfamily	1,55589E-05	1,55589E-05	0	0
K00972_ko00650	Glyoxylateanddicarboxylatemetabolism	Metabolism	Carboxylatemetabolism	Metabolism	carboxylateanddicarboxylatemetabolism_E1.1.1.36	1,55589E-05	1,55589E-05	0	0
K17872_ko00170	Pantothenateandcobalaminbiosynthesis	Metabolism	Carboxylatemetabolism	Metabolism	carboxylateanddicarboxylatemetabolism_E1.1.1.36	1,55589E-05	1,55589E-05	0	0
K00904_ko00230	Uridineandthiouridinebiosynthesis	Metabolism	Nucleotidebiosynthesis	Metabolism	carboxylateanddicarboxylatemetabolism_E1.1.1.36	1,55589E-05	1,55589E-05	0	0
K10000_ko02010	Transports	EnvironmentalInformationProcessing	Membranetransport	Membranetransport	Membranetransport	0,000157955	6,6443E-05	0	0
K00716_ko01053	Transports	EnvironmentalInformationProcessing	Membranetransport	Membranetransport	Membranetransport	0,000157955	6,6443E-05	0	0
K1802_ko04110	Celastrol	CellularProcesses	Cellgrowthanddeath	CellularProcesses	CellularProcesses	1,03726E-05	1,03726E-05	0	0
K10283_ko01023	Pertussis	HumanDiseases	Infectiousdiseases	HumanDiseases	Infectiousdiseases	1,03726E-05	1,03726E-05	0	0
K08093_ko00030	Pentosephosphatepathway	Metabolism	Carboxylatemetabolism	Metabolism	carboxylateanddicarboxylatemetabolism_E1.1.1.36	1,03726E-05	1,03726E-05	0	0
K03023_ko00140	Transports	EnvironmentalInformationProcessing	Membranetransport	Membranetransport	Membranetransport	1,03726E-05	1,03726E-05	0	0
K13938_ko00785	Lipidmetabolism	Metabolism	Lipidmetabolism	Metabolism	lipidmetabolism	1,03726E-05	1,03726E-05	0	0
K09972_ko02010	Transports	EnvironmentalInformationProcessing	Membranetransport	Membranetransport	Membranetransport	1,03726E-05	1,03726E-05	0	0
K10175_ko02020	Transports	EnvironmentalInformationProcessing	Membranetransport	Membranetransport	Membranetransport	1,03726E-05	1,03726E-05	0	0
K05780_ko00440	Phosphonateandphosphinatemetabolism	Metabolism	Metabolism	Metabolism	metabolism	1,03726E-05	1,03726E-05	0	0
K09995_ko02010	Transports	EnvironmentalInformationProcessing	Membranetransport	Membranetransport	Membranetransport	1,03726E-05	1,03726E-05	0	0
K07672_ko02020	Two-componentsystem	EnvironmentalInformationProcessing	Signaltransduction	Two-componentsystem	OmpKfamily	1,03726E-05	1,03726E-05	0	0
K01557_ko00350	Tyrosinemetabolism	Metabolism	Aminoacidmetabolism	Metabolism	tyrosinemetabolism	1,03726E-05	1,03726E-05	0	0
K03788_ko00740	Riboflavinmetabolism	Metabolism	Aminoacidmetabolism	Metabolism	riboflavinmetabolism	1,03726E-05	1,03726E-05	0	0
K13584_ko04112	Celastrol	CellularProcesses	Cellgrowthanddeath	CellularProcesses	CellularProcesses	1,03726E-05	1,03726E-05	0	0
K07687_ko02020	Two-componentsystem	EnvironmentalInformationProcessing	Signaltransduction	Two-componentsystem	OmpKfamily	1,03726E-05	1,03726E-05	0	0
K02080_ko00052	Galactosemetabolism	Metabolism	Carboxylatemetabolism	Metabolism	carboxylateanddicarboxylatemetabolism_E1.1.1.36	1,03726E-05	1,03726E-05	0	0
K03368_ko00830	Retinolmetabolism	Metabolism	Metabolism	Metabolism	retinolmetabolism	1,03726E-05	1,03726E-05	0	0
K13919_ko00630	Glyoxylateanddicarboxylatemetabolism	Metabolism	Carboxylatemetabolism	Metabolism	carboxylateanddicarboxylatemetabolism_E1.1.1.36	1,03726E-05	1,03726E-05	0	0
K03080_ko00040	Pentoseandglucuronateinterconversions	Metabolism	Carboxylatemetabolism	Metabolism	carboxylateanddicarboxylatemetabolism_E1.1.1.36	1,03726E-05	1,03726E-05	0	0
K02865_ko03010	Ribosome	GeneticInformationProcessing	Transcription	Transcription	Transcription	1,03726E-05	1,03726E-05	0	0
K07702_ko02020	Two-componentsystem	EnvironmentalInformationProcessing	Signaltransduction	Two-componentsystem	OmpKfamily	1,03726E-05	1,03726E-05	0	0
K08196_ko00270	Cysteineandhomocysteinemetabolism	Metabolism	Aminoacidmetabolism	Metabolism	cysteineandhomocysteinemetabolism	1,03726E-05	1,03726E-05	0	0
K02193_ko02010	Transports	EnvironmentalInformationProcessing	Membranetransport	Membranetransport	Membranetransport	1,03726E-05	1,03726E-05	0	0
K14048_ko05120	EpithelialcellsignalinginHelicobacteriuminfection	HumanDiseases	Infectiousdiseases	HumanDiseases	Infectiousdiseases	1,03726E-05	1,03726E-05	0	0
K03414_ko02030	Bacterialchemotaxis	OrganismalSystem	Cellmotility	Chemotaxis	chemotaxis	1,03726E-05	1,03726E-05	0	0
K10002_ko02010	Transports	EnvironmentalInformationProcessing	Membranetransport	Membranetransport	Membranetransport	1,03726E-05	1,03726E-05	0	0
K08964_ko00270	Cysteineandhomocysteinemetabolism	Metabolism	Aminoacidmetabolism	Metabolism	cysteineandhomocysteinemetabolism	1,03726E-05	1,03726E-05	0	0
K07780_ko02020	Two-componentsystem	EnvironmentalInformationProcessing	Signaltransduction	Two-componentsystem	OmpKfamily	1,03726E-05	1,03726E-05	0	0
K06857_ko02010	Transports	EnvironmentalInformationProcessing	Membranetransport	Membranetransport	Membranetransport	1,03726E-05	1,03726E-05	0	0
K09689_ko02010	Transports	EnvironmentalInformationProcessing	Membranetransport	Membranetransport	Membranetransport	1,03726E-05	1,03726E-05	0	0
K03236_ko02010	Transports	EnvironmentalInformationProcessing	Membranetransport	Membranetransport	Membranetransport	1,03726E-05	1,03726E-05	0	0
K14075_ko02010	Transports	EnvironmentalInformationProcessing	Membranetransport	Membranetransport	Membranetransport	1,03726E-05	1,03726E-05	0	0
K14979_ko02020	Two-componentsystem	EnvironmentalInformationProcessing	Signaltransduction	Two-componentsystem	OmpKfamily	1,03726E-05	1,03726E-05	0	0
K03081_ko00040	Pentoseandglucuronateinterconversions	Metabolism	Carboxylatemetabolism	Metabolism	carboxylateanddicarboxylatemetabolism_E1.1.1.36	1,03726E-05	1,03726E-05	0	0
K00732_ko00740	Riboflavinmetabolism	Metabolism	Aminoacidmetabolism	Metabolism	riboflavinmetabolism	1,03726E-05	1,03726E-05	0	0
K10006_ko02010	Transports	EnvironmentalInformationProcessing	Membranetransport	Membranetransport	Membranetransport	1,03726E-05	1,03726E-05	0	0
K08350_ko02020	Two-componentsystem	EnvironmentalInformationProcessing	Signaltransduction	Two-componentsystem	OmpKfamily	1,03726E-05	1,03726E-05	0	0
K00077_ko00051	Fructoseandmannosemetabolism	Metabolism	Carboxylatemetabolism	Metabolism	carboxylateanddicarboxylatemetabolism_E1.1.1.36	1,03726E-05	1,03726E-05	0	0
K04719_ko00740	Riboflavinmetabolism	Metabolism	Aminoacidmetabolism	Metabolism	riboflavinmetabolism	1,03726E-05	1,03726E-05	0	0
K10353_ko00230	Purinemetabolism	Metabolism	Nucleotidebiosynthesis	Metabolism	carboxylateanddicarboxylatemetabolism_E1.1.1.36	1,03726E-05	1,03726E-05	0	0
K14570_ko03008	Ribosome	GeneticInformationProcessing	Transcription	Transcription	Transcription	1,03726E-05	1,03726E-05	0	0
K03410_ko02030	Bacterialchemotaxis	OrganismalSystem	Cellmotility	Chemotaxis	chemotaxis	1,03726E-05	1,03726E-05	0	0
K02877_ko03010	Ribosome	GeneticInformationProcessing	Transcription	Transcription	Transcription	1,03726E-05	1,03726E-05	0	0
K07690_ko02020	Two-componentsystem	EnvironmentalInformationProcessing	Signaltransduction	Two-componentsystem	OmpKfamily	1,03726E-05	1,03726E-05	0	0
K03238_ko03013	RNATransport	EnvironmentalInformationProcessing	Membranetransport	Membranetransport	Membranetransport	1,03726E-05	1,03726E-05	0	0
K13923_ko00630	Glyoxylateanddicarboxylatemetabolism	Metabolism	Carboxylatemetabolism	Metabolism	carboxylateanddicarboxylatemetabolism_E1.1.1.36	1,03726E-05	1,03726E-05	0	0
K13317_ko00521	Polyketidesugarunitbiosynthesis	Metabolism	Metabolism	Metabolism	polyketidesugarunitbiosynthesis	1,03726E-05	1,03726E-05	0	0







**Supplementary Table 25**

List of identified analytes together with retention times in the two chromatographic dimensions ( $t_{R}$  and  ${}^2t_{R}$ ), experimental and tabulated linear retention indices ( $I^E_S$ ), normalized 2D volume and relative standard deviation (RSD%) over three replicated analyses from each diet regimen sample.

Analytes	$t_{R}$ (min)	${}^2t_{R}$ (s)	Exp $I^E_S$	Ref $I^E_S$	SD		L-Fr		S-Fr	
					Norm 2D Volume	RSD%	Norm 2D Volume	RSD%	Norm 2D Volume	RSD%
2-Butanone	5.02	0.517	-	900	5138694	11.3	5631898	7.1	5569975	0.6
Butanal	5.55	0.655	926	911	411362	8.9	271685	2.3	174077	9.3
3-Methylbutanal	6.02	0.828	960	-	654043	18.5	269406	9.8	463418	7.8
1-Methoxy-2-propanone	6.15	0.483	969	-	65635	6.1	54745	5.8	106606	6.3
1,1'-Oxybis-butane*	6.69	2.000	1003	-	235165	4.3	212164	3.3	253346	0.6
2-Pentanone	6.89	0.621	1013	1011	65431	16.1	-	-	-	-
Isoxazole	7.95	0.828	1061	-	265560	14.6	452941	15.7	199116	19.3
2,3-Pentanedione	8.55	0.931	1085	1076	884781	13.1	60210	17.2	-	-
Butyl acetate	8.89	1.448	1098	1100	21735	19.5	28854	17.3	32086	13.6
Hexanal	9.22	1.414	1110	1105	396840	12.7	173438	9.3	146149	1.3
2-Methyl-3-Hexanone	10.49	1.862	1155	-	25307	5.8	29376	6.0	34021	9.8
1-Butanol	11.09	0.724	1174	1175	1204294	11.7	401598	2.4	406819	5.9
2-Methylbutyl propanoate	11.09	2.449	1174	-	355481	8.2	1430224	1.9	1519475	4.6
3-Methyl-4-heptanone	11.29	2.345	1180	-	54378	1.4	63909	1.3	69875	2.8
3-Heptanone	11.42	1.897	1184	1167	31167	5.8	36638	10.2	29809	0.7
Heptanal	12.49	1.862	1216	1206	161709	16.0	95965	14.2	58851	9.3
2-Ethyl hexanal	12.55	2.414	1218	1216	351699	16.7	358964	8.0	332911	3.7
Pyridine	12.62	0.897	1220	-	6421261	10.4	73487	16.4	69223	6.9
Limonene	12.82	2.690	1226	1224	84920	16.1	465263	9.7	469188	8.2
3-Methyl-1-butanol	13.22	0.860	1238	1237	-	-	99615	4.0	118542	9.7
1,8-Cincole	13.35	2.862	1241	1245	43666	14.4	13611	0.3	-	-
1-(Chloromethoxy)-2-methyl-propane*	13.49	3.138	1245	-	38713	5.0	34792	17.2	50115	11.3
Butyl butanoate	13.62	2.517	1249	1243	7849331	4.5	8426060	7.3	9551280	4.9
Pentanol	14.82	0.897	1280	1274	24600	17.0	38194	2.0	28335	2.9

1-Butanol-3-methylpropanoate	15.09	1.483	1287	-	78221	20.5	84066	6.3	81943	0.7
Octanal	16.49	2.242	1324	1319	339710	15.3	89546	3.2	64821	11.2
2-Ethyl-2-hexenal	16.89	2.207	1334	1336	551382	13.2	565609	7.6	597980	5.9
6-Methyl-5-hepten-2-one	18.35	1.793	1371	1365	37763	7.6	43166	13.7	50728	0.4
Hexanol	18.89	1.000	1383	1386	636568	23.9	348981	2.2	290444	18.0
2-Propylhexanal	19.82	3.276	1405	-	87392	12.7	-	-	-	-
Nonanal	20.69	2.517	1429	1423	328418	22.0	393118	4.8	207225	1.3
1-Octen-3-ol	20.89	2.035	1434	1430	55234	14.9	59144	9.4	58307	10.6
2-Butoxy ethanol	20.95	1.069	1435	1435	18569	17.1	-	-	22972	13.5
1-Hepten-3-ol	22.82	1.207	1481	-	62592	13.1	55609	16.9	35653	7.4
Acetic acid	22.82	0.448	1481	1479	1279002	9.4	925652	17.8	770146	8.5
Heptanol	23.02	1.173	1486	1465	327093	19.6	297805	0.9	148568	14.0
2-Ethyl-1-hexanol	24.42	1.310	1522	1518	907920	19.4	1056351	12.5	815905	12.1
1H-Pyrrole	25.22	0.586	1543	1534	41440	8.0	69348	15.5	37818	3.9
Benzaldehyde	26.02	1.069	1563	1555	740857	27.5	99365	8.4	260884	20.3
Propanoic acid	26.29	0.517	1569	1564	135266	17.0	-	-	50900	14.8
Octanol	27.15	1.310	1591	1585	1121374	10.1	294466	6.4	224653	11.2
Butanoic acid	29.75	0.517	1659	1661	571958	19.8	77417	15.7	73686	15.1
Phenylacetaldehyde	30.55	1.104	1679	-	809122	7.4	462549	9.9	556029	8.4
Nonanol	31.15	1.414	1694	1695	574209	17.7	855342	1.4	465283	6.1
2-Propyl-1-heptanol	31.42	1.621	1700	-	1061702	20.1	19174	13.5	38284	13.0
2-Methyl butanoic acid	31.42	0.586	1700	1705	24362	16.5	-	-	-	-
3-(Methylthio)-1-propanol	33.15	0.793	1749	1744	65522	8.8	40929	15.0	30139	3.6
Pentanoic acid	33.95	0.586	1770	1768	18263	16.2	-	-	-	-
Decanol	34.95	1.517	1797	1781	68509	16.5	136539	4.5	107723	12.5
Hexanoic acid	37.75	0.621	1876	1873	42652	12.4	65044	12.3	49914	17.1
Butyl benzoate	38.55	1.790	1898	1903	1262029	13.1	1311705	18.8	1319326	3.3
Phenylethyl Alcohol	40.02	0.828	1943	1944	138203	17.6	97147	1.6	97156	10.5
6,10-Dimethyl-5,9-undecadien-2-ol*	41.69	1.724	1992	-	490283	16.8	123955	4.5	142311	4.7
Dodecanol	42.09	1.724	2004	-	62850	17.9	65189	0.9	54807	13.1
Phenol	43.02	0.586	2034	2026	56667	15.2	89277	1.7	107727	14.2
4-Methyl phenol	45.49	0.621	2109	2100	144082	4.8	124970	6.3	127323	8.3
Indole	56.02	0.724	2465	2460	192902	7.8	192077	4.2	82313	2.2

\*Tentatively identified